

**Studies of conformational and functional transitions
of N-acetyl galactosamine binding lectins from
Bauhinia purpurea and *Wisteria floribunda***

Thesis Submitted to AcSIR
For the Award of the Degree of
DOCTOR OF PHILOSOPHY
in
BIOLOGICAL SCIENCES



by

Agrawal Sanskruthi Bhickchand

Registration Number: 10BB15J26040

Under the guidance of

Dr. Mahesh Kulkarni

(Research Supervisor)

Dr. Sushama Gaikwad

(Research Co- Supervisor)

DIVISION OF BIOCHEMICAL SCIENCES
CSIR-NATIONAL CHEMICAL LABORATORY
PUNE – 411008, INDIA

November 2019



Dedicated to

My beloved Family &

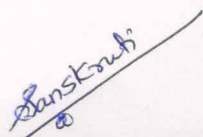
my Grandfather,

late Mr. Vaijanath Agrawal

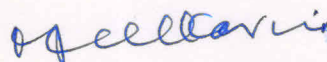
CERTIFICATE

This is to certify that the work incorporated in this Ph.D. thesis entitled "**Studies of conformational and functional transitions of N-acetyl galactosamine binding lectins from *Bauhinia purpurea* and *Wisteria floribunda***" submitted by **Ms. Agrawal Sanskruthi Bhickchand** to Academy of Scientific and Innovative Research (AcSIR) in fulfillment of the requirements for the award of the Degree of **Doctor of Philosophy**, embodies original research work under our supervision/guidance. We further certify that this work has not been submitted to any other University or Institution in part or full for the award of any degree or diploma. Research material obtained from other sources has been duly acknowledged in the thesis. Any text, illustration, table etc., used in the thesis from other sources, have been duly cited and acknowledged.

It is also certified that this work done by the student, under my supervision, is plagiarism free.



Ms. Agrawal Sanskruthi Bhickchand
(Student)



Dr. Mahesh J. Kulkarni
(Research Supervisor)



Dr. Sushama M. Gaikwad
(Research Co-Supervisor)

DECLARATION OF THE CANDIDATE

I declare that the thesis entitled, "**Studies of conformational and functional transitions of N-acetyl galactosamine binding lectins from *Bauhinia purpurea* and *Wisteria floribunda***" submitted by me for the Degree of **Doctor of Philosophy** is the record of work carried out by me during the period from 29th December 2014 to 22nd May 2019 under the guidance of **Dr. Mahesh J. Kulkarni and Dr. Sushama M. Gaikwad** and has not formed the basis for the award of any Degree, Diploma, Associateship, Fellowship, titles in this or any other University or other Institute of higher learning. I further declare that the material obtained from other sources has been duly acknowledged in the thesis.

Date: 6th Nov 2019


Ms. Agrawal Sanskruthi Bhickchand

Signature of the candidate

Acknowledgement

The path towards this Thesis had been a truly astonishing. In its completion I would like to thank many people who challenged, supported and stuck with me in this way.

Foremost, I would like to express my sincere gratitude to my advisor **Dr. Sushama M. Gaikwad** for the continuous support of my Ph.D study and related research, for her patience, motivation, and immense knowledge. Her guidance helped me in all the time of research and writing of this thesis. I could not have imagined having a better advisor and mentor for my Ph.D study. Her care, understanding nature always gave me a homely atmosphere during my tenure.

Besides her, I would like to express by heartfelt gratitude to thank **Dr. Mahesh J. Kulkarni** for his unconditional support and advice during the work.

I am grateful to **Dr. Amanpreet Kaur Sidhu**, my MSc. Dissertation guide, former colleague and friend for her continuous motivation to develop keen interest in research and pursue Ph.D. She was always present morally in all the up-downs of my life. Discussions with her always pushed me to think differently and accept the challenges positively.

My sincere thanks goes to the rest of my thesis committee: **Dr. Dhanasekaran Shanmugam**, **Dr. Subaschandrabose Chinnathambi** and **Dr. Amol Kulkarni**, for their insightful comments and encouragement, but also for the hard question which incited me to widen my research from various perspectives.

I would like to thank all my collaborators: from NCL **Dr. Deepanjan Ghosh**, **Ms. Siddhanta** and **Dr. Durba Sengupta** for their valuable contribution in *in-silico* study. **Dr. Neha Gupta** and **Dr. Sameer Bhagyawant** from SOS in Biotechnology, Jiwaji University, Gwalior for help in Cell culture work. **Ms. Aishwarya** and **Dr. Mayurika Lahiri** from IISER, Pune for help in MTT assay. I must thank **Dr. Moneesha Fernandes** for the CD facility and **Dr. Siddhart Bhosale** for technical help in time resolved fluorescence studies.

I owe my sincere gratitude to my seniors and my friends –**Dr. Sayli**, **Dr. Priya**, **Dr. Ekta** and **Dr. Ameya** for their advices and assistance with various problems. I express warm feelings for **Priya di** and **Ekta di** with whom I have spend wonderful time in and out of lab, care and love which I received from them as younger one. Many thanks to other friends from

NCL **Dr. Snehal More, Dr. Ruby, Dr. Vijay, Dr. Preeti , Dr. Amruta, Manisha di, Uma, Sheetal, Tejashree, Isha and Swarali** for providing good atmosphere in department. I take this opportunity to thank **Dr. Varsha Parasharami** faculty at Plant tissue culture division, NCL, for giving me opportunity to work with her and organize a workshop which help me learn new things and gave me a different experience in general.

I would like to express my love and heartfelt thanks to my past and present roommates and friends **Dr. Sneha, Dr. Arati, Dr. Nivedita, Dr. Jyotsana, Komal, Sneha, Mamta, Gauri, Neelam and Pranita** for being great roomies and for taking care of me as and when required. I would like to take efforts to specially thank **Gauri and Komal** for taking care of me during my physical and emotional breakdowns. I will always treasure the memories of joyfull time spent with them.

I have no words to express my gratitude to my family, thank you for encouraging me in all of my pursuits and inspiring me to follow my dreams. I am especially grateful to my parents, who supported me emotionally. I always knew that you believed in me and wanted the best for me. Thanks to my life-coach, my **late Grandfather** because I owe it all to you. Thank you for teaching me that my job in life was to learn, to be happy, and help others. Thanks to my **Grandmother** she was always keen to know what I was doing and how I was proceeding, although it is likely that she has never grasped what it was all about! Thank you to my **Mother**, for guiding me as a person, keeping patience, listening all to my work stories and being my friend whenever needed. **Papa** mere listening to your voice once in a day made my day and vanished all my problems. **Chachu** who stood always as a strong pillar besides me as my guardian and best friend in all the ups-down of my life. My brother **Dr. Adarsh** who always believed in me and stood by me in all my decisions. Though younger he always took care of me as elder brother. Even I am thankful to **Chachu** and **Adarsh** for help in CSIR-800 project. Last but not the least I would like to extend my warm thanks to all my **Buha, Pupaji, Mama, Masi** and all other family members who were always appreciating and supporting in some or other ways.

I take opportunity to sincerely thank my extended family and my best friends who mean lot to me **Amanpreet Mam, Irum di, Akanksha, Ajinkya, Bhushan, Kalpesh, Saniya and Shweta** for all the love, care and support. Cheers! To our lifelong friendship. Thanks to my friend cum sister **Akanksha** for her selfless love, care and dedicated efforts which pushed me a lot for completion of my thesis. I would also like to thank

Ashwini di, Aarati di and Vedanti who helped me in my initial phase of my PhD. and there support helped me to adjust in Pune as I was new comer to city.

I thank **God** for giving me strength and for blessing me with wonderful people around who added happiness to my life.

I also would like to thank **staff of Biochemical Sciences Division, CSIR-National Chemical Laboratory, Student Academic Office (SAO- NCL) and AcSIR (NCL campus)** for helping me directly or indirectly during course of my stay and study in the division.

Finally, I thank the **scientists and Head(s), Division of Biochemical Sciences, the Director(s) of CSIR-National Chemical Laboratory and AcSIR (Academy of Scientific and Innovative Research)** for allowing me to submit this work in the form of the thesis and lastly, **Indian Council of Medical Research (ICMR), India**, for the financial assistance.

Thanks for all your encouragement!

Agrawal Sanskruthi Bhickchand

Contents

	Page No.
Abbreviations	1-2
Abstract	3-5
Chapter 1 Introduction	7 -43
1.1 Protein folding	7
1.1.1 Protein misfolding and aggregation	8
1.1.2 Diseases caused due to Protein misfolding	10
1.1.3 Studying folding/ unfolding transitions of proteins	11
1.1.4 Techniques to study protein folding	11
1.1.5 Structure-function relationship of proteins	14
1.2 Lectins	15
1.2.1 Historical background	16
1.2.2 Detection of lectin	17
1.2.3 Occurrence and Biological Role of Lectin	17
1.2.4 Classification of Lectins	18
1.2.5 Lectin-Sugar Interactions	19
1.2.6 Applications of Lectins	22
1.2.7 Recently solved structures of lectin	26
1.2.8 Legume lectins	31
1.3 Objective of the present thesis	32
References	33
Chapter 2 Sugar binding studies of BPL and WFL	44-59
Abstract	45
2.1 Introduction	45
2.2 Materials and Methods	47

2.3	Results and discussion	49
2.4	Conclusion	57
	References	58
Chapter 3	Structural and functional transition studies of BPL and WFL	60-85
	Abstract	61
3.1	Introduction	61
2.2	Materials and Methods	62
2.3	Results and discussion	67
<i>Section I</i>	<i>Thermal transition studies</i>	67
<i>Section II</i>	<i>Chemical denaturation studies</i>	74
<i>Section III</i>	<i>Characterization of molten globule like intermediate</i>	79
	References	84
Chapter 4	Anticancer activity of BPL and WFL on Breast cancer	89-99
4.1	Introduction	89
4.2	Materials and Methods	90
4.3	Results	93
4.4	Discussion	97
	References	99
	Summary and conclusion	103-104
	List of publications and posters presented	105-106

LIST OF ABBREVIATIONS USED

ANS	1-anilino-8-naphthalenesulfonate
Asp	Aspartic acid
BPL	<i>Bauhinia purpurea</i> lectin
CD	Circular dichroism
DCFH-DA	Dichloro dihydro fluorescein diacetate
DMEM	Dulbecco's modified eagle medium
FBS	Fetal bovine serum
GalNAc	N-acetyl D-galactosamine
GdnHCl	Guanidine hydrochloride
Glu	Glutamic acid
Gly	Glycine
GSA	<i>Griffonia simplicifolia</i> agglutinin
HA	Hemagglutinating activity
Ile	Isoleucine
LacdiNAc	β -D-GalNAc-[1 \rightarrow 4]-DGlcNAc
LDH	Lactate dehydrogenase
k_a	Association constant
kDa	Kilo Dalton
K_{sv}	Stern-Volmer (dynamic) quenching constant
MCF-7	Michigan Cancer Foundation-7
MD	Molecular dynamics
MG	Molten globule
MRE	Mean Residual Ellipticity
MTT	3-(4,5-dimethylthiazol-2-yl)-2,5-diphenyl-tetrazolium bromide
NRMSD	Normalized root mean square deviation
PAGE	Polyacrylamide gel electrophoresis
PBS	Phosphate buffer saline
PDB	Protein Data Bank
Pro	Proline
RIPs	Ribosome inactivating proteins
RMSD	Root mean square deviation
RMSF	Root mean square fluctuation

ROS Reactive oxygen species

SDS Sodium dodecyl sulphate

Ser Serine

T-antigen Thomsen-Friedenreich (Gal β 1-3GalNAc)

Trp Tryptophan

WFL *Wisteria floribunda* lectin

WGA Wheat germ agglutinin

Abstract of the thesis

Chapter 1: Introduction

The importance and updates in protein folding/unfolding research have been discussed in this section. Significance of studying the structure-function relationship of proteins through various experimental and theoretical approaches has also been presented. The importance of lectins in terms of classification, structure and function is given. The available information, recent developments in lectins with applications are summarised as the basis of studies undertaken in thesis.

Chapter 2: Sugar binding studies of BPL and WFL

Sugar binding studies of two novel medicinally important legume lectins from *Bauhinia purpurea* (BPL) and *Wisteria floribunda* (WFL) were performed. The Homology model of BPL was constructed to predict the three dimensional structure, locate the tryptophan residues and evaluate the environment therein. The three dimensional structure of BPL monomer with bound metal ions Ca^{2+} represented the typical legume lectin fold presenting the jelly roll motif. Model thus constructed was docked with sugars (GalNAc and T-antigen) to find out amino acid residues involved in sugar binding and their binding energies. The hydrogen bonds and hydrophobic interactions occurring between these sugars and the protein were studied and ligand interactions diagrams were generated. The docked pose of T-antigen (-8.313) showed two fold increase in docking score compared to GalNAc (-4.008). The binding constants K_a of BPL for GalNAc and T-antigen disaccharide (Gal β 1-3GalNAc α O-Me) as determined by intrinsic fluorescence spectroscopy (in solution studies) were $5.0 \times 10^3 \text{ M}^{-1}$ and $1 \times 10^4 \text{ M}^{-1}$, respectively. Thus, binding affinities determined by *in silico* and *in solution* studies correlate well. Sequence and structural alignments of BPL and WFL showed longer loop D in WFL making it more specific to LacdiNAc over GalNAc/Gal β 1-3 GalNAc.

Chapter 3: Structural and functional transitions studies of BPL and WFL

BPL and WFL possessing extended sugar binding site were investigated for functional and conformational transitions using biochemical and biophysical techniques as well as bioinformatical tools. The results on the studies of the two unexplored lectins have been

presented together (In III sections) to get deeper understanding of the structural and functional elements responsible for similar or diverse properties.

Section I deals with thermal transitions studies of BPL and WFL. Structural and functional transitions were monitored at different temperatures using biophysical techniques and hemagglutination assay. Detail investigations of aggregation were done by Molecular Dynamics simulations. Based on hemagglutination activity assay, BPL was functionally stable up to 40 °C whereas WFL is functionally stable upto 70 °C. CD scan for both the lectins showed peculiar alteration in the structure indicated by increase in the negative ellipticity at 212–215 nm and decrease in the positive ellipticity between 190 and 200 nm showing conversion of atypical to typical beta sheet. BPL did not aggregate when heated upto 90 °C, while WFL got aggregated at 85 °C as indicated by increase in the light scattering intensity. Molecular dynamics simulation studies of WFL showed difference in RMSD and RMSF at 85 °C compared to that at 25°C.

Section II comprises of chemical denaturation studies in presence of chaotropic agent GdnHCl which revealed multistate unfolding of lectins. Tryptophans in denatured BPL and WFL (GdnHCl 6.0 M) exhibited higher polar environment than at pH 8.0 due to unfolding. The far-UV CD spectra of BPL showed complete loss in structure in > 3M GdnHCl and which correlated well with functional loss of activity (≥ 3.0 M). Similar results were observed in WFL, complete loss in structure was observed in 5M GdnHCl. Overall it's a multistate unfolding of protein. Substantial decrease in retention time (by 1.2–1.8 min) due to increase in Stoke's radius in presence of 1.0 M GdnHCl was observed in size exclusion chromatography. SEC studies showed that dissociation and unfolding of the proteins occurred simultaneously.

In Section III, detection and detailed characterization of acid induced molten globule like intermediates is discussed. At pH 1.0, both the lectins exhibited molten globule like structures, which were characterized further and were found to respond in a different way towards denaturants.

Chapter 4: Anticancer activity of lectins from *Bauhinia purpurea* and *Wisteria floribunda* on Breast cancer MCF-7 cell lines

MTT assay on human breast cancer cell line MCF-7 was performed to examine cytotoxic effect of BPL and WFL. These agglutinins caused remarkable concentration-dependent antiproliferative effect. The values were approximately 446 μgml^{-1} (2.2 μM) and 329

μgml^{-1} (2.8 μM) for BPL and WFL, respectively. The level of LDH released from the cells significantly increased after 24 hr of exposure to 500 $\mu\text{g/ml}$ of lectins against untreated cells. Intracellular ROS production was measured by DCFH oxidation in cells treated with lectin at a dosage of 500 $\mu\text{g/ml}$ for 24 hr. There was a significant 2-3 fold increase in the ROS generation as compared to untreated cells. The BPL and WFL 500 $\mu\text{g/ml}$ treatment for 24 hr caused a significant ($P < 0.05$) increase in caspase-3 activation compared to tamoxifen and control. The inhibitory effect of these lectins was shown to be a consequence of lectin cell surface binding and triggering S and G2 phase arrest revealed by flow-cytometry studies. Apoptotic signal is amplified by activation of caspase-3 executing cell death.

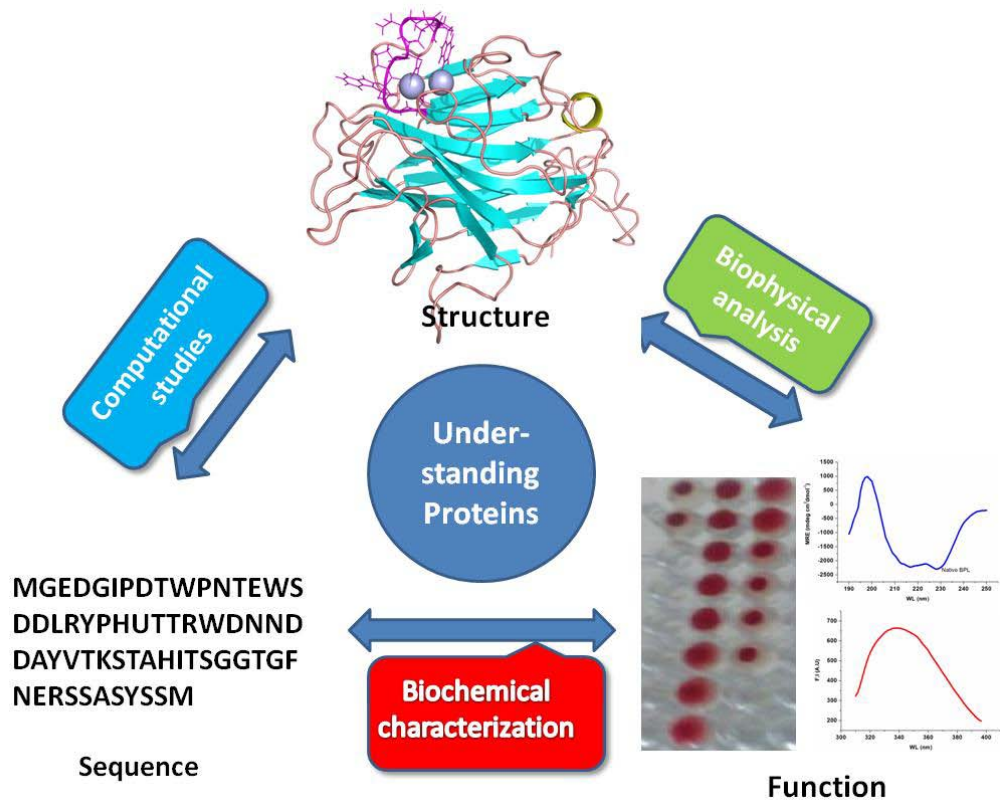
Summary and conclusion

The study of protein folding started as a challenge in basic sciences and still motivates researchers for understanding protein- structure function relationship. To understand the structure function correlation, information comes from the primary structure i.e amino acid sequence and associated tertiary structure of protein. This chapter discusses highlights of thesis and summarises characteristics of two legume lectins under study.

The biochemical, biophysical and *in silico* studies on both the GalNAc binding plant lectins described here not only confirm the applicability but also enhance our understanding of the lectin function and protein structure at molecular level. Loss in cell viability and apoptosis of the cancer cells in presence of lectins suggests that both the lectins BPL and WFL may possibly have potential as an anticancer agent in future.

Chapter 1

Introduction



1. Introduction

1.1 Protein Folding

Protein folding is an active field of research comprising aspects of biochemistry, biology, chemistry, computer science and physics. Fundamental principles of protein folding apply in aiding genome research, in the understanding of disease pathologies and construction of new proteins with special functions [1]. Detailed pathways of folding are not known completely, advances have been made in the understanding of this complex process through experimental and theoretical approaches [2]. As proposed by Anfinsen [3] “the process by which proteins fold into their functional structures is dictated by the chemical blueprints encoded into their amino acid sequence.”

The proteins are synthesized from amino acids at a high rate in hierarchical folding process in a living cell. Amino acid sequences readily fold into α -helices or β -sheets, followed by different interactions between them to form stable structures and the process continues until complete polypeptide is folded [4]. Protein folding is initiated by a spontaneous collapse of the polypeptide into a compact state driven by non polar interactions among hydrophobic amino acids [5]. Tertiary structure of a protein is held together by four different bonds and interactions such as hydrogen bonds, hydrophobic and hydrophilic interactions, ionic bonds and disulphide bonds, if any (Fig.1A). Quaternary structure is the three-dimensional structure of a multi-subunit protein and the way in which subunits fit together by the non-covalent interactions and in some cases, disulfide bonds.

From thermodynamic perspective, the folding process is a kind of free-energy funnel. The unfolded states have more number of conformations compared to native and have both high conformational entropy and free energy [2]. Very few intramolecular interactions that will exist in the native conformation are there in unfolded state. As folding proceeds, the thermodynamic path down the funnel reduces the number of species present, leading to decrease in entropy and free energy. Depressions on the sides of the free-energy funnel show semi-stable intermediates that can slow down the folding process [3, 5-6]. A single or a small set of native conformations are seen at the bottom of the funnel (Fig.1B).

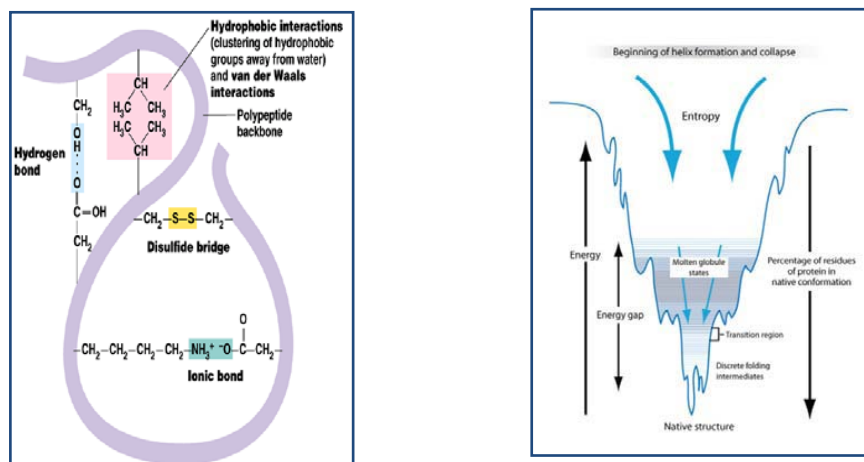


Figure 1. Protein folding: A. Types of interactions involved in polypeptide chain formation (adapted from Pearson Education Inc., publishing as Benjamin Cummings) **B. The thermodynamics of protein folding depicted as a free-energy funnel** (adapted from <https://www.learner.org/courses/physics/visual>)

1.1.1 Protein misfolding and aggregation

A stringent quality control system in the cellular machinery ensures proper protein folding, trafficking and degradation [7]. Still, a number of proteins fail to reach or maintain their native conformation leading to protein misfolding. Misfolded proteins cannot be refolded by chaperones and are targeted to proteasome or lysosome for degradation [8]. The stability of a native protein depends on parameters viz temperature, pH, ionic strength, and solvent composition. The intramolecular bonds responsible for stability and integration of the protein are susceptible for dislocation. Perfectly folded proteins remain stable for long term in biological environment and interact specifically with their natural ligands. Misfolded or partially folded states usually aggregate as they are major kinetic traps in the folding pathway. These states normally show exposed hydrophobic amino acid residues and regions of unordered polypeptide backbone which are mainly buried in the native state. Similar to intramolecular folding, aggregation is association of two or more non-native protein molecules largely driven by hydrophobic forces resulting into the formation of amorphous structures (Fig.2). Aggregation can also lead to formation of highly ordered, fibrillar aggregates called amyloid, in which β -strands run perpendicular to the long fibril axis (cross- β structure). Formation of amyloid fibrils is generally toxic to cells and may lead to the neurodegenerative diseases [6].

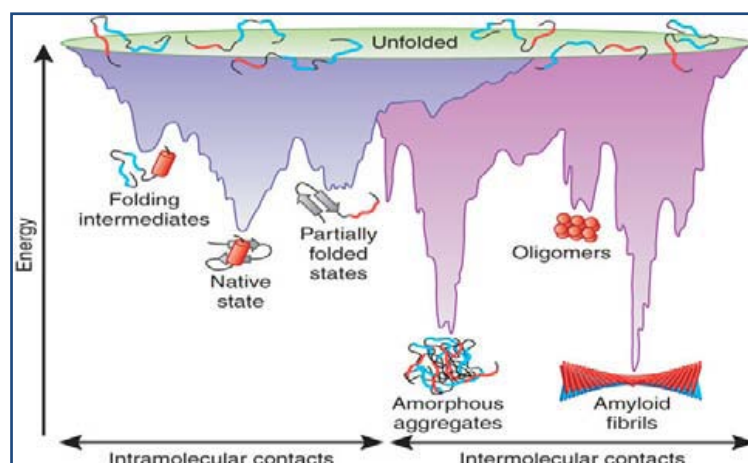


Figure 2: Energy landscape of protein folding and misfolding

<http://www.ghrnet.org/index.php/jbmr/article/viewFile/1027/1397/6798>

1.1.2 Diseases caused due to Protein misfolding

Protein misfolding follows two pathophysiological pathways, (i) due to toxic aggregates, e.g. neurodegenerative diseases such as Alzheimer's, Huntington's or Parkinson's disease; (ii) due to inappropriate folding, accelerated degradation or aggregation of proteins because of genetic variation [9-12]. In the second group of disorders, missense mutations typically lead to reduced folding, decreased proteolytic and thermal stability, enhanced protein degradation and aggregation, resulting into a non-functional phenotype [13]. The list of few diseases caused due to protein misfolding and amyloid aggregation has been summarized in Table 1.

Table 1: Examples of human diseases associated with protein misfolding and amyloid aggregation (Modified from ref [11] and [14])

Disease	Symptom	Aggregating protein or peptide	Structure of protein or peptide
Alzheimer's disease (AD)	Memory loss	Amyloid β peptide	Intrinsically disordered
Spongiform encephalopathies	Impairment of brain function	Prion protein	Intrinsically disordered α -helical

(TSE)			
Parkinson's disease (PD)	Progressive movement disorder	α -Synuclein	Intrinsically disordered
Amyotrophic lateral sclerosis (ALS)	Motor neuron disease	Superoxide dismutase 1	β -sheet and Ig- like
Huntington's disease (HD)	Uncontrolled movement	Huntingtin (polyQ)	Most intrinsically disordered
Light chain amyloidosis	Plasma cell disorder	Immunoglobulin light chains	β -sheet and Ig- like
Hemodialysis- related amyloidosis	Deposition of amyloid fibrils consisting of β 2- microglobulin	β 2-microglobulin	β -sheet and Ig- like
Type II diabetes	Metabolic disorder, Increase in blood sugar	Amylin	Intrinsically disordered

1.1.3 Studying folding/ unfolding transitions of proteins

Knowledge of folding-unfolding transitions between native and denatured conformations serves in understanding biological function of the protein [15]. Protein folding involves collapse of disordered and extended polypeptide chain to form a globular compact protein. Estimation of molecular dimensions and core packing are vital elements of the folding process. Changes in the fluorescence of tryptophan or tyrosine or the extrinsic fluorophores such as 8-anilino-1-naphthalenesulphonate (ANS), are used as indirect probes which have numerous applications. Direct probes used in the study of accessibility of ionic fluorescence quenchers such as iodide or acrylamide have also been developed [16].

Changing the composition of the system by the addition of co-solvents to the solution or by changing the thermodynamic state of the system (temperature, pressure, pH), equilibrium between the folded and the unfolded states can be shifted in any direction [17]. Urea and guanidium hydrochloride (GdnHCl) induce disorder and favour

the unfolded state of proteins, and are therefore known as denaturants/ chaotropes. Studies on solvent mediated structural and conformational transitions of proteins can provide insight into their stability, folding pathways, and intermolecular aggregation behaviour [18, 19].

Enthalpy, entropy and free energy are the thermodynamic state functions for protein folding. These thermodynamic properties can be used as tools to study protein conformational changes under different environmental conditions. Free energy of protein folding and protein denaturation is equal. Entropy is most important parameter as when a protein molecule is denatured it leads to increased randomness of system which is direct measure of entropy [20].

Detailed understanding of protein-ligand interaction studies is beneficial for structure based drug design. One of the important aspects of interaction is relationship between structure of protein and binding thermodynamics [21]. Thermodynamics of protein-ligand interaction can be studied using techniques like steady state or time resolved fluorescence spectroscopy, surface plasmon resonance and isothermal titration calorimetry.

1.1.4 Techniques to study protein folding

Major advances in elucidating the mechanism of protein folding have been chiefly derived from the development of methods that can monitor fast transitions between structurally dynamic ensembles [22]. The experimental techniques for studying protein folding monitor the gradual unfolding or folding of proteins and observe conformational changes using standard noncrystallographic techniques like fluorescence and circular dichroism. The computational techniques for protein structure prediction are related to, but are distinct from experimental studies of protein folding [6, 23]. The use of novel methods of initiating refolding and combination of theoretical and experimental approaches has lead to an in depth understanding of several aspects of the folding process. Techniques have been listed in Table 2.

Table 2: Techniques for studying protein folding.

Technique	Information content
Intrinsic fluorescence [24]	Environment of tryptophan and tyrosine (through measurement of intensity and λ_{\max})

Far UV CD [25]	Secondary-structure content, measures the difference in absorbance of right and left circularly polarized light by a substance.
Near UV CD [25]	Packing of aromatic residues, measures the difference in absorbance of right and left circularly polarized light by a substance.
Raman spectroscopy [26]	Solvent accessibility, conformation of aromatic residues, observe vibrational, rotational, and other low-frequency modes in a system
Infrared spectroscopy [27]	Secondary-structure content, involves the interaction of infrared radiation with matter.
ANS (1-anilino-8-naphthalene sulfonic acid) binding [26]	Exposure of aromatic surface area
Förster resonance energy transfer [28]	Molecular ruler, dependent on the distance between two fluorophores
Fluorescence correlation spectroscopy [29]	Diffusion time (and hence size and shape), a correlation analysis of fluctuation of the fluorescence intensity.
Anisotropy [24]	Correlation time measurements provide information about shape and size of molecule
Small-angle X-ray scattering [30]	Radius of gyration, elastic scattering of X-rays due to inhomogeneities in the nm-range.
Absorbance [31]	Environment of chromophore
Real-time NMR [32]	Structural information via chemical shifts and measurement of NOEs (Nuclear Overhauser effects)
Native-state hydrogen exchange [33]	Global stability, detection of metastable states
Protein engineering [34]	Role of an individual residue in determining the rate of folding, stability of a species of interest
Differential scanning Calorimetry(DSC) or	Conformational energetics of protein, difference in the amount of heat required to increase the temperature of a

microcalorimetry [35]	sample and reference is measured as a function of temperature
Different scanning fluorimetry (DSF) [36]	Thermophoresis gives melting temperature of protein
Differential static light scattering (DSL) [37]	Temperature of aggregation of a protein

Theoretical approach: New theoretical and computational approaches have emerged including various bioinformatics tools, multiple sequence alignments, structure-prediction web servers, physics-based force fields etc. These techniques are employed to match the experiments in providing an overall picture of the protein structure. The computational methods available for protein structure determination include homology modelling, fold recognition via threading, and ab initio methods [38]. Tremendous amount of sequence and structural data of proteins and modern experimental and bioinformatics methods have enhanced our understanding about the protein sequence→structure→dynamics→function relationship [39]. This helps to understand the interaction of proteins with their substrate or other molecules such as ligands, which can become a drug candidate [40]. The main goal of 'structure-based drug design' is to predict the binding modes and affinities of different compounds upon interaction with the protein binding sites, and is achieved by 'docking' approach. There are a number of programs written to carry out such analysis. In general, many conformations are generated for the small molecule (substrate or ligand), either prior to docking or during the docking routine. Each conformation is positioned in the active site in a variety of orientations, the combination of conformation and orientation is known as a "pose". Further, several such poses are selected and ranked by a scoring function to determine the best overall pose and the binding energy and affinity are calculated [38, 41]. The new frontiers now lie in the physics based modelling to predict conformational changes, understand protein motions, design synthetic proteins and improve protein modeling based on the laws of physics [42].

Molecular dynamics simulations: Molecular dynamics (MD) simulations imitate the physical motions of atoms in the protein molecule present in the actual environment. The interaction of atoms is allowed to occur for a certain period of time, which helps to compute their trajectory through and around the protein molecule. Simulation gives detail information about individual motion of atoms as a

function of time. Over the period, enormous alternative approaches to classical MD simulation have been developed e.g. Monte-Carlo sampling of conformational space, simulated annealing, hybrid Quantum Mechanics/Molecular Mechanics (QM/MM), steered MD, Brownian dynamics, coarse-grained dynamics, normal vibration modes analysis, molecular docking simulations and other non-dynamic methods. These methods have brought about brilliant applications and developments in biomolecular simulation. In the past few years, few widely used MD simulation packages like NAMD, AMBER and GROMACS, have significantly improved their algorithmic sophistication and parallel performance, which can deliver up to ~10-100 ns/day/workstation/cluster [43]. MD simulations are used to study protein aggregation and model the aggregate structures based on the assessment of sequence determinants of protein aggregation. The amino acid composition impacts aggregation propensity which is highly applicable to protein evolution, protein design, and the pathogenicity due to certain amino acid substitutions. The increased hydrophobic content in a peptide would lead to increased aggregation propensity [44, 45].

1.1.5 Structure-function relationship of proteins

Understanding the relationships between protein structure and function is a primary focus in structural biology which has important consequences in biochemistry, genetics, molecular biology, bioinformatics and protein engineering. One way to study this problem is to understand how nature has re-constructed proteins for newer functions through evolutionary processes. This approach has potential to give information about important characteristics of protein structures and the definite mode in which they perform their functions. To understand the structure-function theory, vital structural information is dictated by the primary amino acid sequences and the tertiary structures. Understanding of the existing series of family folds and associated evolutionary relationships, latest research in investigation of the "protein universe" at the tertiary structural level have provided key features. Although tertiary structure database is small, the sequence databases are huge and compile the entire genome sequences of several bacteria, an archaeon and a microbial eukaryote. Using the great harmony of protein sequence and structural data, computational approaches to solve the "structure-function" problem can help to understand the associations between protein structure and function.

Besides computational approach, one of the widely used approach is to subject the native and active conformation of a protein to various physicochemical stress conditions and monitor the changes occurring in its conformation and function at each step. Generally native proteins are marginally stable i.e. free energy gap between the folded and unfolded states in typical proteins under physiological conditions is rather small (20 to 65 kJ/mol). Therefore, when the balance between the interactions involved in stabilizing or destabilizing particular structure is disturbed by harsh environment like extreme temperature, pH and chaotropes, it may lead to structural and functional alterations in protein [46]. When a protein loses its quaternary/tertiary/secondary structure, but not its primary sequence, it is considered to be denatured. Denatured proteins are generally non-functional. For some proteins, denaturation can be fully or partially reversed. Since the primary structure of the polypeptide is still intact, it may be able to re-fold into its functional form provided it is subjected to its normal condition, else denaturation is irreversible. It has long time ago been observed that some proteins can refold after denaturation even when kept alone in a test tube. Since this happens spontaneously, their amino acid sequence must contain all the information required for folding. However, not all proteins are able to fold/refold this way, how proteins normally fold in a cell seems to be complicated. Several proteins which do not fold by themselves are assisted by chaperones (chaperonins). In some cases, the structure of a protein remain stable, but the liable active site tends to lose its geometry and hence the activity. Contrary to this, the active site may get unusually stabilized and highly active. A polypeptide can even adopt a more flexible conformation different from its functional native form, due to changes in environment [18, 47-48]. Exploring structure-function relationships of proteins can help in establishing the factors responsible for their stability.

The present study uses a combination of various experimental and theoretical approaches to investigate the structural and functional transitions of two unexplored legume lectins. The following section gives details about basic information, structure and applications of lectin.

1.2 Lectins

Lectins are proteins of non immune origin with the ability to recognize and bind special sugars existing on cell surfaces [49]. Lectins are known to be ubiquitous, being present in most species like viruses, bacteria, fungi, invertebrates, vertebrates and plants. They can bind to the carbohydrate moieties on the surface of erythrocytes and agglutinate them

[50]. Due to their ability to agglutinate red blood cells they are also called as hemagglutinins.

1.2.1 Historical background

The first evidence for hemagglutinin came in 1860, when S.W. Mitchell observed the agglutination of pigeon blood by the venom of the rattlesnake [51]. Later, first study focused on the origin of hemagglutination was H. Stillmark's thesis in 1888, where the so called ricin from *Ricinus communis* was examined and named as phytohemagglutinin [52].

Earlier lectins were detected and characterized in plants, further, numerous lectins from microorganisms (*Staphylococcus aureus* and *Vibrio*) and from animals (horseshoe crab, lobster) were isolated [53]. The first viral lectin identified in early 1950's was influenza virus hemagglutinin. In 1980's first lectin from protozoan and the first fungal lectin from common mushroom *Agaricus bisporus* were isolated. Historical timeline gives a glimpse of further development in lectinology (Fig.3). Today, lectins are known to be ubiquitous, present in most species [54].

About 42 lectins are available commercially (in Sigma-Aldrich/ Vector Labs, USA) for application in analytical and clinical industry. More than 40 reviews have been published on various aspects of lectins. Though lectins are studied since 130 years, they are still an attractive topic of research for the biologists.

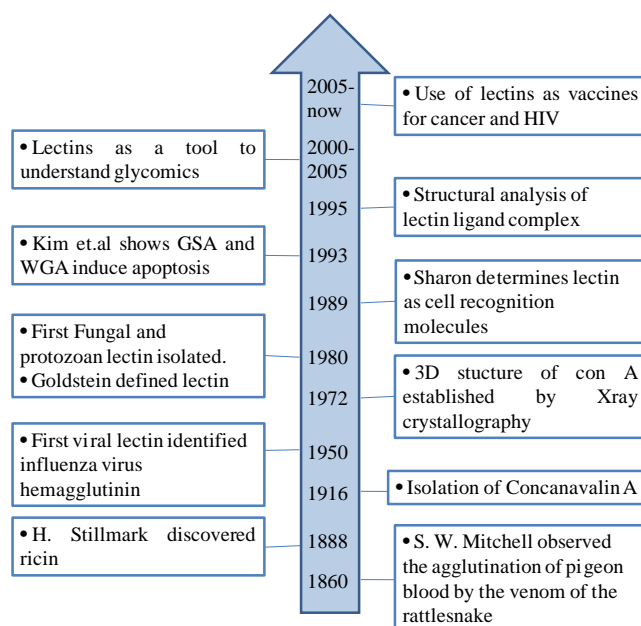


Figure 3: Timeline describing development of lectinology

(GSA: *Griffonia simplicifolia* Agglutinin WGA: Wheat Germ Agglutinin)

1.2.2 Detection

Hemagglutination using rabbit RBC's is regularly used to detect the presence of lectins in any biological source [55]. The lectin should bind to the cells and form cross-bridges between them for agglutination to occur. The erythrocytes can be used directly or after treating with trypsin, pronase or neuraminidase [56]. A technique like enzyme multiplied assay has also been used [57].

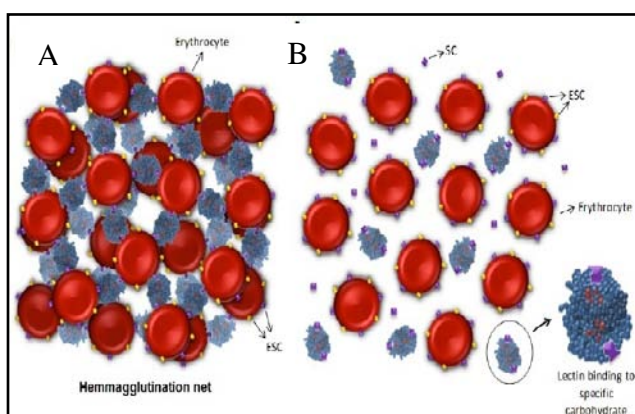


Figure 4: Scheme of hemagglutinating activity (HA) and inhibition of HA assays. A. The lectin sample induces hemagglutination due to lectin linkage to erythrocyte surface carbohydrate (ESC). **B.** HA inhibition occurs when lectin sample is incubated with

carbohydrate prior to addition of erythrocytes; binding of a specific carbohydrate (SC) to lectin sites extinguish net formation. Adapted from ref [58].

1.2.3 Occurrence and Biological Role of Lectin

1.2.3.1 Viral Lectins

Influenza virus hemagglutinin (HA) is the best studied example of viral lectins. HA binds to cell surface receptors, and it mediates release of the viral genome into the cytoplasm through membrane fusion. Sialic acid is the essential component of the influenza virus receptor to which HA binds [59]. Other viral lectins include those from foot-and-mouth disease and HIV [56].

1.2.3.2 Fungal Lectins

The first fungal lectins were isolated from fruiting bodies of mushrooms *Agaricus campestris* and *Agaricus bisporus* [60, 61]. Fungal lectins participate in formation of mycelium structures which help pathogenic fungi to penetrate into the host organism [62]. Later on, lectins were isolated from *Grifolia*, *Ganoderma*. Mushroom lectins have been studied from *Lactarius deliciosus*, *Boletus edulis*, *Laetiporus sulphureus* etc. The first fungal lectin of which the structure was solved was from *Aleuria aurantia*.

1.2.3.3 Bacterial Lectins

Bacterial lectins occur generally in the form of sub microscopic, elongated, multisubunit protein appendages and known as pili (threads) or fimbriae (hairs). They interact with glycoprotein and glycolipid receptors on host cells [63]. The two classes are: (1) Adhesins, present on the surface of the bacteria helping them in adhering to the host surface leading to colonization, and (2) Toxins, secreted in the surrounding.

1.2.3.4 Animal Lectins

The first animal lectin activity was observed in snakes. Thrombolectin from *Bothrops atrox* was the first lectin isolated in pure form in 1980 [64]. Animal lectins belong to eight structurally different families are classified into intracellular and extracellular lectins. The intracellular lectin families are calnexin family, M-type, L-type and P-type which are responsible for functioning in trafficking, sorting and targeting through secretory pathway. On the other hand, the extracellular lectin families comprise of C-type, R-type, siglecs and galectins which are secreted into the extracellular matrix or body fluids, they are involved in cell adhesion, migration, cell signalling and pathogenic interactions.

1.2.3.5 Plant Lectins

Plant lectins comprise largest group of lectins studied with respect to structural and functional aspects. First plant lectin to be reported was Ricin from castor bean plants in 1888. Majority of plant lectins have been obtained from seeds. Some of the lectins from *Sambucus*, *Allium*, *Sophora*, *Vicia* etc. are localized in vegetative and storage tissues [65]. Sumner and Howell first crystallized and then extensively studied Concanavalin A (Con A), a lectin from jack beans [66]. Structure-function studies and possible applications of lectins grew rapidly in last few years. They play role in defense against phytopathogens as well as against predators. Some lectins from plants like *Phaseolus vulgaris* (French bean), *Ricinus communis* (castor bean), *Galanthus nivalis* (snowdrop), *Triticum vulgare* (wheat) protect from herbivorous animals whereas *Hevea brasiliensis* (rubber tree), *Urtica dioica* (stinging nettle), *Solanum tuberosum* (potato) lectin have been shown to play role in protection from fungal attack [67].

1.2.4 Classification of Lectins

Earlier, plant lectins used to be classified on basis of monosaccharide specificity into five groups. Lectins specific for (i) Mannose/Glucose (Man/Glu) (ii) Galactose/N-acetyl Galactosamine (Gal/GalNAc) (iii) Glucose/N-acetyl Glucosamine (Glc/GlcNAc) (iv) Fucose and (v) N-acetyl neuraminic acid were reported [65]. After several years of extensive and advance research; based on the transcriptome and biochemical analysis, now there are twelve families of plant lectins (Table 3)

Table 3: Classification of lectin based on transcriptome and biochemical analysis
(Ref: [68] and [69])

Lectin family	Specificity	Example/s
<i>Agaricus bisporus</i> agglutinin	T-antigen	<i>Marchantia polymorpha</i> ABA
Amaranthins	T-antigen	<i>Amaranthus</i> species
Class V Chitinase	High mannose N-glycans	<i>Robinia pseudoacacia</i> chitinase-related agglutinin
Cyanovirin family	High mannose N-glycans	<i>Nostoc ellipsoforum</i>
EEA family	High mannose N-glycans	<i>Euonymus europaeus</i>
GNA family (<i>Galanthus nivalis</i>)	Mannose and High mannose N-glycans	Tulip lectin (TxLC-I), <i>G. nivalis</i> lectin
Proteins with hevein domains	Chitin	Potato lectin
Jacalins	Mannose and galactose	lectins from other <i>Artocarpus</i> species
Proteins with legume lectin domain	Galactose, GalNAc, T-antigen	<i>Canavalia ensiformis</i> , <i>Phaseolus vulgaris</i> , <i>Glycine max</i>

LysM domains	Chitin	<i>Arabidopsis thaliana</i> , <i>Pteris ryukyuensis</i>
Nictaba family	Chitin	<i>Nicotiana tobacum</i> agglutinin (Nictaba)
Ricin-B family	Galactose and GalNAc	<i>Ricinus communis</i> agglutinin

1.2.5 Lectin-Sugar Interactions

Based on the amino acid sequences of lectins studied so far, it is inferred that the saccharide binding property of the lectins resides in a polypeptide sequence, named as “Carbohydrate-recognition domain” (CRD) [70]. Fine changes in the disposition of amino acid side chains near the sugar-binding sites dictate the differential binding of sugars to lectins [71]. Recognition events impose a stringent geometry upon both the ligand and the corresponding receptor, thus conferring unique sugar-specificities upon lectins. Carbohydrates can interact with lectins *via* hydrogen bonds, metal coordination bonds and van der Waal’s and hydrophobic interactions. Water molecules often act as bridges in these interactions. These forces involved in lectin-sugar interactions have been discussed below:

1. **Hydrogen bonding:** The characteristic of the interaction of lectins and other carbohydrate-binding proteins with hydroxyl group of sugar is that the hydroxyl group (OH) acts simultaneously as a hydrogen-bond donor and acceptor [71]. Selectivity ultimately results from co-operative hydrogen bonding between the hydroxyl groups as well as amine and carboxyl groups of many carbohydrates (Fig.5A). Hydroxyl groups of sugars establish hydrogen bonds with the side chains of polar amino acids like aspartic acid, asparagines, glutamine, glutamic acid, serine and arginine, amine and carbonyl groups of backbone. The specificity towards a given sugar type is rendered to the protein by the typical stereochemical arrangement of the hydroxyl groups [72].

2. **Apolar interactions:** Clustering of three or more adjacent C-H groups due to the typical steric disposition of hydroxyl groups occurring in some sugars creates hydrophobic pockets on the sugar surface. These can establish apolar contacts with hydrophobic residues in proteins, especially the aromatic rings of tryptophan, tyrosine and phenyl alanine. The attractive forces are due to 1) entropy generating from the mutual protection of both apolar surfaces from the water and 2) the enthalpy of non-conventional

hydrogen bonds between the partially positively charged C-H groups and the quadrupole formed by the aromatic ring π -system [73]. In all the lectin-Gal complex structures, the apolar patch of the Gal β stacks against that of tryptophan or phenylalanine. This **stacking** arrangement implies that the Gal ring is parallel to the plane of the aromatic ring (Fig.5B) [74].

3. **Other interactions:** Besides above interactions, forces involved in the recognition of sachharides by their protein receptors include salt bridges between electrically charged residues of a few sugars, e.g. sialic acid, and amino acid residues with opposite charge. Other remarkable interaction involves the divalent cation coordination bridging particular sugar hydroxyls and negatively charged aspartates or glutamates. Example of this interaction is C-type family proteins which involve Ca^{2+} ions to recognize their carbohydrate ligands [72].

4. **Extended binding:** The term ‘extended site’ describes binding sites that interact specifically with more than one sugar residue to provide increased affinity, the feature also called as subsite multivalency. Lectins have increased selectivity towards a target through multiple binding by mechanism of additional binding in subsites and subunit multivalency [70]. The primary binding site is important in subsite binding for carbohydrate recognition, and secondary binding site helps in enhancing the affinity of the lectin for specific oligosaccharides. Although the legume lectins *Lathyrus ochrus* isolectin II (LOL II) and Con A are Man/Glc specific, they exhibit different oligosaccharide choices. LOL II has much higher affinity for oligosaccharides with additional α (1–6)-linked fucose residues unlike Con A. Another example is from *Artocarpus* genus where lectins from *A. integrifolia*, *A. lakoocha* and *A. hirsuta* have extended binding site for T-antigen [75]. In subunit multivalency, subunits of the same lectin contribute to binding by recognizing different chains or extensions in a branched oligosaccharide [76].

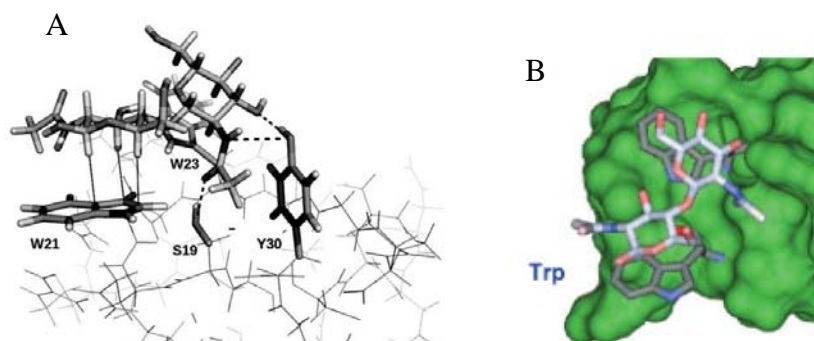


Figure 5: Protein-carbohydrate interactions governing the recognition of chitobiose by hevein **A.** Dashed lines represent hydrogen bonds established between the sugar and polar residues of the protein (S19 and Y30), solid lines indicate CH- π interactions with the W21 indole ring. **B.** Stacking interaction between chitobiose and Tryptophan.

1.2.6 Applications of Lectins

Lectins have applications either in their soluble form or immobilized derivatives. They have huge functions in biochemistry and cell biology. Lectins are also useful in medical field e.g. in detection of cell surface alteration during cancer development. Multiple lectins have applications in biological research, both as agents and tools. The applications and mechanisms of action as biological agents are briefly listed below (Table 4). Lectins have now emerged as biological tool which are used as probes in various identification and detection kits. Some of the examples of lectins as biological tools are given below (Table 5).

Table 4: Lectins as biological agents. (adapted from Dan et. al [77])

Activity	Lectins	Targets	Mechanisms
Anti-tumor	Con A (from <i>Jack beans</i>)	Hepatoma(Mice-P)	Binds with tumor cells in a mannose-specific manner and induces autophagy
	Mistletoe lectins	Pancreatic cancer (Mice-P), head and neck cancer (human-N), breast cancer (human-P)	Induce apoptosis or inhibit protein synthesis

Anti-HIV	BanLec(from banana) cyanovirin-N (from <i>Nostocellipsosporum</i>) Lectins(from leek, stinging nettle, and HHA)	HIV virus (in vitro) SARS-CoV(in vitro)	Bind to the glycosylated HIV-1 envelope protein (gp 120) and block cellular entry Interfere with the glycans on the spike during virus entry and virus release
Anti-insect	AJL (from <i>Arisaema jacquemontii blume</i>) MuBL and MuHL (respectively isolated from <i>Myracrodruon urundeuva</i> bark and heartwood, respectively)	<i>Bactrocera cucurbitae</i> larvae <i>Aedes aegypti</i>	Decreases the activity of acid phosphatase and alkaline phosphatase Increase larval mortality

Anti-fungal	Lectin from <i>Curcuma amarissima</i> Roscoe TEL (<i>Talisia esculenta</i>)	<i>Fusarium oxysporum</i> , <i>Exserohilum turanicum</i> , and <i>Colletotrichum cassiicola</i> <i>F. oxysporum</i> , <i>Colletotrichum lindemuthianum</i> , and <i>Saccharomyces cerevisiae</i>	Not explained Crosslinks chitin and prevents cell expansion at tip of the growing hyphae
Anti-bacterial	Ch-salectin (cloned from <i>Crassostrea hongkongensis</i>) HSL (<i>H. scabra</i> lectin)	<i>Escherichia coli</i> , <i>Vibrio alginolyticus</i> , <i>Bacillus thuringiensis</i> , and <i>Staphylococcus aureus</i> <i>Staphylococcus</i> sp., <i>Serratia</i> sp., <i>Proteus</i> sp., <i>Proteus</i> sp., etc.	Binds to a sialic acid containing protein fetuin and inhibits the growth of bacteria Binds to the glycoconjugate moiety on the surface of bacteria and enhances the phagocytosis rate

Table 5: Lectins as Biological tools. (adapted from Dan et. al [77])

Types of tools	Representative	Application	Companies
Lectins for histochemistry and cytochemistry	Lectin from <i>Ulex europaeus</i> -Atto 488 conjugate (19337)	For the detection of α -L-fucose by microscopy, flow cytometry and fluorescence in situ hybridization, etc.	Sigma-Aldrich
	WGA, Alexa FluorR _ 488 Conjugate (W11261)	For the detection of N-acetylglucosamine and sialic acid residues by microscopy and flowcytometry	Life Technologies
	Horseradish peroxidase (HRP)-conjugated <i>Limax flavus</i> lectin (LFA) (H-5101-1)	For the detection of sialic acid (generic term for derivatives of N-acetylneuraminic acid and N-glycolylneuraminic acid)	EY Laboratories
	DIG Glycan Differentiation Kit (11210238001)	For differentiation between complex and high-mannose chains, differentiation between α (2,3) and α (2,6) linkage of terminal sialic acids, and identification of the core disaccharide Gal β (1,3)GalNAc of O-glycans	Roche

Columns for glycoprotein isolation	Con A lectin resin (89804) Lentil Lectin-Sepharose 4B (17-0444-01)	For the isolation of glycoproteins containing alpha-linked mannose and terminal glucose residues For the purification of a number of glycoproteins and other carbohydrate containing molecules	Thermo Scientific GE Healthcare Life Science
Lectin microarrays	PlexArrayR Lectin Array Kit I (BG-L-K001) Lectin Array 40 (GA-Lectin-40)	For glycoprotein screening (label free) For glycoprotein screening (fluorescence labeling)	Plexera RayBiotech

1.2.7 Recently solved structures of lectin

In last few years, the number of lectin structures increased enormously, resulting in almost 1800 deposited structures of more than 470 different lectins (lectin 3D <http://glyco3d.cermav.cnrs.fr>). Table below gives a brief account of the recently studied (last 5 yrs) lectins from various sources which are structurally diverse with different sugar specificity (Table 6). Most of the lectins have shown promising results as anticancer/ anti-HIV activity.

Table 6: Recently released structures of lectins

Sr. No.	Lectin source/ PDB ID./ Reference	Specificity	Fold	Application/ effect
Plant				
1	Jacalin-related lectin from <i>Ananas comosus</i> stem (AcmJRL) 6FLW [78]	Mannose	β -prism	

2	<i>Oryzata</i> 5XFH [79]	High mannose-type glycans	β -prism	Insecticidal
3	<i>Canavalia bonariensis</i> seeds 5U3E [80]	Mannose/Glucose	Jelly roll motif	Antiglioma effect
4	<i>Platypodium elegans</i> seeds (PELa) 5U38 [81]	High mannose-type glycans	β -sandwich	Nociceptive effect
5	<i>Dioclea lasiocarpa lectin</i> (DLL) 5UUY [82]	Mannose/Glucose	Jelly roll motif	vasodilator effect/ Antiglioma activity
6	<i>Wisteria floribunda</i> (Japanese wisteria) 5KXB [83]	GalNAc, LacdiNAc	Jelly roll motif	Cancer glycomarker/ diagnosis
7	<i>Bauhinia forficata</i> (Orchid tree) 5T20 [84]	GalNAc/Tn-antigen	Jelly roll motif	Inhibit Melanoma cells
8	<i>Colocasia esculenta</i> (Tarin) 5T1X [85]	Mannose	β -prism II fold	Mitogenic effect
9	<i>Momordica charantia</i> (Bitter gourd) 4Z8S [86]	Galactose		insulinomimetic activity
10	<i>Centrolobium tomentosum</i> (Arariba) 5EYX [87]	Mannose/Glucose	β -sandwich	Inflammatory activity
11	<i>Vatairea macrocarpa</i> (Amargo) 4XXA [88]	GalNAc		Cancer diagnosis and prognosis
12	<i>Dioclea sclerocarpa</i> 4NOT [89]	Mannose	Jelly roll domain.	Vasorelaxant effect
13	<i>Parkia biglobosa</i> 4MQ0 [90]	Mannose	β -prism domain	Antinociceptive and anti-inflammatory effect

14	<i>Cymosema roseum</i> 4MYE	Mannose		
15	<i>Canavalia boliviana</i> (Jack beans) 4K20 [91]	Mannose	Canonical dimer α/β sandwich	anti-inflammatory effect
16	<i>Ipomoelin from sweet potato</i> 4DDN [92]	Glucose/Mannose	Canonical β -prism fold	Defense against insect
Human				
17	Galectin -2 5EWS [93]	β -galactoside/lactose	Homodimer consists of β -strands	Apoptosis/ Cell signaling
18	Intelectin-1 4WMQ [94]	Glycan epitopes on microbes (β -galpyranose)	Homooligomer (Highly twisted β -sheet)	Microbial surveillance
19	langerin CRD 13 4N34 [95]	High mannose structures		
Animal				
20	<i>Saxidomus purpuratus</i> (SPL-2) 6A7S [96]	GalNAc/GlcNAc		
21	<i>Dario rerio galectin-1-L2</i> 6E20 [97]	Galactose	Dimer consisting of β -sheet	Modulate 1HNV attachment to epithelial cells
22	<i>Crenomytilus grayanus</i> 5F8S [98]	Galactose/Globotriose	β -trefoil fold	Antifungal, antibacterial, anticancer activity
23	<i>Mytilus californianus</i> 5VBK [99]	Galactose	β -trefoil fold	Growth inhibition in microbes

24	<i>Bothrops jararacuss</i> 5F2Q			
25	Xenopus Embryonic Epidermal 4WN0 [100]	Galactofuranose	barbell-shaped dimer of trimers	Opsonin for phagocytosis
26	Carp FEL 4RUQ [101]	GlcNAc	β -propeller	Role in innate immunity/embryonic development
Fungus				
27	<i>Pholiota squarrosa</i> (PhoSL) 6A86 [102]	GlcNAc	B-prism scaffold	Biomarker/diagnosis tool for cancer
28	<i>Aspergillus fumigatus</i> (AFL) 4UOU [103]	Fucose	β -propeller	Role in pathogenicity
29	Epithelial Adhesin 1 A domain (Epa1A) from <i>Candida glabrata</i> 4AF9 [104]	Gal β 1-3 GalNAc	Antiparallel β -sandwich motif	
30	<i>Rhizoctonia solani</i> 4G9M [105]	GalNAc	β -trefoil fold	Insecticidal activity
31	<i>Coprinopsis cinerea</i> 4USP [106]	GlcNAc(Fuca1, 3) β 1,4GlcNAc	β -trefoil fold	Defense against predators
32	<i>Lyophyllum decastes</i> 4NDS [107]	α -galactosyl	Unique fold with 5 antiparallel β sheet and 2 α helices packed against each other	Defense against predators, antitumor effect
Bacteria				

33	<i>Kordia zhangzhouensis</i> 6HTN [108]	Fucose	Beta-propeller	
34	<i>Photorhabdus asymbiotica</i> (PHL) 5MXE [109]	Fucose	Beta-propeller	Role in pathogenicity
35	<i>Photorhabdus luminescens</i> 5C9L [110]	Fucose	Beta-propeller	Defense against nematodes
36	<i>Putative Fml fimbrial adhesin FmlD</i> 5LNG [111]	galactose β 1-3 N-acetylgalactosamine	β -sandwich	Role in Urinary tract infection
37	<i>Pseudomonas aeruginosa LecB</i> 5A6Q [112]	Fucosylated N-glycans	homotetramer with the four carbohydrate recognition domains (CRD)	Virulence factor required for adhesion and biofilm formation
38	<i>Pseudomonas aeruginosa LecA</i> 4CPB [113]	Divalent galactose	β -prism II fold	Virulence factor involved in lung injury, mortality, and cellular invasion
39	<i>Burkholderia oklahomensis</i> 4GK9 [114]	Man α (1-6)Man disaccharide unit	β -barrel	Anti-HIV activity
40	<i>Mycobacterium smegmatis</i> 4OIT [115]	Mannose	β -prism II fold	
41	<i>Vibrio vulnificus</i> Hemolysin/Cytolysin 4OWL [116]	N-Acetyl-D-Lactosamine Bound	β -trefoil fold	Role in Pathogenesis

42	<i>Psuedomonas fluorescens</i> 4FBO [117]	α 3, α 6- mannopentaose	β -barrel	Anti-HIV activity
43	<i>Myxococcus Xanthus</i> 4FBR [117]	α 3, α 6- mannopentaose	β -barrel	Anti-HIV activity

1.2.8 Legume lectins

The most studied group of Plant lectins include those purified from Leguminosae family [118]. Previous studies have revealed that most of the legume lectins are dimers or tetramers of approx. 30 kDa. They are characterized by legume lectin fold which remains conserved in all the lectins. This fold is also called “Jelly roll motif” which is characterized by a six stranded nearly flat ‘back’ β -sheet, a seven stranded curved ‘front’ β -sheet and several loops that connect the sheets (Fig. 6A, 6B). Though all legume lectins are related at molecular level, they show variation in carbohydrate binding/specificity. For example, the legume lectin soybean (*Glycine max*) agglutinin (SBA, SBL) binds N-acetyl D-galactosamine/galactose; Concanavalin A (*Canavalia ensiformis*) lectin (ConA) binds glucose/ mannose and gorse (*Ulex europaeus*) lectin (UEA1) binds L-fucose. Recently studied other legume lectins from Chickpea, *Bauhinia forficata*, *Sophora japonica*, *Amaranthus caudatus* bind N- acetyl D-galactosamine/galactose whereas *Dioclea lasiocarpa*, *Canavalia bonariensis*, *Dioclea sclerocarpa*, *Platypodium elegans* bind mannose/Glucose.

The seeds of leguminous plants are the richest sources of lectins [119]. Lectins, ‘natural mutants of the quaternary state’ are the excellent model systems for studies of multisubunit proteins as well as for the significance of oligomerization on their stability and structural integrity [120, 121]. There are different modes of oligomerization in legume lectins like canonical, handshake, back to back, noncanonical interface and the unusual interfaces (Fig. 6C-E) [122].

1.2.8.1 GalNAc binding *Sophora japonica* lectin

Sophora japonica (Family: Fabaceae), also known as Chinese Scholar Tree or Japanese Pagoda Tree is a leguminous plant. It has medical applications in the treatment of health disorders like uterine bleeding, haemorrhoids, chest congestion, constipation etc [123].

The plant seed lectin is a tetrameric protein with molecular mass of 120 kDa, shows maximum stability at pH 8.5 in presence of Ca^{2+} ions and specificity towards N-acetyl D-galactosamine (GalNAc) [124, 125]. Homology Model constructed by Yadav et. al showed a typical legume lectin monomer (Fig.6F). Secondary structure majorly comprises of Type III β turns. Further studies have shown that SJL has extended binding site for T-antigen [126].

1.2.8.2 Glucose/mannose binding *Dioclea lasiocarpa* lectin (PDB ID: 5UUY)

Dioclea lasiocarpa lectin (DLL) is glucose/mannose specific lectin. It is a tetrameric protein with a molecular mass of 25 kDa [82]. Structural studies revealed DLL has a Jelly roll motif. The monomers are packed in a tetramer by two canonical dimers, both stabilized by noncovalent interactions (Fig. 6G). Each chain of the tetramer has a metal-binding site and carbohydrate recognition domains of the same specificity. Docking studies have shown DLL binds more specifically to mannose. It has shown antiproliferative activity against various cancer cell lines. Further studies showed DLL is most effective on C6 glioma cells at small concentration.

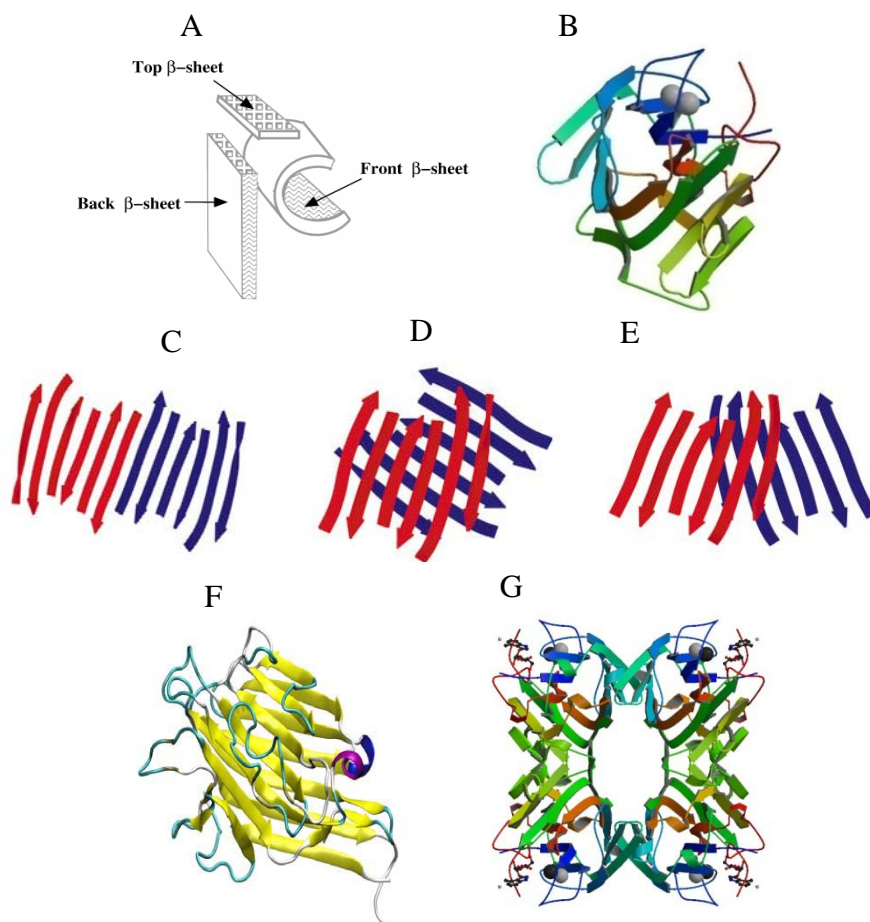


Figure 6: Typical legume lectin A. Schematic representation of a legume lectin subunit in terms of sheets **B.** Crystal Structure of the lectin from Concavalin A (PDB ID: 1DQ6) **C.** Canonical type interface in Con A, pea lectin **D.** Handshake interface of ECorL, WBA I **E.** Back-to-back interface of GS IV and PNA (1-4 and 2-3) **F.** Homology model constructed monomer of *Sophora japonica* **G.** Tetrameric crystal structure of *Dioclea lasiocarpa* lectin (DLL) (PDB ID: 5UUY).

1.3 Objective of the present thesis

The thesis work is based on the investigations of two N-acetylgalactosamine binding leguminous lectins from *Bauhinia purpurea* and *Wisteria floribunda*. Although few reports on applications and structural studies on these lectins are available, *in solution* and *in silico* functional and conformational transition investigations were limited. Functional and/or structural novelty of two GalNAc binding lectins was studied by monitoring the transitions under various denaturing and physicochemical stress conditions and checking anticancer activity of two lectins.

Biochemical characterization and sugar binding studies were carried out using hemagglutination and its inhibition assays, respectively. Biophysical studies were performed by using fluorescence and circular dichroism (CD). The microenvironment of the tryptophan residue was studied by performing solute quenching experiments. Homology model of the *Bauhinia purpurea* lectin (BPL) was constructed. Protein ligand docking (*in-silico*) and sugar binding (*in-solution*) studies of the D-galactose and its derivatives to BPL were carried out to identify the amino acid residues involved and binding energies. Molecular dynamics thermal simulations were performed for *Wisteria floribunda* lectin (WFL) to study aggregation in detail. Acid induced molten globule like species were detected in both lectins which were characterized further in detail.

Cytotoxic and antiproliferative effect of BPL and WFL on MCF7 cell lines was checked using MTT assay, LDH leakage assay, ROS assay and caspase 3 assay. Further cell cycle analysis was performed to check population of cells undergoing apoptosis.

References

1. J. Yon (2001) Protein folding: a perspective for biology, medicine and biotechnology. Braz. J. Med. Biol. Res. 34, 419-435.
2. C. Dobson (2003) The nature and significance of protein folding. Nature. 426, 884-890.

3. C. Anfinsen (1973) Principles that govern the folding of protein chains. *Science*. 181, 223-230.
4. A. Fersht (2008) From the first protein structures to our current knowledge of protein folding: delights and skepticisms. *Nat. Rev. Mol. Cell Biol.* 9, 650-654
5. S. Radford (2000) Protein folding: progress made and promises ahead. *Trends Biochem. Sci.* 25,611-618.
6. F. Hartl, and M. Hayer-Hartl (2009) Converging concepts of protein folding in vitro and in vivo, *Nature Struct. Biol.*16, 574-81.
7. S.L. Lindquist and J.W. Kelly (2011) Chemical and biological approaches for adapting proteostasis to ameliorate protein misfolding and aggregation diseases—progress and prognosis. *Cold Spring Harbor perspectives in biology.* 3(12), a004507.
8. R.A. Denny, L.K. Gavrin and E. Saiah (2013) Recent developments in targeting protein misfolding diseases. *Bioorganic and medicinal chemistry letters.* 23(7), 1935-1944.
9. F. Chiti and C. Dobson (2006) Protein misfolding, functional amyloid and human disease. *Annu. Rev. Biochem.* 75, 333-66.
10. C. Ross and M. Poirier (2004) Protein aggregation and neurodegenerative diseases. *Nat. Med.* S10- S17.
11. T. Knowles, M. Vendruscolo and C. Dobson (2014) The amyloid state and its association with protein misfolding diseases. *Nature.* 15, 384-396
12. A. Muntau and S. Gersting (2010) Phenylketonuria as a model for protein misfolding diseases and for the development of next generation orphan drugs for patients with inborn errors of metabolism. *J. Inherit. Metab. Dis.* 33, 649-658.
13. D. Eisenberg and M. Jucker (2012) The amyloid state of proteins in human diseases. *Cell.* 148, 1188-1203.
14. C.M. Gomes (2012) Protein misfolding in disease and small molecule therapies. *Current Topics in Medicinal Chemistry.* 12, 2460-2469.
15. H. Kim, S. Kim, Y. Jung, J. Han, J-H. Yun, I. Chang et al. (2016) Probing the Folding-Unfolding Transition of a Thermophilic Protein, MTH1880. *PLoS ONE.* 11(1), e0145853.
16. K.W. Plaxco and C. Dobson (1996) Time-resolved biophysical methods in the study of protein folding, *Current Opinion in Structural Biology.* 6, 630-636.

17. D.R. Canchi and A.E. García (2013) Cosolvent effects on protein stability. *Annu.Rev. Phys.Chem.* 64, 273-293.
18. A. Varshney, G. Rabbani, G. Badr and R.H. Khan (2014) Cosolvents induced unfolding and aggregation of keyhole limpet hemocyanin. *Cell Biochem. Biophys.* 69(1), 103-113.
19. S.K. Ramasamy, C.G Suresh, J.A. Brannigan, G.G. Dodson and S.M. Gaikwad (2007). Bile salt hydrolase, the member of ntn-hydrolase family: differential modes of structural and functional transitions during denaturation. *IUBMB Life.* 59(2), 118– 125.
20. S.N. Gummadi (2003) What Is the Role of Thermodynamics on Protein Stability? *Biotechnol. Bioprocess Eng.* 8, 9-18.
21. T.S.G. Olsson, M.A. Williams, W.R. Pitt, J.E. Ladbury (2008) The thermodynamics of protein–ligand interaction and solvation: Insights for ligand design, *J. Mol. Biol.* 384(4), 1002-1017.
22. B. Ahmad and R.H. Khan (2005) Protein Folding: From Hypothesis Driven to Data Mining. *Pakistan journal of biological sciences.* 8 (3), 487-492.
23. A. Bartlett and S. Radford (2009) An expanding arsenal of experimental methods yields an explosion of insights into protein folding mechanisms. *Nature Struct. Biol.* 16, 582-588.
24. C. Royer (2006) Probing protein folding and conformational transitions with fluorescence. *Chem.Rev.* 106, 1769-1784.
25. S. Kelly, T. Jess, and N. Price (2005) How to study proteins by circular dichroism. *Biochim. Biophys. Acta.* 1751, 119-139.
26. G. Balakrishnan, C.M. Weeks, A. Ibrahim and T.S. Soldatova (2008) Protein dynamics from time resolved UV Raman spectroscopy. *Curr. Opin. Struct. Biol.* 18, 623-629.
27. H. Fabian and D. Naumann (2004) Methods to study protein folding by stopped-flow FTIR. *Methods*, 34, 28-40.
28. B. Schuler and W. Eaton (2008) Protein folding studied by single-molecule FRET. *Curr. Opin. Struct Biol.* 18, 16-26.
29. E. Haustein and P. Schwille (2007) Fluorescence correlation spectroscopy: novel variations of an established technique. *Annu. Rev. Biophys. Biomol. Struct.* 36, 151-169.

30. J. Lipfert and J. Doniach (2007) Small-angle X-ray scattering from RNA, proteins, and protein complexes, *Annu. Rev. Biophys. Biomol. Struct.* 36, 307-327.
31. H. Roder, K. Maki and H. Cheng (2006) Early events in protein folding explored by rapid mixing methods. *Chem. Rev.* 106, 1836-1861.
32. H. Dyson and P. Wright (2005) Elucidation of the protein folding landscape by NMR. *Methods Enzymol.* 394, 299-321.
33. M. Krishna, L. Hoang, Y. Lin, and S. Englander (2004) Hydrogen exchange methods to study protein folding. *Methods*, 34, 51-64.
34. A. Zarrine-Afsar and A. Davidson, A. (2004) The analysis of protein folding kinetic data produced in protein engineering experiments. *Methods*, 34, 41-50.
35. C.M. Johnson (2013). Differential scanning calorimetry as a tool for protein folding and stability. *Archives of biochemistry and biophysics*, 531(1), 100-109.
36. R.J. Johnson, C.J. Savas, Z. Kartje, and G.C. Hoops (2014) Rapid and adaptable measurement of protein thermal stability by differential scanning fluorimetry: updating a common biochemical laboratory experiment. *Journal of Chemical education*, 91, 1077–1080.
37. G.A. Senisterra and P.J. Finerty Jr (2009) High throughput methods of assessing protein stability and aggregation. *Molecular Bio Systems*, 5(3), 217-223.
38. A. Breda, N. F. Valadares, O. Norberto de Souza, et al. (2006) Protein Structure, Modelling and Applications [Updated 2007 Sep 14]. In: Gruber A, Durham AM, Huynh C, et al., editors. *Bioinformatics in Tropical Disease Research: A Practical and Case-Study Approach* [Internet]. Bethesda (MD): National Center for Biotechnology Information (US); 2008. Chapter A06.
39. M. John, F. Krzysztof, K. Andriy, S. Torsten and T. Anna (2014). Critical assessment of methods of protein structure prediction (CASP)-round x. *Proteins*. 82(2), 1–6.
40. E. J. Dodson (2007) Computational biology: Protein predictions *Nature*. 450, 176-177.
41. H. Alonso, A. A. Bliznyuk and J. E. Gready (2006). Combining docking and molecular dynamic simulations in drug design. *Med. Res. Rev.* 26, 531–568.
42. K. A. Dill, S. B. Ozkan, M. S. Shell and T. R. Weik (2008). The Protein folding problem. *Annu. Rev. Biophys.* 37, 289–316.

43. S. Patodia, A. Bagaria and D. Chopra (2014) Molecular dynamics simulation of proteins: A brief overview. *J. Phys. Chem. Biophys.* 4-6.
44. R. Redler, D. Shirvanyants, O. Dagliyan, F. Ding, D. Nam Kim, P. Kota, E. Proctor, S. Ramachandran, A. Tandon and N. Dokholyan (2014) Computational approaches to understanding protein aggregation in neurodegeneration, *J. Mol. Cell Biol.* 6, 104-115.
45. R. Nelson, M. Sawaya and M. Balbirnie (2005) Structure of the cross- β spine of amyloid-like fibrils, *Nature.* 435, 773-778.
46. D. Nelson and M. Cox (2005) Chapter 4: Three dimensional structure of proteins. *Lehninger: Principles of Biochemistry (4th Ed.)* W.H. Freeman and Company, New York, 2005.
47. S. B. Rohamare, V. S. Dixit, P. K. Nareddy, D. Sivaramakrishna, M. J. Swamy and S. M. Gaikwad (2013). Polyproline fold—in imparting kinetic stability to an alkaline serine endopeptidase. *Biochim. Biophys. Acta.* 1834, 708–716.
48. S. Dalal, S. V. More, S. Shankar, R. S. Laxman and S.M. Gaikwad (2014). Subtilase from *Beauveria* sp.: conformational and functional investigation of unusual stability, *Eur. Biophys. J.* 43, 393-403.
49. Z. Zuo, H. Fan, X. Wang, W. Zhou, and L. Li (2012) Purification and characterization of a novel plant lectin from *Pinellia ternata* with antineoplastic activity. *Springer Plus*, 1-13.
50. S.K. Lam and B.T. Ng (2011) Lectins: production and practical applications. *Appl Microbiol Biotechnol.* 89, 45-55
51. S.W. Mitchell (1860) Researches upon the venom of the rattlesnake: with an investigation of the anatomy and physiology of the organs concerned. *Smithsonian Contribution to Knowledge XII.*
52. H. Stillmark (1888) Über Ricin ein giftiges Ferment aus den Samen von *Ricinus communis* L. Und einige anderen Euphorbiaceen. *Inaugural Dissertation Dorpat, Tartu.*
53. R. Hamid, A. Masood, H.I. Wani and S. Rafiq (2013) Lectins: Proteins with diverse Applications, *J. Appl. Pharm. Sci.* 3, S93-S103
54. N. Sharon (2007) Lectins: Carbohydrate-specific reagents and biological recognition molecules, *J. Biol. Chem.* 282 (5), 2753–276
55. M.M. Burger (1974) Assays for agglutination with lectins. *Methods in Enzymo.* 32, 615–621.

56. N. Sharon and H. Lis (1972) Lectins: cell-agglutinating and sugar-specific proteins. *Science*. 177, 949–959.
57. M. Ghosh, B.K. Bachhawat and A. Surolia (1979) Rapid and Sensitive Assay for Detection of nanogram Quantities of Castor-Bean (*Ricinus communis*) Lectins, *Biochem. J.* 183, 185-188.
58. A.F.S. Santos, T. H. Napoleão, R.F. Bezerra, E. V. M. M. Carvalho, M. T. S. Correia, P. M. G. Paiva, and L. C. B. B. Coelho (2013) Strategies to obtain lectins from distinct sources. *Advances in Medicine and Biology*. 63, 34-60
59. N.K. Sauter, J.E. Hanson, G.D. Glick, J.H. Brown, R.L. Crowther, S.J. Park, J.J. Skehel, and D.C. Wiley (1992) Binding of influenza virus hemagglutinin to analogs of its cell-surface receptor, sialic acid: analysis by proton nuclear magnetic resonance spectroscopy and X-ray crystallography. *Biochemistry*, 31, 9609–9621.
60. H.J. Sage and J.J. Vazquez (1967) Studies on a hemagglutinin from the mushroom *Agaricus campestris* . *J. Biol. Chem.* 242 (1), 120-125.
61. Presant and S. Kornfeld (1972) Characterization of the Cell Surface Receptor for the *Agaricus bisporus* hemagglutinin. *J. Biol. Chem.* 247(21), 6937-6945.
62. F. Khan and M.I Khan (2011) Fungal lectins: Current molecular and biochemical perspective. *Int. J. Biol. Chem.* 5(1), 1-20.
63. A. Varki, R.D. Cummings, J.D. Esko, H.H. Freeze, P. Stanley, C.R. Bertozzi, G.W. Hart, and M.E. Etzler, *Essentials of Glycobiology*. 2nd edition. Cold Spring Harbour.
64. D.C. Kilpatrick (2002) Animal lectins: a historical introduction and overview. *Biochimica et Biophysica Acta.*, 1572, 187– 197.
65. N. Sharon, H. Lis (2007) *Lectins* .2nd edition, Springer.
66. J.B. Sumner and S.F. Howell (1936) The identification of the Hemagglutinin of the Jack bean with Concanavalin A. *J. Bacteriol.* 32, 227.
67. H.J. Gabius (1997) Animal lectins. *Eur J Biochem.* 243 (3), 543–576.
68. E.J.M. Van Damme, W.J. Peumans, A. Pusztai, and S. Bardocz (1998b). *Handbook of plant lectins: properties and biomedical applications*. John Wiley & Sons, Chichester. 452.
69. H. Singh and S.P. Sarathi (2012) Insight of Lectins- A review. *International Journal of Scientific and Engineering Research*, 3(4), 1-9.

70. S. Elgavish and B. Shaanan (1997) Lectin—carbohydrate interactions: different fold, common recognition principles. *TIBS, Review, Elsevier science ltd.*,462-467
71. W.I. Weis and K. Drickamer (1996) Structural basis of lectin carbohydrate recognition. *Annu.Rev. Biochem.* 65, 441-73.
72. M. Fernández-Alonso, D. Díaz, M. Berbis, F. Marcelo, J. Cañada and J. Jiménez-Barbero (2012) Protein-carbohydrate interactions studied by NMR: from molecular recognition to drug design, *Curr. Protein Pept. Sci.* 13, 816-830.
73. J. Jiménez-Barbero, F. Cañada, J. Asensio, N. Aboitiz, P.Vidal, A. Canales, P. Groves, H.Gabius and H. Siebert (2006) Hevein domains: an attractive model to study carbohydrate-protein interactions at atomic resolution, *Adv. Carbohydr. Chem. Biochem.* 60, 303-354.
74. J.L. Asensio, F. Anaarda, J. Javier and Jimenez-Barbero (2013) Carbohydrate aromatic interactions, *Acc. Chem. Res.* 46 (4), 946–954.
75. S.M. Gaikwad and M.I. Khan (2007) Binding of T-Antigen disaccharides to *Artocarpus hirsuta* lectin and Jacalin are energetically different, *Photochem. Photobio.* 82, 1315-1318.
76. S.S Komatha, M. Kavithab, and M.J. Swamy (2006) Beyond carbohydrate binding: new directions in plant lectin research. *Org. Biomol.* 4, 973-988
77. X. Dan, W. Liu and T.B. Ng (2015) Development and Applications of Lectins as Biological tools in Biomedical Research. *Med. Res. Rev.* 1-27.
78. A. Mohamed, F. Georges, V. Julie ,H. Raphaël, M. Rachida, S. Eric, V.B. Arnaud, M. André, C. Paulette and K. Frédéric (2018) Biochemical and structural characterization of a mannose binding jacalin-related lectin with two-sugar binding sites from pineapple (*Ananas comosus*) stem, *Scientific Reports.* 11508, 8.
79. M. Nagae, S.K. Mishra, S. Hanashima, H. Tateno and Y. Yamaguchi (2017) Distinct roles for each N-glycan branch interacting with mannose-binding type Jacalin-related lectins Oryzata and Calsepa. *Glycobiology.* 27 (12),1120-1133
80. B.S. Cavada, M.T.L. Silva, V.J.S. Osterne, V.R. Pinto-Jr., A.P.M. Nascimento, I.A.V. Wolin, I.A. Heinrich, C.A.S. Nobre, C.G. Moreira, C.F. Lossio, C.R.C. Rocha, J.L. Martins, K.S. Nascimento, R.B. Leal (2018) *Canavalia bonariensis* lectin: Molecular bases of glycoconjugates interaction and antiglioma potential. *Int. J. Biol. Macromo.* 106, 369-378.
81. B.S. Cavada, D.A. Araripe, I.V. Silva, V.R. Pinto-Jr., V.J.S. Osterne, A.H.B Neco, E.P.P. Laranjeira, C.F. Lossio, J.L.A. Correia, A.F. Pires, A.M.S. Assrey

- and K.S. Nascimento (2018) Structural studies and nociceptive activity of a native lectin from *Platypodium elegans* seeds (nPELa). [Int. J. Biol. Macromo. 107, 236-246.
82. K.S. Nascimento, M.Q. Santiago, V.R. Pinto-Jr, V.J.S. Osterne, F.W.V. Martins, A.P.M. Nascimento, I.A.v. Wolin, I.A. Heinrich, M.G.Q. Martins, M.T.L. Silva, C.F. Lossio, C.r.C. Rocha, R.B. Leal, B.S. Cavada (2017) Structural analysis of *Dioclea lasiocarpa* lectin: A C6 cells apoptosis-inducing protein. Int. J. Biochem. Cell Biol. 92, 79-89
83. O. Haji-Ghassemi, M. Gilbert, J. Spence, M.J. Schur, M.J. Parker, M.L. Jenkins and S.V. Evans (2016) Molecular basis for recognition of the cancer glycomarker, LacdiNAc(GalNAc[β 1 \rightarrow 4]GlcNAc), by *Wisteria floribunda* agglutinin, J. Biol. Chem. 291, 24085–24095.
84. J. Lubkowski, S.V. Durbin, M.C. Silva, D. Farnsworth, J.C. Gildersleeve, M.L. Oliva, and A. Wlodawer (2017) Structural analysis and unique molecular recognition properties of a *Bauhinia forficata* lectin that inhibits cancer cell growth. FEBS J. 284, 429-450.
85. P.R. Pereira, J.L. Meagher, H.C. Winter, I.J. Goldstein, V.M.F. Paschoalin, J.T. Silva and J.A. Stuckey (2017) High-resolution crystal structures of *Colocasia esculenta* tarin lectin. Glycobiology. 27 (1), 50–56.
86. T. Chandran, A. Sharma and M. Vijayan (2015) Structural studies on a non-toxic homologue of type II RIPs from bitter gourd: Molecular basis of non-toxicity, conformational selection and glycan structure. J. Biosci. 40(5), 929-941
87. A.C. Almeida, V.J.S. Osterne, M.Q. Santiago, V.R. Pinto-Jr, J.C.S. Filho, C.F. Lossio, F.L.F. Nascimento, R.P.H. Almeida, C.S. Teixeira, R.B. Leal, P. Delatorre, B.A.B. Rocha, A.M.S. Assreuy, K.S. Nascimento and B.S. Cavada (2016) Structural analysis of *Centrolobium tomentosum* seed lectin with inflammatory activity, Arch. Biochem. Biophys. 596, 73-83.
88. B.L. Sousa, J.C.S. Filho, P. Kumar, M.A. Graewert, R. I. Pereira, M.S.R. Cunha, K.S. Nascimento, G.A. Bezerra, P. Delatorre, K.D. Carugo, C. S. Nagano, K. Gruber and B.S. Cavada (2016) Structural characterization of a *Vatairea macrocarpa* lectin in complex with a tumor-associated antigen: A new tool for cancer research, Int. J. Biochem. Cell Biol. 72, 27-39.
89. J.L.A. Correia, A.S.F. Nascimento, J.B. Cajazeiras, A.C.S. Gondim, R.I. Pereira, B.L. Sousa, A.L.C. Silva, W. Garcia, E.H. Teixeira, K.S. Nascimento, B.A.M.

- Rocha, C.S. Nagano, A.H. Sampaio and B.S. Cavada (2011) Molecular Characterization and Tandem Mass Spectrometry of the Lectin Extracted from the Seeds of *Dioclea sclerocarpa* Ducke. *Molecules*. 16, 9077-9089.
90. A.U. Bari, M.Q. Santiago, V.J.S. Osterne, V.R. Pinto-Junior, L.P. Pereira, J.C.S. Filho, H. Debray, B.A.M. Rocha, P. Delatorre, C.S. Teixeira, C.C. Neto, A.M.S. Assreuy, K.S. Nascimento and B.S. Cavada (2016) Lectins from *Parkia biglobosa* and *Parkia platycephala*: A comparative study of structure and biological effects. *Int. J. Biol. Macromo.* 92,194-201.
91. G.A. Bezerra, R. Viertlmayr, T.R. Moura, P. Delatorre, B.A.M Rocha , K.S. Nascimento, J. G. Figueiredo, I.G.A. Bezerra, C.S. Teixeira, R.C. Simões, C.S. Nagano, N.M.N. Alencar, K. Gruber and B.S. Cavada (2014) Structural Studies of an Anti-Inflammatory Lectin from *Canavalia boliviana* Seeds in Complex with Dimannosides. *PLoS ONE*. 9(5), e97015. doi:10.1371/journal.pone.0097015,
92. Y.C. Chen, H.S. Chang, H.M. Lai, and S.T. Jeng (2005) Characterization of the wound inducible protein ipomoelin from sweet potato. *Plant Cell Environ*, 28, 251–259.
93. Si. Yunlong, S. Feng, J. Gao, Y. Wang, Z. Zhang, Y. Meng, Y. Zhou, G. Tai and J. Su (2016) Human galectin-2 interacts with carbohydrates and peptides non-classically: new insight from X-ray crystallography and hemagglutination, *Acta Biochim. Biophys. Sin.* 939–947.
94. D.A. Wesener, K. Wangkanont, R. McBride, X. Song, M.B. Kraft, H.L. Hodges, L.C. Zarling, R.A. Splain, D.F. Smith, R.D. Cummings, J.C. Paulson, K.T. Forest and L.L. Kiessling (2015) Recognition of microbial glycans by human intelectin-1. *Nat Struct Mol Biol.* 22(8), 603-10.
95. H. Feinberg, T.J. Rowntree, S.L. Tan, K. Drickamer, W.I. Weis, M.E. Taylor (2013) Common polymorphisms in human langerin change specificity for glycan ligands. *J Biol Chem.* 288(52), 36762-71.
96. H. Unno, S. Itakura, S. Higuchi, S. Goda, K. Yamaguchi and T. Hatakeyama (2019) Novel Ca²⁺ independent carbohydrate recognition of the C-type lectins, SPL-1 and SPL-2, from the bivalve *Saxidomus purpuratus*. *Protein Science.* 28, 766-778.
97. A. Ghosh, A. Banerjee, L.M. Amzel, G.R. Vasta, M.A. Bianchet, Structure of the zebrafish galectin-1-L2 and model of its interaction with the infectious

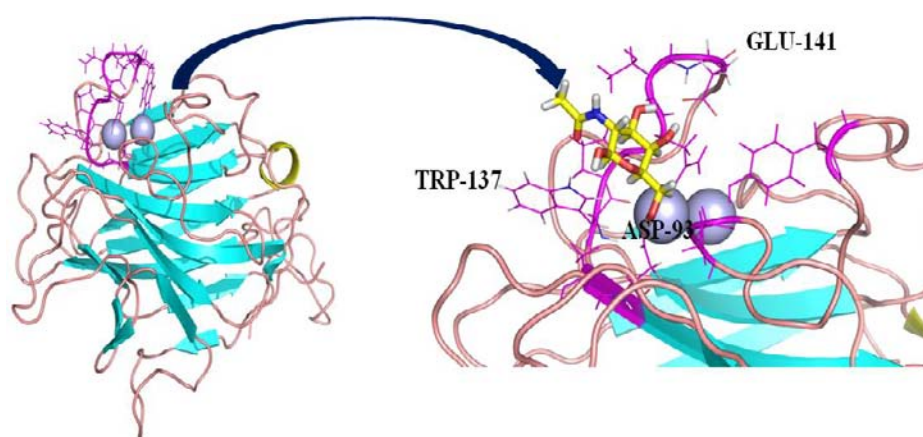
- hematopoietic necrosis virus (IHNV) envelope glycoprotein. *Glycobiology*. 29 (5) 419–430.
98. M. Jakob, J. Lubkowski, B.R. O'Keefe and A. Wlodawera (2015) Structure of a lectin from the sea mussel *Crenomytilus grayanus* (CGL), *Acta Cryst. F71*, 1429–1436
99. E.G. Maldonado, P.C. Sánchez and A.H. Santoyo (2017) Molecular and functional characterization of a glycosylated Galactose-Binding lectin from *Mytilus californianus*. *Fish Shellfish Immunol.* 66, 564-574.
100. K. Wangkanont, D.A. Wesener, J.A. Vidani, L.L. Kiessling, and K.T. Forest (2016) Structures of *Xenopus* embryonic epidermal Lectin reveal a conserved mechanism of microbial Glycan Recognition *J. Biol. Chem.* 291, 5596-5610.
101. S. Capaldi, B. Faggion, M.E. Carrizo, L. Destefanis, M.C. Gonzalez, M. Perduca, M. Bovi, M. Galliano and H.L. Monaco (2015). Three-dimensional structure and ligand-binding site of carp fiselectin (FEL). *Acta Cryst. D71*, 1123-1135.
102. K. Yamasaki, T. Kubota, T. Yamasaki, I. Nagashima, H. Shimizu, R. Terada, H. Nishigami, J. Kang, M. Tateno and H. Tateno (2019) Structural basis for specific recognition of core fucosylation in N-glycans by *Pholiota squarrosa* lectin (PhoSL), *Glycobiology*, 29 (7) ,576–587.
103. J. Houser, J. Komarek, G. Cioci, A. Varrot, A. Imberty, M. Wimmerova. (2015). Structural insights into *Aspergillus fumigatus* lectin specificity: AFL binding sites are functionally non-equivalent. *Acta Cryst. D71*, 442-453.
104. M. Maestre-Reyna, R. Diderrich, M.S. Veelders, G. Eulenburg, V. Kalugin, S. Brückner, P. Keller, S. Rupp, H.U. Mösch and L.O. Essen (2012). Structural basis for promiscuity and specificity during *Candida glabrata* invasion of host epithelia. *Proc Natl Acad Sci U S A.* 109(42), 16864-9.
105. V.T. Skamnaki, W.J. Peumans, A.L. Kantsadi, M.A. Cubeta, K. Plas, S. Pakala, S.E. Zographos, G. Smaghe, W.C. Nierman, E.J. Damme and D.D. Leonidas (2013), Structural analysis of the *Rhizoctonia solani* agglutinin reveals a domain swapping dimeric assembly. *FEBS J.* 280, 1750-1763.
106. S.B. Martinez, K. Stutz, R. Sieber, M. Collot, J.M. Mallet, M. Hengartner, M. Schubert, A. Varrot and M. Künzler (2017) Dimerization of the fungal defense lectin CCL2 is essential for its toxicity against nematodes, *Glycobiology*. 27 (5), 486–500.

107. A.V. Eerde, E. M. Grahn, H. C Winter, I. J Goldstein, U. Krengel (2015) Atomic-resolution structure of the α -galactosyl binding *Lyophyllum decastes* lectin reveals a new protein family found in both fungi and plants. *Glycobiology*. 25 (5), 492–501.
- 108.F. Bonnardel, A. Kumar, M. Wimmerova, M. Lahmann, S. Perez, A. Varrot, F. Lisacek and A. Imberty (2019) Architecture and Evolution of Blade Assembly in β -propeller lectins, *Structure*, 27(5), 764-775.
109. G. Jančaříková, J. Houser, P. Dobeš, G. Demo, P. Hyršl and M. Wimmerová (2017) Characterization of novel bangle lectin from *Photorhabdus asymbiotica* with dual sugar-binding specificity and its effect on host immunity. *PLoS Pathog.* 13(8), e1006564.
- 110.A. Kumar, P. Sýkorová, G. Demo, P. Dobeš, P. Hyršl, and M. Wimmerová (2016) A Novel Fucose-binding Lectin from *Photorhabdus luminescens* (PLL) with an Unusual Heptabladed β -Propeller Tetrameric Structure *J. Biol. Chem.* 291, 25032-25049.
- 111.M.S. Conover, R.S Taganna, J. Kalas V, De Greve H, J.S. Pinkner, K.W. Dodson H. Remaut and S.J. Hultgren (2016) Inflammation-Induced adhesin-receptor interaction provides a fitness advantage to uropathogenic *E.coli* during chronic infection. *Cell Host Microbe*. 20(4), 482-492.
112. R. Sommer, S. Wagner, A. Varrot, C. M. Nycholat, A. Khaledi, S. H^aussler, J.C. Paulson, A. Imbertyc and A. Titz (2016) The virulence factor LecB varies in clinical isolates: consequences for ligand binding and drug discovery. *Chem. Sci.*, 7, 4990-5001.
113. A. Novoa, T. Eierhoff, J. Topin, A. Varrot, S. Barluenga, A. Imberty, W. Römer and N. Winssinger (2014) A LecA Ligand Identified from a Galactoside-Conjugate Array Inhibits Host Cell Invasion by *Pseudomonas aeruginosa*. *Angew. Chem. Int. Ed.*, 53, 8885-8889.
114. M.J. Whitley, W. Furey, S. Kollipara and A.M. Gronenborn (2013) Burkholderia agglutinin is a canonical two domain OAA-family lectin: structures, carbohydrate binding, and anti-HIV activity. *FEBS J.* 280(9), 2056–2067.
115. D. Patra, P. Mishra, A. Surolia and M. Vijayan (2014) Structure, interactions and evolutionary implications of a domain-swapped lectin dimer from *Mycobacterium smegmatis*, *Glycobiology*. 956–965.

116. K. Kaus, J.W. Lary, J.L. Cole and R. Olson (2014) Glycan specificity of the *Vibrio vulnificus* hemolysin lectin outlines evolutionary history of membrane targeting by a toxin family. *J Mol Biol.* 426(15), 2800-12.
117. L.M. Koharudin, S. Kollipara, C. Aiken and A.M. Gronenborn (2012) Structural insights into the anti-HIV activity of the *Oscillatoria agardhii* agglutinin homolog lectin family. *J Biol Chem.* 287(40), 3796-811.
118. H.C. Silva, Pinto L. da S. Teixeira, K.S. Nascimentoa, B.S. Cavada and A.L.C. Silva (2014) BUL: A novel lectin from *Bauhinia unguolata* L. seeds with fungistatic and antiproliferative activities. *Process Biochem.* 49, 203–209
119. M. Etzler (1998) From structure to activity: New insights into the functions of legume lectins. *Trends Glycosci. Glycotech.* 10, 247-55.
120. L. Remy, T. Hamelryck, J. Bouckaert and W. Lode (1998) Legume lectin structure. *Biochimica et Biophysica Act.*, 1383, 9-36.
121. V. Srinivas, B. Reddy, N. Ahmad, C. Swaminathan and A. Surolia (2001) Legume lectin family, the 'natural mutants of the quaternary state', provide insights into the relationship between protein stability and oligomerization. *Biochimica et Biophysica Acta.* 1527, 102-111.
122. K. Brinda, N. Mitra, A. Surolia and S. Vishveshwara (2004) Determinants of quaternary association in legume lectins, *Prot. Sci.* 13, 1735-1749.
123. J. Kim, H. Yun-Choi (2008) Anti-platelet effects of flavonoids and flavonoid glycosides from *Sophora japonica*, *Arch. Pharm. Res.* 31, 886-890.
124. R. Poretz, H. Riss, J. Timberlake and S. Chien, (1974) Purification and properties of the hemagglutinin from *Sophora japonica* seeds, *Biochemistry.* 13, 250-256.
125. A. McPherson, C. Hankis and L. Shannon (1987) Preliminary X-ray diffraction analysis of crystalline lectins from the seeds and leaves of *Sophora japonica*, *J. Biol. Chem.* 262, 1791-1794.
126. P. Yadav, G. Shahane, S. Ramasamy and D. Sengupta (2016) Structural – functional insights and studies on saccharide binding of *Sophora japonica* seed lectin, *Int. J. Biol. Macromol.* 91, 75–84.

Chapter 2

Sugar binding studies of BPL and WFL



Archives of Biochemistry and Biophysics 662 (2019) 134–142



Contents lists available at ScienceDirect

Archives of Biochemistry and Biophysics

journal homepage: www.elsevier.com/locate/yabbi



Investigation of structural and saccharide binding transitions of *Bauhinia purpurea* and *Wisteria floribunda* lectins[☆]



Sanskruithi B. Agrawal^{a,b}, Deepanjan Ghosh^{a,b}, Sushama M. Gaikwad^{b,*}

^aAcademy of Scientific and Innovative Research (AcSIR), India

^bCSIR National Chemical Laboratory, Dr Homi Bhabha Road, Pune, 411008, India

ARTICLE INFO

Keywords:
Lectin
Saccharide binding
Homology model
Conformation
Thermal aggregation
Molten globule

ABSTRACT

Two novel medicinally important legume lectins from *Bauhinia purpurea* (BPL) and *Wisteria floribunda* (WFL) possessing extended sugar binding site were investigated for functional and conformational transitions using biochemical and biophysical techniques as well as bioinformatical tools. Homology model of BPL was constructed using the Schrodinger suite and docked with N-acetyl galactosamine and T-antigen disaccharide (Gal β 1-3GalNAcO-Me). The longer loop D in the structure of WFL compared to that in BPL was found to be responsible for its specificity to LactiNac (β -D-GalNAc-[1 \rightarrow 4]-DGlcNAc) over Gal β 1-3GalNAc. BPL remained functionally stable up to 40 °C whereas WFL remained stable upto 70 °C indicating the strength of the sugar binding site

Abstract

Sugar binding studies of two novel medicinally important legume lectins from *Bauhinia purpurea* (BPL) and *Wisteria floribunda* (WFL) were carried out. The homology model of BPL was constructed to predict the three dimensional structure, locate the tryptophan residues and evaluate the environment therein. The three dimensional structure of BPL monomer with bound metal ions Ca^{2+} represented the typical legume lectin fold presenting the jelly roll motif. Model thus constructed was docked with sugars (GalNAc and T-antigen) to find out amino acid residues involved in sugar binding and their binding energies. The hydrogen bonds and hydrophobic interactions taking place between BPL and these sugars were studied and diagrams of ligand interactions were generated. The docked pose of T-antigen (-8.313) showed two fold increase in docking score compared to GalNAc (-4.008). The binding constants k_a of BPL for GalNAc and T-antigen disaccharide (Gal β 1-3GalNAc α O-Me) as determined by intrinsic fluorescence spectroscopy (*in solution* studies) were $5.0 \times 10^3 \text{ M}^{-1}$ and $1 \times 10^4 \text{ M}^{-1}$, respectively. Thus, binding affinities determined by *in silico* and *in solution* studies correlate well. Sequence and structural alignments of BPL and WFL showed longer loop D in WFL making it more specific to LacdiNAc over GalNAc/Gal β 1–3 GalNAc.

2.1 Introduction

Being the specific sugar /oligosaccharide binding proteins, lectins are widely used to study role of cell surface carbohydrates, to isolate and characterize glycoconjugates and to detect sugar moieties on normal and tumor cell surfaces [1-4]. Cellular glycan binding property which confers antitumor property to lectins has drawn increasing attention of cancer biologists [1]. The broad range binding site architecture of lectins from minor/shallow grooves to deeper pockets provide extended binding site to sugars. The hydrogen bonds, hydroxyl groups and aromatic side chain stacking interactions contribute majorly to sugar binding [2]. Non-covalent interactions of lectins with sugars are highly specific and reversible [4]. They can also bind to free-floating glycans including monosaccharides. This glycan architecture is changed in transformed cells which can be detected by lectins. Hence, study of sugar binding to lectins is important [3, 4].

The two lectins selected for the present studies are from *Bauhinia purpurea* and *Wisteria floribunda* (Family: Fabaceae), leguminous plants commonly called as Camel foot's tree or Butterfly tree and Japanese wisteria, respectively. *Bauhinia purpurea* is used as antidiarrheal, astringent and as a poison antidote [5]. *Bauhinia purpurea* lectin (BPL)

binds to T-antigen and has also showed elevated binding in metastatic urine [6-7]. *Wisteria floribunda* lectin (WFL) binds N-glycans terminating in β -linked N-acetylgalactosaminides especially ones with LacdiNAc (β -D-GalNAc-[1 \rightarrow 4]-DGlcNAc) termini, and to terminal galactose residues with lower affinity [8-10]. LacdiNAc is a cancer glycomarker associated with leukemia, prostate, pancreatic, ovarian, and liver cancers [9]. WFL is currently considered as the most prominent diagnostic lectin against cholangiocarcinoma. It is a malignant tumor arising from the epithelial lining of the intrahepatic biliary tract. With the help of lectin microarray profiling, Matsuda et. al have shown that WFL can differentiate between normal and carcinoma cells [11]. Thus, both the lectins have high medicinal value.

The seed lectins from the plants *Bauhinia purpurea* and *Wisteria floribunda* are tetrameric proteins with molecular mass of 197 kDa and 116 kDa, respectively, show maximum stability at pH 8.0 and specificity towards N-acetyl D-galactosamine (GalNAc) [8, 12]. Molecular cloning of the *Bauhinia purpurea* lectin has been reported earlier [6], whereas cloning and crystal structure of *Wisteria floribunda* lectin has been recently reported [9, 13]. The lectins show 43% sequence identity to each other.

The present chapter deals with *in solution* and *in silico* studies of sugar binding studies of *Bauhinia purpurea* and *Wisteria floribunda* lectin. Hemagglutination assay which is a routine method for detection of lectins was performed. Hemagglutination inhibition assay was done to check sugar binding specificity. Fluorescence titration studies were performed to determine sugar binding affinity of BPL to different sugars. SPR based sugar binding studies for WFL have been already reported where KD for GalNAc α -pNP was 92.4 μ M, for LacdiNAc β -pNP 5.45 μ M, and for Gal β -pNP, 0.47 mM indicating high affinity for the respective saccharides [9].

Homology modelling, molecular docking studies of BPL and detailed investigation of differential sugar binding to both the lectins BPL and WFL were performed. *In silico* study provided information about three dimensional structures of protein, different secondary structural elements and geometry of sugar binding sight. Computational tools were used for construction, validation of model and to perform docking studies.

2.2 Materials and Methods

2.2.1 Materials

Bauhinia purpurea and *Wisteria floribunda* lectins were procured from Vector Labs, USA. Galactose and its derivatives like N-acetyl D-galactosamine, methyl α D-galactopyranoside, methyl β D-galactopyranoside, 6-O methyl D-galactopyranose, lactose, melibiose, gal β 1-3 GalNAC β 1-OMe and other sugars like glucose were obtained from Sigma-Aldrich. All other chemicals used were of analytical grade. Buffers were prepared in Milli Q water. Rabbit blood for the hemagglutination assay was procured from animal house of the National Institute of Virology, Pune, India.

2.2.2 Protein preparation

BPL was dissolved in Tris HCl pH 8.5 (10 mM) buffered saline (150 mM) with CaCl_2 (1 mM) and was stored at 4°C until further use. Buffer was filtered through 2 μm filter membrane before use.

2.2.3 Protein Estimation

Protein concentration was determined based on absorbance of solution at 280 and molar extinction coefficient (ϵ). ($\epsilon_{280 \text{ nm}} 0.1\%$ for BPL 1.75, for WFL 0.89).

2.2.4 Sodium dodecyl sulfate-polyacrylamide gel electrophoresis (8% SDS-PAGE)

Electrophoresis was carried out according to Laemmli's protocol [14] with minor modifications. BPL sample (15 μg) was run on 8% SDS Gel.

2.2.5 Matrix assisted laser desorption ionization -Time of flight (MALDI-TOF)

The molecular mass of BPL was also determined by MALDI-TOF mass spectrometry using a Voyager DE-STR (Applied Biosystems) equipped with a 337 nm nitrogen laser. 5 μl of the BPL (1 mg/ml) was mixed with 30 μl of sinapinic acid and spotted on MALDI target plate and analyzed.

2.2.6 Erythrocyte preparation

Rabbit erythrocytes were washed with PBS (Phosphate buffered saline, 20 mM potassium phosphate buffer, pH 7.2, containing 150 mM NaCl) and a 3% (v/v) suspension of erythrocyte was prepared in the same buffer.

2.2.7 Hemagglutination assay

Hemagglutination assay was performed in tris buffer saline (pH 8.0 with Ca^{2+}) using standard 96 well microtitre plates by the two-fold serial dilution method. A 50 μl aliquot of the erythrocytes suspension was mixed with 50 μl of serially diluted lectin and agglutination was examined visually after incubation for one hour. A unit of hemagglutination activity (U) is expressed as the reciprocal of the highest dilution (titre) of the lectin that showed complete agglutination. The specific activity of the lectin is defined as the number of hemagglutination units/mg of the protein. To study the effect of metal ions, the lectin was treated with CaCl_2 , MgCl_2 , MnSO_4 (effective concentration of 1mM) and also with EDTA (1 mM) and hemagglutination assay was performed.

2.2.8 Hemagglutination inhibition assays

Hemagglutination inhibition assays were performed as described above except that serially diluted sugar solutions (25 μl from 0.5 M stock) were pre-incubated for 15 min at room temperature with 25 μl of the lectin. Erythrocyte suspension (50 μl) was then added, mixed and the plates were examined visually after one hour.

2.2.9 Fluorescence based titration studies of sugar binding

For titration experiment, stock solution of 5 mM T-antigen α O-Me and 5 mM GalNAC were used. Sugars were added in 3–10 μl aliquots to BPL solution (70 $\mu\text{g/ml}$). After mixing the solution well, the samples were excited at 295 nm and the emission was recorded from 310 to 400 nm on a Perkin Elmer LS-50B spectrofluorimeter. Slit widths of 7 nm each were set for excitation and emission monochromators and the spectra were recorded at 100 nm/min. The baseline was corrected by subtracting the signal produced by buffer solution. The fluorescence intensity at 338 nm (λ_{max} of the lectin) was considered for further analysis. Corrections were also made to compensate the dilution effect upon addition of ligand to the lectin. The association constants (k_a) were calculated according to the equation described by Chipman et al. [15]. The abscissa intercept of the plot of $\log [C]$ against $\log \{ (\Delta F) / (F_c - F_\infty) \}$, where $[C]$ is the free ligand concentration, yielded k_a value for lectin-ligand interaction according to the relationship:

$$\log [F_o - F_c / F_c - F_\infty] = \log k_a + \log [C] \quad (1)$$

where F_c is the fluorescence intensity of the lectin at any point during the titration, F_∞ is the fluorescence intensity at saturation binding, $[C]$ is the free ligand concentration.

2.2.9 Homology model construction and validation of BPL

The homology model of BPL was generated using Schrodinger version 15.3. Model was further refined through energy minimization using prime suit of Schrodinger. The model was checked for quality on PDB sum and validated by Ramchandran plot [16]. The RMSD between model and template was calculated by the Carbon alpha fitting method from PyMOL 1.8.x (www.pymol.org) program.

2.2.10 Docking studies of BPL

The structures of all the ligands used in the present study were obtained from ZINC database (<http://zinc.docking.org>) and refined using LigPrep 3.7 suit of Schrödinger. Similarly, using Protein preparation utility, hydrogen atoms were added to the BPL model and restrained minimization was carried out. The processed receptor and ligand structures were docked using Glide 6.9. The binding site was defined as a grid box of innerbox dimension 10*10*10 Å. Receptor grid generation was followed by ligand docking where the ligand was docked flexibly using extra precision mode in Glide. Free energy of binding was roughly estimated using an empirical scoring function called GlideXP Score, which includes electrostatic, van der Waals interaction and other terms for rewarding or penalizing interactions that are known to influence ligand binding. Based on Glide score, the best docked complex was selected and was visualized with PyMOL 1.8.x.

2.3 Result and Discussion

In solution studies of sugar binding to BPL

2.3.1 SDS PAGE and MALDI-TOF analysis of protein

BPL has molecular mass of 197 kDa and is a homotetrameric protein (monomer of 34 kDa) with 290 amino acids. *Bahuinia purpurea* lectin showed a single band in SDS-PAGE with molecular mass of approximately 34 kDa and showed a single major peak of 32,000 Da in MALDI.

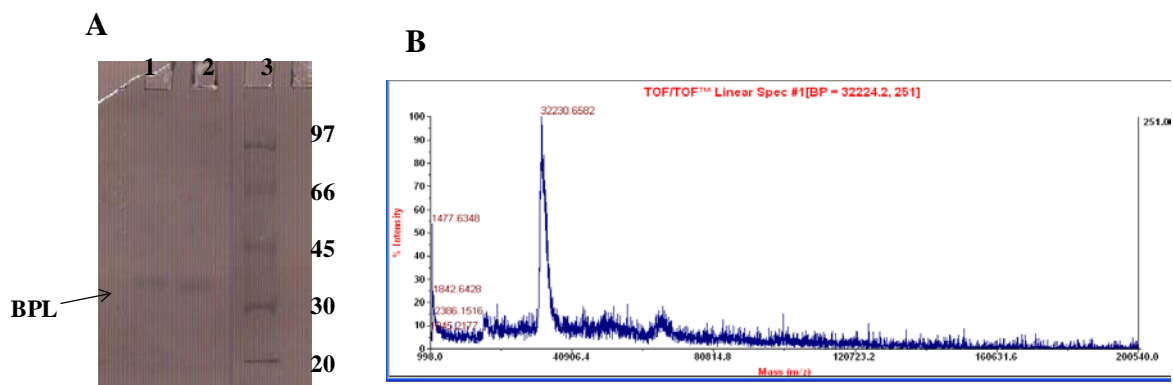


Figure 1: **A.** SDS-PAGE analysis of BPL showed a single band. **B.** 32 kDa sharp peak was observed in MALDI analysis.

2.3.2 Hemagglutination and hemagglutination inhibition assay

Functional studies of BPL were carried out using hemagglutination assay in tris buffer saline (pH 8.0) with Ca^{2+} . The hemagglutination titre was obtained to be 1280 U/ mg of protein. The activity remained stable in presence of Ca^{2+} (Table 1) as compared to other metal ions (Mg^{2+} , Mn^{2+} and EDTA).

Simple sugars like glucose and mannose did not show inhibition of the hemagglutinating activity of the lectin. Hemagglutination was inhibited by galactose and its derivatives like D-galactosamine, N-acetyl D-galactosamine, methyl α -D-galactopyranoside, methyl β - D-galactopyranoside, 6-O methyl D-galactopyranose, lactose, melibiose, gal β 1-3 GalNAC β 1-OMe (Table 2). The minimum inhibitory concentration for galactose and N-acetyl galactosamine were found to be 120 μM and 24.3 μM , respectively. T-antigen (Gal β 1-3 GalNAC β 1-OMe) showed high affinity to BPL with 1 μM inhibitory concentration.

Table 1: Effect of Metal ions on *Bahunia purpurea* lectin hemagglutination activity

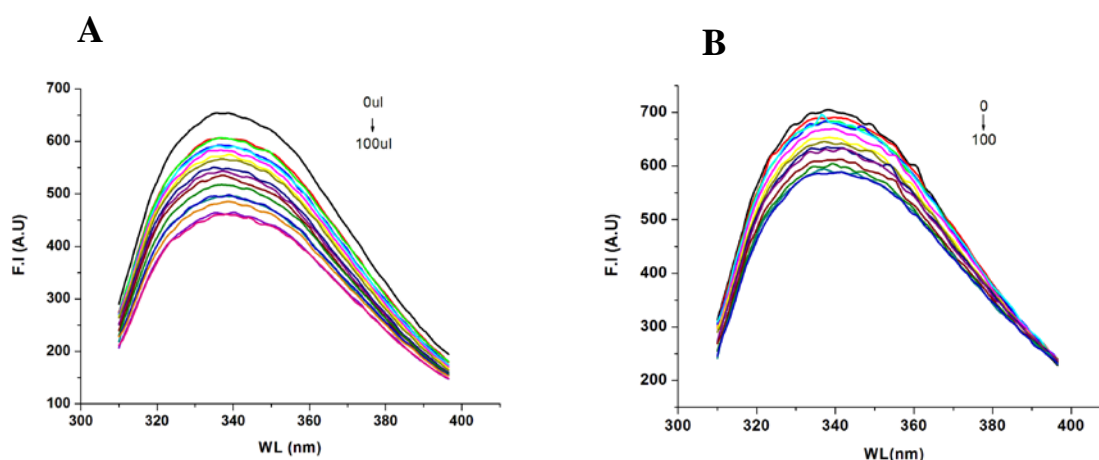
Lectin + Metal ion/s (1 mM)	Residual hemagglutination activity(%)
Mn^{2+}	50
Mg^{2+}	50
Ca^{2+}	100
Control	100
EDTA	50

Table 2: Hemagglutination activity inhibition by *Bahuinia purpurea* lectin in presence of sugars.

Sugar	Minimum inhibitory concentration (μM)
Glucose	ND
Mannose	ND
Galactose	120
N-acetyl galactosamine	24.3
Methyl α - D galactopyranoside	1170
Methyl β - D galactopyranoside	293
6-O Methyl D galactopyranose	390
Lactose	195
Melibiose	98
Gal β 1-3 GalNAC β 1-OMe	1

ND: Not detected**2.3.3 Fluorescence based titration studies of sugar binding**

The titrations of BPL with GalNAc and T-antigen leading to fluorescence quenching were performed (Fig 2A, 2B). The value of F_{∞} was derived from the graph by plotting $F_0/\Delta F$ vs $1/C$ as shown in Figure 2C and 2D. The plot of $\log [\Delta F / (F_c - F_{\infty})]$, versus $\log [C]$ was used to calculate the binding constant k_a and the values were, $5.0 \times 10^3 \text{ M}^{-1}$ and $1 \times 10^4 \text{ M}^{-1}$, respectively (Fig 2E, 2F).



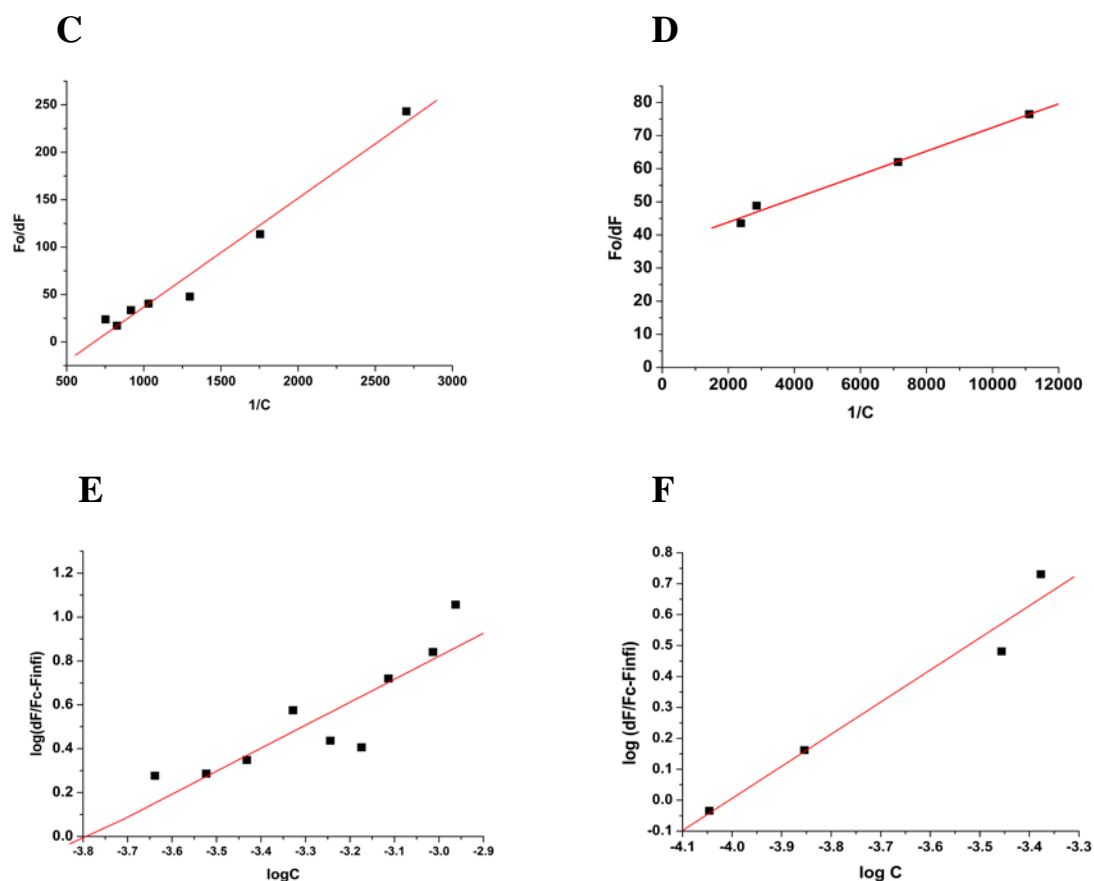


Figure 2: Sugar binding studies of BPL; The fluorescence change during titration of **A.** GalNAc **B.** T-antigen. **C and D** (F_{∞}) is obtained from Y-intercept of plot $F_0/\Delta F$ versus $1/C$. **E and F.** A double log plot of $\log(\Delta F/F_c - F_{\infty})$ versus $\log C$. The X-intercept of plot gives k_a value for interaction between BPL and GalNAc/T-antigen, respectively.

***In silico* studies of sugar binding**

The Homology model of *Bauhinia purpurea* lectin (BPL) was constructed to predict the three dimensional structure, locate the tryptophan residues and evaluate the environment therein. Model thus constructed was docked with sugars (GalNAc and T-antigen) to find out amino acid residues involved in sugar binding and their binding energies. The available structure of *Wisteria floribunda* lectin WFL (PDB ID: 5KXB) was aligned with modeled BPL to locate molecular and structural basis of difference in sugar binding.

2.3.4. Model construction and validation

Bauhinia purpurea seed lectin (BPL) sequence BLAST analysis exhibited 78% identity with *Bauhinia forficata* (PDB ID: 5T55) seed lectin sequence. Hence, homology model for BPL was built using the crystal structure of 5T55 with the help of the Schrodinger

suite. The 3D structure of BPL monomer with bound Ca^{2+} metal ions displayed the typical legume lectin fold representing the jelly roll motif consisting of a six stranded nearly flat 'back' β -sheet, a seven stranded curved 'front' β -sheet and several loops that connect the sheets (Fig.3A) [17]. PDB sum analysis showed 3.8 % helix, 37.4 % sheets and 58.8 % turns and unordered structure (Fig.3B) [16]. Model validation with Ramachandran plot from PROCHECK showed 76.2 % residues in the most favored regions; 21.6 % in allowed regions and 0.4 % in the disallowed region, acceptable G Factor -0.44 . RMSD of constructed model when superimposed to template was 0.735 (Fig.3C). The ProSA analysis of the model showed a Z-score of -6.32 which was comparable to that of the template confirming the reliability of the constructed model of BPL (Fig.3D) [18].

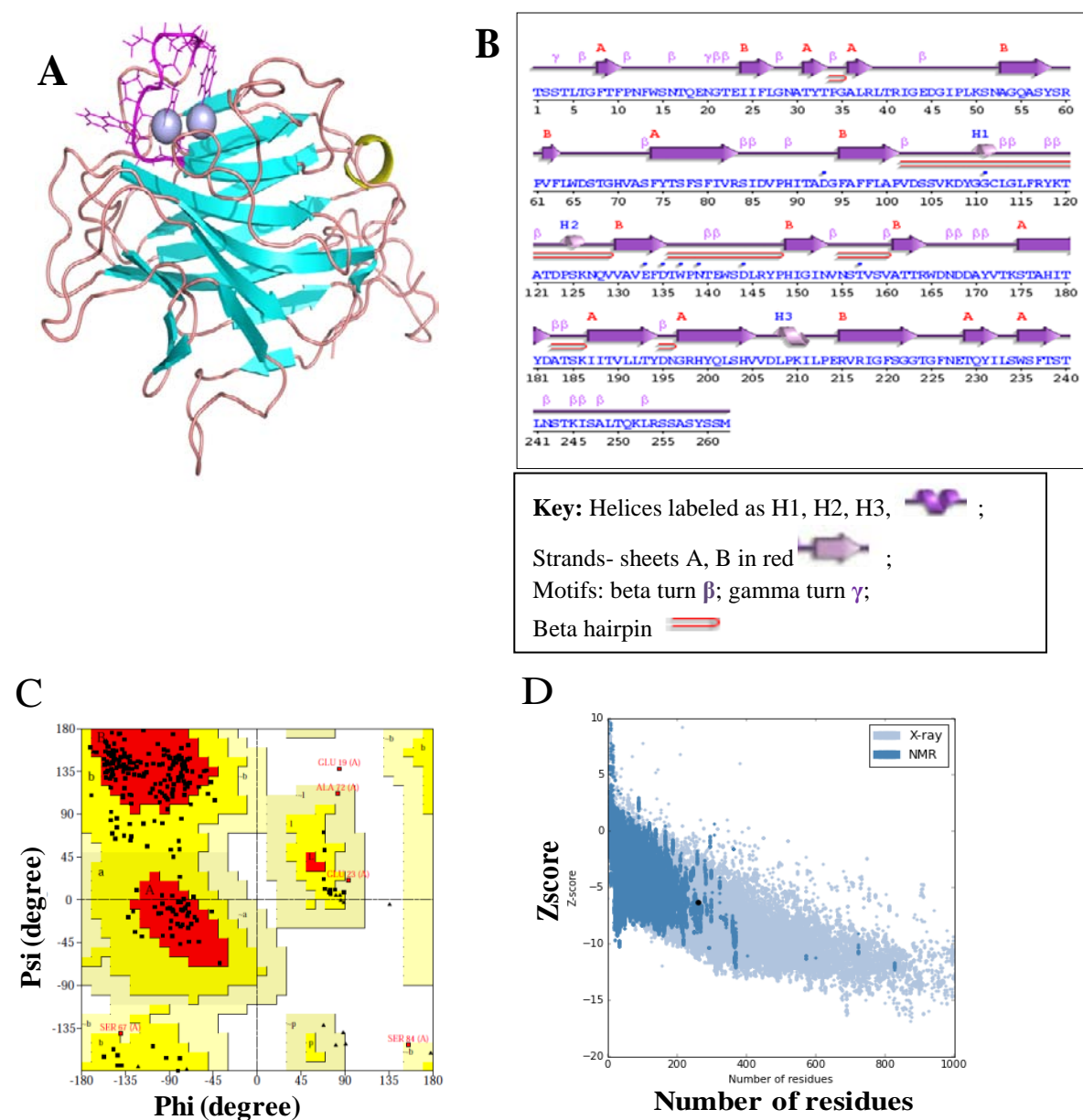
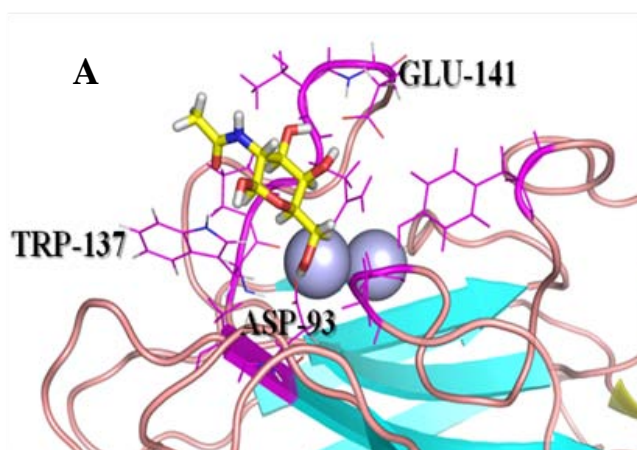


Figure 3: **A.** Cartoon representation of BPL monomer constructed by Schrodinger using 5T55 as template. The bound calcium ions are represented as spheres colored in light blue, helices in yellow color, cyan color for β -sheets, salmon color for turns, purple for sugar binding pocket (Fig drawn in Pymol). **B.** The ‘wiring diagram’ shows the secondary structure elements of protein (α -helices and β -sheets) together with various structural motifs such as β and γ -turns, and β -hairpins. **C.** Validation of Homology model by Ramchandran plot using PROCHECK and **D.** Zplot using PROSA analysis.

2.3.5 Docking with ligands

Yamamoto et al. (1992) reported nine amino acid sequence DTWPNTEWS (BP-9) as sugar binding region in *Bauhinia purpurea* lectin using affinity chromatography. This region from 135 to 143 amino acid residues remains conserved in many leguminous lectins [6]. To the predicted binding pocket of BPL, GalNAc and T-antigen were docked (Fig.4A). The hydrogen bonds and hydrophobic interactions forming between the sugars and BPL were studied and ligand interactions diagrams were generated (Fig. 4B, C, D and E). The residues involved in these interactions with docking score of ligands have been compiled in Table 3. Asp-93 is the common residue forming hydrogen bond. In spite of tryptophan being involved in sugar binding, no stacking interactions between the aromatic residue and pyranose ring were observed as mentioned by Asensio et al. [19]. The docked pose of T-antigen (-8.313) showed two fold increase in docking score compared to GalNAc (-4.008). The binding constants k_a of BPL for GalNAc and T-antigen disaccharide as determined by intrinsic fluorescence spectroscopy (*in solution* studies) were $5.0 \times 10^3 \text{ M}^{-1}$ and $1 \times 10^4 \text{ M}^{-1}$, respectively (Fig. 1E and F). Thus, binding affinities determined by *in silico* and *in solution* studies correlate well with each other.



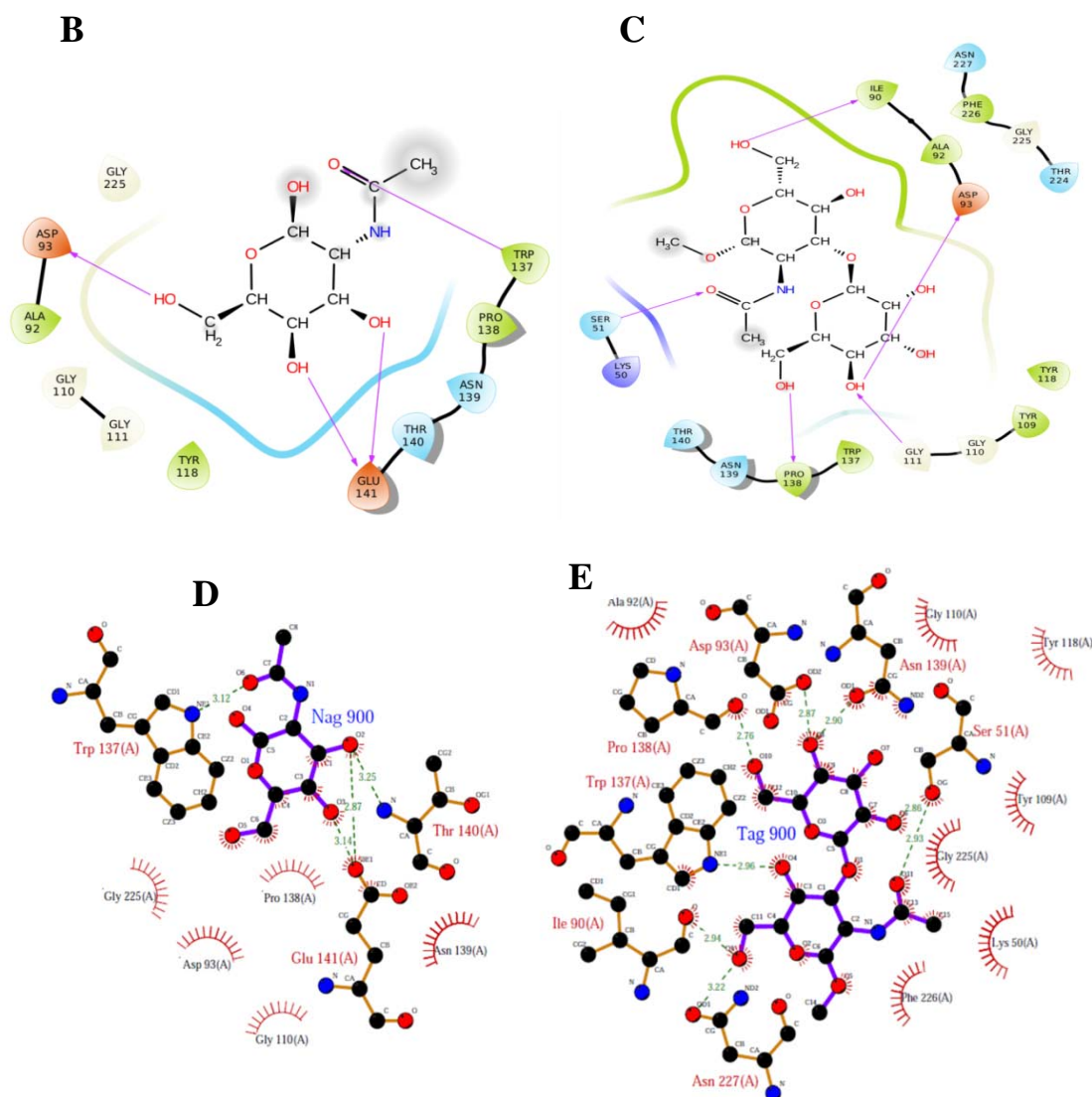


Figure 4: Docking studies; A. Sugar binding pocket of docked BPL showing the ligand molecule GalNAc (colored by element) and amino acid residues involved in formation of binding site. Detailed view of the binding region of BPL with ligands **B.** GalNAc **C.** T-antigen showing interactions of the proton donor and other residues in and around the binding site represents H bond. Interactions between **D.** GalNAc (Nag 900) **E.** T-antigen (Tag 900) and the residues on the BPL generated by the LIGPLOT. Ligand bonds are shown in thick purple lines, while non-ligand bonds (i.e., belonging to those BPL residues to which the GalNAc is hydrogen-bonded) are shown with thin orange bonds. Hydrogen bonds are shown by green dashed lines with the bond length printed in the middle. Hydrophobic contacts between BPL and GalNAc are indicated by brick-red spoked arcs. Other atoms involved in hydrophobic contacts have spokes coming out of the individual atoms.

Table 3: Docking score, glide score and residues involved in sugar binding of BPL.

Sugar (Ligand)	GalNAc	Tantigen
Dock score	-4.008	-8.313
Emodel	-30.325	-58.481
Ligand bound amino acids (Hydrogen bonds)	Asp93, Trp137, Glu141	Asp93, Ile90, Pro138, Ser51, Gly111

2.3.6 Detailed Structural investigation of differential sugar binding to BPL and WFL

Sequence and structural alignments of BPL and WFL showed loop C of BPL comprising of nine conserved amino acids from 135 to 143 residues DTWPNTEWS (Fig.5A). Tryptophan at 137 is replaced by phenylalanine in WFL (PDB Id: 5KXB). Proline at position 138 in BPL makes loop C rigid. It can be noted that loop D of BPL is small comprising of 223–227 amino acid residues TGFNE whereas WFL loop D is longer with residues 214–223 GLSKDHSVETH which makes it more specific to LacdiNAc over GalNAc/Galβ 1–3 GalNAc (Fig.5B).

Soga et al. have also shown that the length and composition of loop D of lectins are involved in determining the sugar-binding specificity [20]. Furthermore, WFL structure reported by Haji-Ghassemi et al. revealed a hydrophobic groove complementary to the GalNAc and, to a minor extent, to the GlcNAc sugar ring. The smaller hydrophobic surface area considerably increases the affinity for LacdiNAc over GalNAc. The strong affinity of WFL for LacdiNAc has also been reported using surface plasmon resonance where binding constant k_a is reported to be 5.45 μM [9].

A

```

BAA02049.1  GEDGIPLKSNAGQASYSRPVFLWDSTG-HVASFYTSFSFIVRSIDVPHITADGFAFFLAP  59
BAZ95724.1  ----EPVYSSLGRALYYAPIHIWDSNTDTVANFVTSFSFVIDAPN-KAKAADGLAFFLAP  55
          *: *  ** *  * : : ** .  ** *  ***** : : :  : *****

BAA02049.1  VDSSVKDYGGCLGLFRYKTATDPSKNQVAVFDTWPNTEWSDLRYPHIGINVNSTVSV  119
BAZ95724.1  VDTEPQKPGGLLGLFHDDRH--NKSNIHIVAVEFTFKNS-W-DPEGTHIGINVNSIVSRK  111
          ** : .  ** ***** :  ..* : ***** : * : * * .  ***** **

BAA02049.1  TTRWDNDDAYVTKSTAHTYDATSKIITVLLTYD-NGRHYSLSHVVDLPKILPERVRIGF  178
BAZ95724.1  TTSDLENGEVAN--VVISYQASTKLTASLVYPPSSSTSYILNDVVDLKQILPEYVRVGF  169
          ** ** : :  * : :  .  * : * : * : * : * .  * * .  ***** : ***** **

BAA02049.1  SGGTGFNE----TQYILSWSFTSTLNSTKISALTQKLRSSA-SYSSM 220
BAZ95724.1  TAASGLSKDHSVETHDVLAWTFSDLPDPSSDDCNLHLSNVLRGSI 216
          : : : * : :  * : * : * * * . . . .  :  * *  . * :

```

Figure 5A: Sequence alignment of BPL and WFL. BAA02049.1 is *Bauhinia purpurea* lectin, BAZ95724.1 is *Wisteria floribunda* lectin. Highlighted residues form loop C and loop D, respectively in both the lectins.

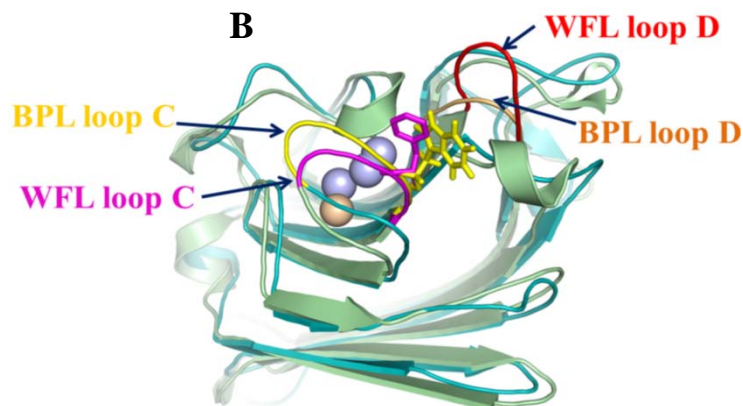


Figure 5B: Structural alignment of BPL and WFL with emphasis on loop C and D. Loop C of BPL and WFL are highlighted in yellow and magenta color, respectively. Tryptophan at 137 position of BPL is replaced by phenylalanine. Loop D of BPL and WFL are highlighted in light orange and red color, respectively.

2.4 Conclusion

The homology model of *Bauhinia purpurea* lectin (BPL) was constructed to predict the three dimensional structure of BPL monomer which represented the typical legume lectin fold. Model thus constructed was docked with sugars (GalNAc and T-antigen) to find out amino acid residues involved in sugar binding and their binding energies. The docking score correlated well with binding constants determined via *in solution* studies. Longer loop D in the structure of WFL compared to that in BPL was found to be responsible for its specificity to LacdiNac (β -D-GalNAc-[1 \rightarrow 4]-DGlcNAc) over Gal β 1-3GalNAc. Detailed understanding of protein-ligand interaction is further beneficial for structure based drug design.

References

1. B. Liu, H. Bian and J. Bao (2010) Plant lectins: potential antineoplastic drugs from bench to clinic, *Cancer Lett.* 287, 1-12.
2. H. Gabius, S. Andre', J. Jimenez-Barbero, A. Romero and D. Soli's (2011) From lectin structure to functional glycomics: principles of the sugar code, *Trends Biochem. Sci.* 36, 298-313.
3. H. Ghazarian, B. Idoni and S. Oppenheimer (2011) A glycobiology review: Carbohydrates, lectins and implications in cancer therapeutics, *Acta Histochem.* 113, 236-247.
4. M. Cameron and B. Davis (2005) Lectins: tools for the molecular understanding of the glycode, *Org. Biomol. Chem.* 3, 1593-1608.
5. T. Kumar and K.S. Chandrashekar (2011) *Bauhinia purpurea* linn: a review of its ethnobotany, phytochemical and pharmacological profile, *Res. J. Med. Plant.* 5, 420–431.
6. K. Yamamoto, Y. Konami and T.A. Osawa (2000) Chimeric lectin formed from *Bauhinia purpurea* lectin and *Lens culinaris* lectin recognizes a unique carbohydrate structure, *J. Biol. Chem.* 275, 129–135.
7. S.A. Fry, B. Afrough, H.J. Lomax-browne, J.F. Timms, L.S. Velentzis and A.J.C. Leathem (2011) Lectin microarray profiling of metastatic breast cancers, *Glycobiology.* 21 1060–1070.
8. T. Kurokawa, M. Tsuda and Y. Sugino (1976) Purification and Characterization of a lectin from *Wisteria floribunda* seeds, *J. Biol. Chem.* 251, 5686–5693.
9. O. Haji-Ghassemi, M. Gilbert, J. Spence, M.J. Schur, M.J. Parker, M.L. Jenkins and S.V. Evans (2016) Molecular basis for recognition of the cancer glycomarker, LacdiNAc(GalNAc[β1→4]GlcNAc), by *Wisteria floribunda* agglutinin, *J. Biol. Chem.* 291, 24085–24095.
10. K. Soga, F. Teruya, H. Tateno, J. Hirabayashi and K. Yamamoto (2013) Terminal Nacetylgalactosamine specific leguminous lectin from *Wisteria japonica* as a probe for human lung squamous cell carcinoma, *PLoS One.* 8, 1–11 <https://doi.org/10.1371/journal.pone.0083886>.
11. A. Matsuda, A. Kuno, T. Kawamoto, H. Matsuzaki, T. Irimura, Y. Ikehara, Y. Zen, Y. Nakanuma, M. Yamamoto, N. Ohkohchi, J. Shoda, J. Hirabayashi and H. Narimatsu (2010) *Wisteria floribunda* agglutinin positive mucin 1 is a sensitive biliary marker for human cholangiocarcinoma, *Hepatology.* 52, 174–182.

12. N.M. Young, D.C. Watson and R.E. Williams (1985) Characterisation of the N-acetyl-D galactosamine specific lectin of *Bauhinia purpurea*, FEBS Lett. 182, 403–406.
13. T. Sato, H. Tateno, H. Kaji, Y. Chiba, T. Kubota, J. Hirabayashi and H. Narimatsu (2017) Glycan recognition engineering of recombinant *Wisteria floribunda* agglutinin specifically binding to GalNAc β 1 , 4GlcNAc (LacdiNAc), Glycobiology. 27,743–754.
14. U. Laemmli (1970) Cleavage of structural proteins during the assembly of the head of bacteriophage T, Nature. 227, 680-685.
15. D. Chipman, V. Grisaro and N. Sharon (1967) The binding of oligosaccharides containing N-acetylglucosamine and N-acetylmuramic acid to lysozyme. The specificity of binding subsites, J. Biol. Chem. 242, 4388–4394.
16. R.A. Laskowski (2001) PDBsum: summaries and analyses of PDB structures, Nucleic Acids Res. 29, 221–222.
17. N. Manoj and K. Suguna (2001) Signature of quaternary structure in the sequences of legume lectins, Protein Eng. Des. Sel. 14, 735–745.
18. M. Widerstein and M. Sippl (2007) ProSA-web: interactive web service for the recognition of errors in three-dimensional structures of proteins, Nucleic Acids Res. 35, W407–W410.
19. J.L. Asensio, Anaarda, F. Javier and J. Jimenez-Barbero (2013) Carbohydrate aromatic interactions, Acc. Chem. Res. 46 (4), 946–954.
20. K. Soga, H. Abo, S.Y. Qin, T. Kyoutou, K. Hiemori, H. Tateno, N. Matsumoto, J. Hirabayashi and K. Yamamoto (2015) Mammalian cell surface display as a novel method for developing engineered lectins with novel characteristics, Biomolecules. 5, 1540–1562.

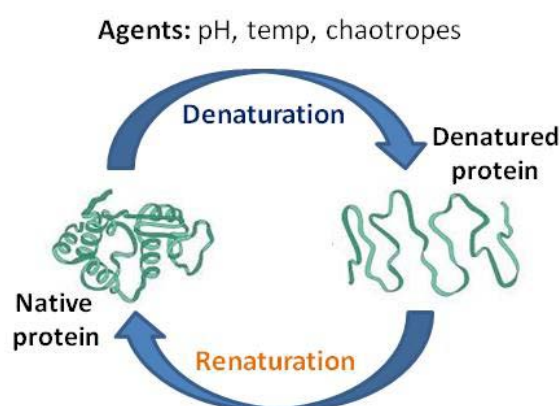
Chapter 3

Structural and functional transition studies of BPL and WFL

Section I: Thermal transition studies

Section II: Chemical denaturation studies

Section III: Characterization of molten globule like intermediate



Archives of Biochemistry and Biophysics 662 (2019) 134–142

Contents lists available at ScienceDirect



Archives of Biochemistry and Biophysics

journal homepage: www.elsevier.com/locate/yabbi



Investigation of structural and saccharide binding transitions of *Bauhinia purpurea* and *Wisteria floribunda* lectins[☆]

Sanskruthi B. Agrawal^{a,b}, Deepanjan Ghosh^{a,b}, Sushama M. Gaikwad^{b,*}

^aAcademy of Scientific and Innovative Research (AcSIR), India

^bCSIR National Chemical Laboratory, Dr Homi Bhabha Road, Pune, 411008, India



ARTICLE INFO

Keywords:
Lectin
Saccharide binding
Homology model
Conformation
Thermal aggregation
Molten globule

ABSTRACT

Two novel medicinally important legume lectins from *Bauhinia purpurea* (BPL) and *Wisteria floribunda* (WFL) possessing extended sugar binding site were investigated for functional and conformational transitions using biochemical and biophysical techniques as well as bioinformatical tools. Homology model of BPL was constructed using the Schrodinger suite and docked with N-acetyl galactosamine and T-antigen disaccharide (Galβ1-3GalNAcαO-Me). The longer loop D in the structure of WFL compared to that in BPL was found to be responsible for its specificity to LacdiNac (β-D-GalNAc-[1 → 4]-DGlcNAc) over Galβ1-3GalNAc. BPL remained functionally stable up to 40 °C whereas WFL remained stable upto 70 °C indicating the strength of the sugar binding site

Abstract

Legume lectins from *Bauhinia purpurea* (BPL) and *Wisteria floribunda* (WFL) possessing extended sugar binding site were investigated for functional and conformational transitions using biochemical and biophysical techniques as well as bioinformatics tools. BPL remained functionally stable up to 40 °C whereas, WFL remained stable upto 70 °C indicating the strength of the sugar binding site geometry. Far-UV CD spectra analysis of both the lectins showed intense but non-specific secondary structure in the range of 65-90 °C. WFL showed rapid aggregation above 80 °C as indicated by light scattering intensity. Molecular dynamics simulation studies of WFL showed difference in RMSD and RMSF in the loop region at 85 °C compared to that at 25°C. The far-UV CD spectra of BPL showed complete loss in structure in >3M GdnHCl and which correlated well with functional loss of activity (≥ 3.0 M). Similar results were observed in WFL, complete loss in structure was observed in 5M GdnHCl. Overall it's a multistate unfolding of the proteins. Decrease in retention time (by 1.2–1.8 min) due to increase in Stoke's radius in presence of 1.0 M GdnHCl was observed in size exclusion chromatography. SEC studies showed that dissociation and unfolding of the proteins occurred simultaneously. At pH 1.0, both the lectins exhibited molten globule like structures, which were characterized further and were found to respond in a different way towards denaturants.

3.1 Introduction

Crucial correlation between structure and function of proteins is observed at molecular level. The biological function of a protein is determined by its three-dimensional (3D) native structure, which in turn is encoded by sequence of amino acids [1]. Nascent polypeptide chain folds into native structure via intermediate steps known as molten globule state. They were first reported in cytochrome c where molten globule state was called as “thermodynamic state” clearly different both from the native and the denatured state [2-3]. This intermediate species has been found for several proteins in mild denaturing conditions, such as acidic or alkaline pH, high temperature, moderate concentrations of urea or guanidinium hydrochloride. Intermediate species acquiring majorly intact secondary and somewhat distorted tertiary structure with exposed hydrophobic residues is particularly called as a “molten-globule” like species [4]. They are more compact than the fully unfolded coil state, but much less than the folded state. Some functional molten globule has been reported earlier in proteins like Photoactive yellow protein (PYP), Clusterin and p53 [5-8]. One of the examples of functional molten globule in plant lectin is from the peanut [9].

The experimental techniques for studying protein folding monitor the gradual unfolding or refolding of proteins and observe conformational changes using standard non-crystallographic techniques like fluorescence and circular dichroism. The computational techniques for protein structure prediction are related to, but are distinct from experimental studies of protein folding [10, 11]. They help a lot in deducing a fine tuning of structure-function relationship.

In the present studies, we have tried to investigate the functional and/or structural novelty by monitoring the respective transitions of BPL and WFL under various denaturing and physicochemical stress conditions. Biophysical techniques like near- and far-UV circular dichroism (CD), fluorescence spectroscopy were employed for this purpose. Native and denatured states of BPL and WFL were studied with respect to the topology of tryptophan residues using time resolved fluorescence and solute quenching technique using steady state fluorescence. The results on the studies of the two unexplored lectins have been presented separately (In III sections) to get deeper understanding of the structural and functional elements responsible for similar or diverse properties.

Section I deals with thermal transitions studies of BPL and WFL. Structural and Functional transitions were monitored at different temperatures using biophysical techniques and hemagglutination assay. Detail investigations of aggregation were done by Molecular dynamics simulations.

Section II comprises of chemical denaturation studies in presence of chaotropic agent GdnHCl which revealed multistate unfolding of lectins.

In Section III, detection and detailed characterization of acid induced molten globule like intermediates is discussed.

3.2 Materials and Method

3.2.1 Materials

Bauhinia purpurea and *Wisteria floribunda* lectin were procured from Vector Labs, USA. Acrylamide, cesium chloride, potassium iodide and guanidine hydrochloride (GdnHCl), sodium dodecyl sulfate (SDS), 8-Anilinonaphthalene-1-sulfonic acid (ANS) and the chemicals, reagents, buffers used for unfolding studies were procured from Sigma-Aldrich, USA. Buffers were prepared in Milli Q water. Rabbit blood for the

hemagglutination assay was procured from animal house of the National Institute of Virology, Pune, India. Buffers and GdnHCl solution were filtered through 2 μm filter membrane prior to use.

3.2.2 Protein preparation

BPL and WFL were dissolved in TBS (10 mM Tris HCl pH 8.0 buffered saline (150 mM NaCl) with CaCl_2 (1 mM) in required concentration. Both lectins were stored at 4 $^\circ\text{C}$ until further use. Protein concentration was determined based on absorbance of solution at 280 and molar extinction coefficient (ϵ). ($\epsilon_{280\text{ nm}}$ 0.1% for BPL 1.75, for WFL 0.89).

3.2.3 Hemagglutination assay

Hemagglutination assay was performed as discussed in Chapter 2, section 2.2.7

3.2.4 Fluorescence measurements

3.2.4.1 Steady state fluorescence studies

Fluorescence measurements of BPL (70 $\mu\text{g/ml}$) and WFL (62 $\mu\text{g/ml}$) were carried out on a Perkin Elmer LS-50B spectrofluorimeter. Each sample was excited at 295 nm (1.0 cm cell path length) and emission was recorded from 310 to 400 nm. Slit widths of 7 nm each were set for excitation and emission monochromators and the spectra were recorded at 100 nm/min. The baseline was corrected by subtracting the signal produced by buffer solution.

3.2.4.2 Time-resolved fluorescence studies

Lifetime measurements were carried out on an FLS-920 single photon counting spectrofluorimeter supplied by Edinburgh Instruments. A laser pico second pulsed light emitting diode (model EPLED-295) was used as the excitation source and a synchronization photomultiplier was used to detect the fluorescence. The diluted Ludox solution was used for measuring Instrument Response Function (IRF). The lectin (1 mg/ml) was excited at 295 nm and emission was recorded at 330 nm. Slit widths of 10 nm each were used for the excitation and emission monochromators. The resultant decay curves were analyzed by a reconvolution fitting program supplied by Edinburgh instruments.

3.2.5 Circular dichroism (CD) spectroscopy

CD spectra of both the lectins were recorded using a Jasco J-815-150S (Jasco, Tokyo, Japan) spectropolarimeter connected to a PTC343 Peltier unit circulating water bath at 28 °C. Far-UV CD spectra was recorded in a rectangular quartz cell of 1mm path length in the range of 190–250 nm at a scan speed of 100 nm/min with a response time of 1 s and a slit width of 1 nm. BPL and WFL at a concentration of 290 µg/ml and 310 µg/ml, respectively were used for all the samples to monitor the secondary structure. Near UV CD spectra of BPL (900 µg/ml) and WFL (1.0 mg/ml) were collected to monitor tertiary structure in the wavelength range of 250–300 nm using a cell of path length 1.0 cm. Each spectrum was recorded as an average of three scanned spectra. Conformational transition studies of lectins were carried out by incubating BPL, WFL under conditions mentioned for respective time periods. All spectra were corrected for buffer contributions and observed values were converted to mean residue ellipticity (MRE) in deg.cm²/dmol defined as

$$\text{MRE} = M\theta_{\lambda} / 10dcr.$$

Where M is the molecular weight of the protein, θ_{λ} is CD in millidegree, d is the path length in cm, c is the protein concentration in mg/ml, and r is the average number of amino acid residues in the protein.

The relative content of various secondary structure elements was calculated by using CDPro software (<http://lamar.colostate.edu/~sreeram/CDPro/main.htm>). Low NRMSD values were observed for analysis with CONTINLL.

3.2.6 Thermal transition studies of BPL and WFL

The samples were incubated at temperatures ranging from 25 to 95 °C with interval of 5 °C for five minutes each. Fluorescence scans and CD measurements were recorded as described above. In a separate experiment, activity of the samples incubated at different temperatures was checked with suitable aliquots using hemagglutination assay. Light scattering was measured at excitation and emission wavelength of 400 nm and the excitation and emission slit widths set at 2.5 and 10 nm respectively, to follow the aggregation of the protein.

The high resolution X-ray crystal structure of *Wisteria floribunda* lectin (5KXB) reported in the Protein Data Bank was taken as a starting point for the simulations. The crystal structure was set-up and simulations were carried out using standard tools in Gromacs version 5.1.4 [12]. The protein was inserted into a cubic water box with a

minimal distance of 13 Å between any protein atom and boundary of the box, with TIP3P water model as applied in CHARMM 36 force field [13]. The system was then subjected to energy minimization using steepest descent algorithm. Two separate stepwise NPT equilibrations were carried out for 2 ns, at temperatures 298 K and 358 K, respectively. Periodic boundary conditions were applied. System components were separately coupled to respective temperature baths at 298 K and 358 K with a coupling time constant of 0.5 ps. A cut-off distance of 1.2 nm was used for van der Waals and short range electrostatic interactions. The Particle-Mesh Ewald (PME) method [14] was applied for long range electrostatic interactions. Isotropic pressure coupling was carried out using Parrinello-Rahman barostat and the volume compressibility was chosen to be $4.5 \times 10^{-5} \text{ bar}^{-1}$ [15]. Two production runs of 5KXB were performed for 150 ns for the said respective temperatures.

3.2.7 Effect of guanidine hydrochloride on BPL and WFL

For GdnHCl mediated denaturation, the denaturant was freshly prepared and pH was adjusted to 8.0 and the solution was filtered through a 0.22 µm syringe filter before use. The lectin samples BPL (290 µg/ml) and WFL (310 µg/ml) were incubated in 0.0–6.0M GdnHCl solution at pH 8.0 for 4 h, 8 h and 24 h. CD measurements were recorded as described above. For Fluorescence scans, concentration of lectin used were 70 µg/ml and 62 µg/ml for BPL and WFL, respectively. All the spectra were corrected for respective blanks of GdnHCl buffer contributions. In a separate experiment, activity of each sample incubated under similar conditions was checked with suitable aliquots using hemagglutination assay.

3.2.8 Size exclusion chromatography

Dissociation of BPL and WFL in presence of Guanidine hydrochloride (GdnHCl) was monitored using WATERS High Performance Liquid Chromatography (HPLC) unit and WATERS gel filtration ProteinPak TM300SW (7.5×300 mm) column. 100 mM Phosphate buffer (with 0.15 M NaCl), pH 7.2 containing different concentrations (0–4.0 M) of GdnHCl served as the mobile phase. 50 µl protein sample (protein stock: 3.0 mg/ml) incubated in 0–4.0 M GdnHCl for one hour each was injected into the column. Flow rate was maintained at 0.5 ml/min and the elution profile was monitored at 280 nm.

3.2.9 Effect of pH on BPL and WFL: fluorescence, CD measurements and hemagglutinating activity

To check the effect of pH on lectins, buffers (25 mM) used were glycine-HCl (pH 1.0-3.0), sodium acetate (pH 4.0), citrate phosphate pH 5.0, sodium phosphate (pH 6.0-7.0), tris-HCl (pH 8.0-10.0) and glycine-NaOH (pH 11.0-12.0). The lectin samples were incubated in pH 1.0-12.0 buffers for 4 h, 8 h and 24 h to attain equilibrium. Intrinsic fluorescence and CD measurements of lectins at different pH were performed as described above. In a separate experiment, activity of each sample incubated was checked with suitable aliquots using hemagglutination assay.

3.2.10 ANS-binding assay

The intermediate states of denatured and native BPL and WFL under different pH and denaturant conditions were analyzed by allowing binding of the hydrophobic dye, 8-anilino-1-naphthalene-sulfonic acid (ANS) to the protein. The final ANS concentration used was 50 μ M, excitation wavelength was 375 nm, and the fluorescence emission was monitored between 400 and 550 nm. Reference spectrum of ANS in each buffer of respective pH and denaturant was subtracted from the spectrum of the sample.

3.2.11 Solute quenching studies

Solute quenching studies were performed for native lectins at pH 8.0, for acid induced molten globule at pH 1.0, and for denatured lectins in GdnHCl (6.0 M) by using a Perkin Elmer LS-50B spectrofluorimeter. The different quenchers like acrylamide (2.5 M) (neutral quencher), iodide (2.5 M), and cesium (2.5 M) (charged quenchers) were added to the lectin samples in small aliquots (3-5 μ l) of quencher stocks, mixed thoroughly and fluorescence spectra were recorded after each addition. Iodide stock solution contained 0.2 M sodium thiosulphate to prevent formation of tri-iodide (I_3^-). Fluorescence intensities were corrected for volume changes before further analysis of quenching data. The steady-state fluorescence quenching data obtained with different quenchers were analyzed by Stern–Volmer (Eq. 1) and modified Stern–Volmer (Eq. 2) equations in order to obtain quantitative quenching parameters

$$F_o/F_c = 1 + K_{sv} [Q] \quad (1)$$

$$F_o/dF = f_a - 1 + 1/[K_a f_a (Q)] \quad (2)$$

Where F_o and F_c are the relative fluorescence intensities in the absence and presence of the quencher, respectively, (Q) is the quencher concentration, K_{sv} is Stern-Volmer

quenching constant, $\Delta F = F_o - F_c$ is the change in fluorescence intensity at any point in the quenching titration, K_a is the quenching constant, and f_a is the fraction of the total fluorophores accessible to the quencher. Equation (2) shows that the slope of a plot of F_o/dF versus $1/Q$ (modified Stern–Volmer plot) gives the value of $(Kaf_a)^{-1}$ and its Y intercept gives the value of fa^{-1} .

3.3 Results and Discussion

Section I: Thermal transition studies

3.3.1 Fluorescence studies of the native lectins

3.3.1.1 Steady-state and lifetime fluorescence measurements of BPL and WFL

Fluorescence spectroscopy has been extensively used to probe the structural changes in the proteins based on tryptophan emission spectra which is dependent on the electronic and dynamic properties of its environment [16]. Fluorescence studies have been extensively used to probe the structural changes in the proteins based on tryptophan emission spectra which is dependent on the electronic and dynamic properties of its environment [16]. The sequence and structure of BPL and WFL revealed the presence of 6 and 4 tryptophans (trp), respectively. The native BPL and WFL showed maximum emission (λ_{max}) of intrinsic fluorescence at 338 nm and at 332 nm, respectively signifying most of the trp residues present in hydrophobic environment (Fig. 1A). The residues are highlighted in model structure of BPL and the available structure of WFL (Fig. 1B and C). Non polar environment for WFL trp residues seems to be more pronounced.

For finer analysis, the lifetimes of fluorescence emission decay of both the lectins were measured in nanosecond domain. After fitting into a bi-exponential curve ($\chi^2 < 1.097$), it could be described by two decay components τ_1 and τ_2 with decay times (with contribution in fluorescence) of 2.65 ns (55.94%) and 0.68 ns (44.06%), respectively in BPL. In WFL, 3.34 ns (86.99%) and 0.42 ns (13.01%) ($\chi^2 < 1.132$) for τ_1 and τ_2 , respectively were detected. Each Trp residue has two different lifetimes corresponding to different excited states 1La and 1Lb. Both lifetimes represent a media of the lifetimes of all the residues of the protein. Thus, in general BPL has all tryptophan residues more exposed than WFL if the lifetimes 2.65 ns and 3.34 ns, respectively are compared. This is

also corroborated by the red shift maximum emission wavelength of BPL in comparison with that of WFL.

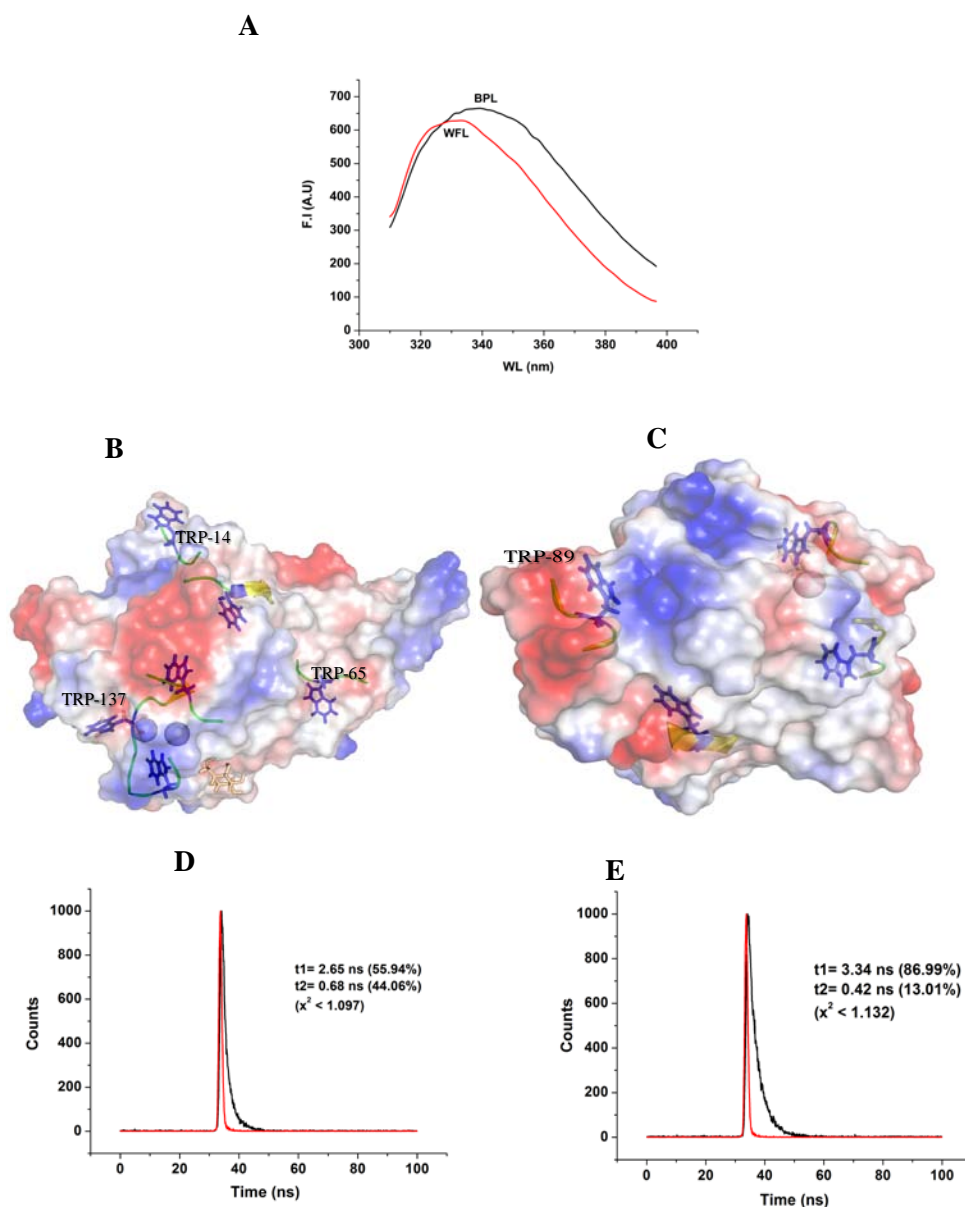


Figure 1: Fluorescence studies: **A.** Intrinsic fluorescence scans of BPL and WFL **B.** Tryptophan residues with their microenvironment charge density highlighted in BPL model and **C.** WFL (PDB ID:5KXB) (Trp in dark blue color, blue color on surface shows positive charge density, red color shows negative charge density [charge density varies according to the color intensity], label shows residues on the surface [Fig drawn in Pymol]) **D. and E.**, time resolved Fluorescence spectra of native BPL and WFL (both 1 mg/ml), respectively.

3.3.1.2 Solute quenching studies

Topological information about protein structure can be obtained from solute quenching of intrinsic tryptophan fluorescence. In the present work, acrylamide, the neutral quencher was found to be the most efficient (Table 1). Downward curvature was observed for ionic quencher KI in case of BPL (Fig. 1F, Fig.1G) indicating two populations of surface tryptophans; one readily accessible to the quencher. Low positive charge density around the surface tryptophan was indicated by Stern–Volmer constants (K_{sv}). WFL showed overall very low positive and negative charge density around the surface tryptophan, residues highlighted near tryptophan in the structure conclude the same (Fig. 1B and 1C). The modified Stern-Volmer plot showed 65% accessibility of tryptophans indicating presence of hydrophobic core for both the lectins (Tables 1A and 1B).

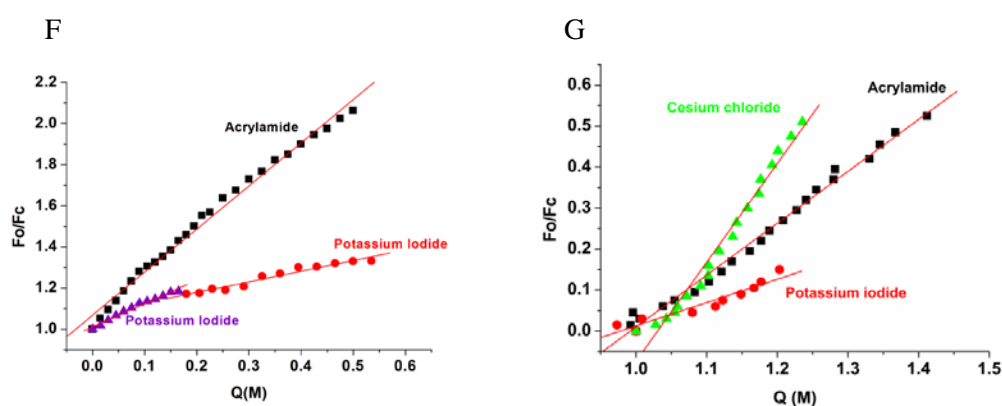


Figure 1F and G: Fluorescence studies: Stern volmer plots for solute quenching with acrylamide, potassium iodide, cesium chloride for native BPL and WFL, respectively.

Table 1A: Parameters of solute quenching of BPL

Quencher	Native BPL			BPL at PH 1.0			Denatured BPL	
	$K_{sv1}(M^{-1})$	$K_{sv2}(M^{-1})$	f_a	$K_{sv1}(M^{-1})$	$K_{sv2}(M^{-1})$	f_a	$K_{sv}(M^{-1})$	f_a
Acrylamide	2.09	-	0.65	2.57	-	0.88	17.3	1.08
Potassium iodide	1.14	0.5	0.54	3.31	1.53	0.65	8.35	0.78

Table 1B: Parameters of solute quenching of WFL

	Native WFL		WFL at PH 1.0		Denatured WFL	
Quencher	$K_{sv1}(M^{-1})$	f_a	$K_{sv1}(M^{-1})$	f_a	$K_{sv}(M^{-1})$	f_a
Acrylamide	0.74	0.65	1.13	0.63	6.7	0.89
Potassium iodide	1.35	0.34	1.28	-	2.66	0.76
Cesium chloride	0.40	0.23	0.5	-	0.9	1.4

3.3.2 Thermal transitions of BPL and WFL

Temperature is the most critical factor affecting protein structure. One of the ways to assess the structural and functional stability of a protein is by monitoring the thermal denaturation. Following thermal denaturation, some proteins may aggregate which is mostly irreversible [18]. Hence parameters like lectin activity, secondary structure transitions and light scattering property were monitored at different temperatures for both BPL and WFL.

3.3.2.1 Functional stability

Based on hemagglutination activity assay, BPL is functionally stable up to 40 °C whereas WFL is functionally stable upto 70 °C. $t_{1/2}$ of BPL activity is 57 °C whereas 80 °C for WFL, indicating WFL is functionally more thermostable as compared to BPL. The difference could be due to the stronger interactions in the binding site geometry of WFL. Complete loss in activity was observed at 70 °C for BPL and 85 °C for WFL (Fig. 2A and B). Thermal transitions in BPL were similar to that reported for *Sophora japonica* lectin [18].

3.3.2.2 CD spectroscopic analysis

Native BPL showed negative ellipticity minima at 228 nm and 215 nm and maxima at 197 nm in far-UV CD spectrum representing presence of atypical β -sheet structure. The CONTINLL program of CDPro software was used to analyze the spectrum which showed the secondary structure elements as 4.1 % α -helix; 41.8 % β -sheets; 21.5 % turns and 32.7 % unordered (Normalised root mean square deviation (NRMSD)=0.072). CDPro analysis

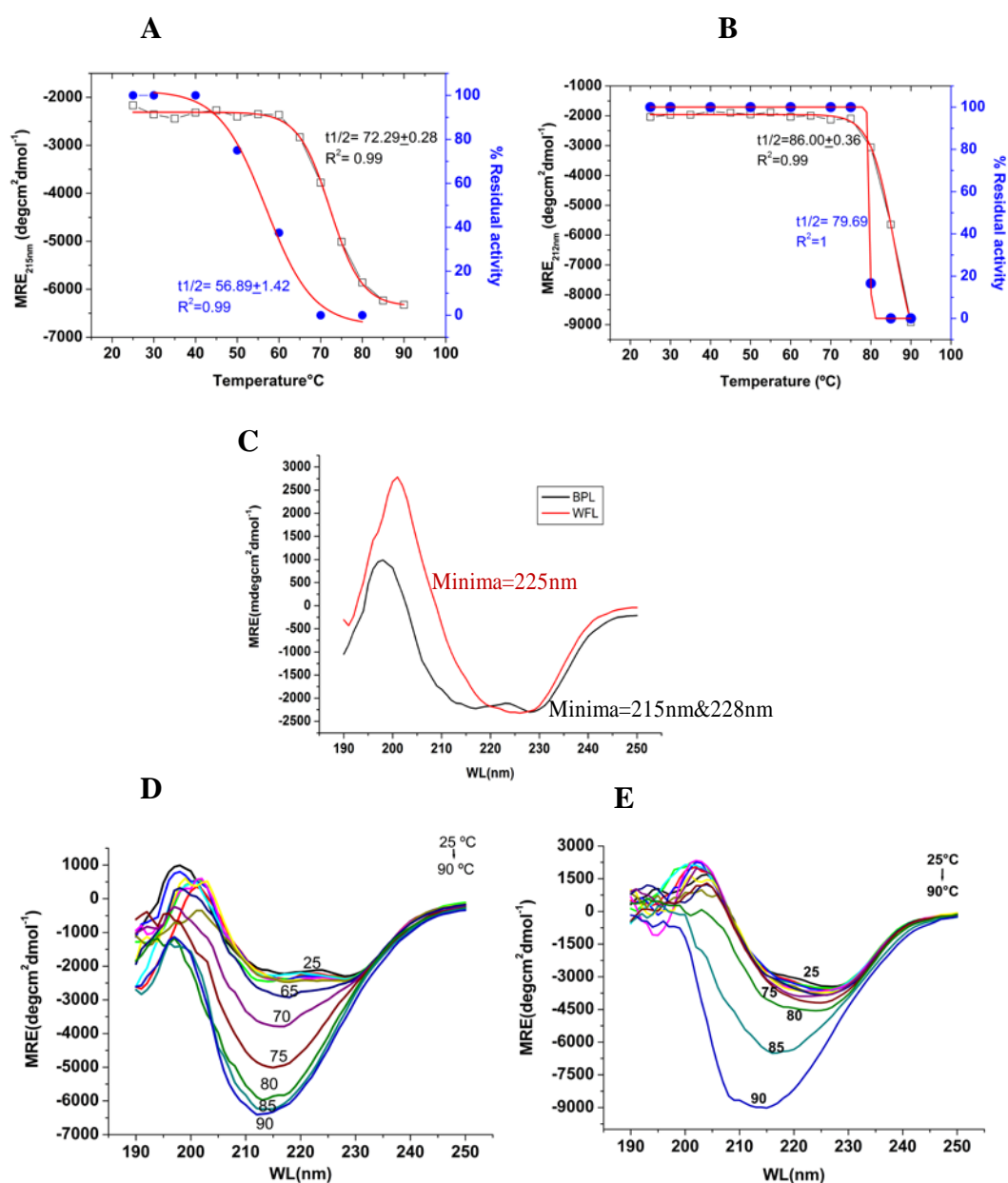
values for BPL were in agreement with the PDB sum analysis mentioned in section 2.3.4 for homology model showing protein is β sheet rich. WFL showed negative ellipticity minima at 225 nm and maxima at 200 nm, secondary structure composition as 5.2 % α -helix; 39.2 % β -sheets; 21.2 % turns and 34.4 % unordered (NRMSD=0.077) (Fig 2C). PDBsum analysis for WFL structure (PDB Id: 5KXB) showed 46.6 % sheets, 5 % helix and 48.3 % turns and unordered structure which also was in agreement with the CDPro analysis.

When MRE at 215 nm was plotted against temperature, T_m of BPL was shown as 70 °C which indicated that loss in function (40 °C) occurs much before the loss in structure of the protein. Both the lectins showed peculiar alteration in the structure indicated by increase in the negative ellipticity at 212-215 nm and decrease in the positive ellipticity between 190 and 200 nm (Fig. 2D and E). This apparently looked like conversion of atypical to typical beta sheet, there could be increase in the unordered structure also. Similar observations were made (increase in negative ellipticity on thermal denaturation) in case of *Ariesaema curvatum* lectin [19]. The alteration of WFL structure at 80 °C correlated well with complete loss of activity at 85 °C. $t_{1/2}$ for MRE was 73 °C in case of BPL and 86 °C for WFL (Fig 2A, 2B).

3.3.2.3 Light scattering studies

BPL did not aggregate when heated upto 90 °C, while WFL got aggregated at 85 °C as indicated by increase in the light scattering intensity (Fig. 2F, G). Secondary structure at this temperature as observed in far UV CD spectra seemed to be increased (Fig. 2E). There was no unfolding of the protein observed before aggregation as no red shift was observed in intrinsic fluorescence spectra (Fig 2H, I). Direct correlation of the aggregation propensity of the proteins with the structural elements has still not been unequivocally proved. To some extent, protein aggregation is related to local concentration of hydrophobic and hydrophilic residues in contiguous blocks of sequence [20]. Thermal aggregation with concomitant loss in secondary structure (both at around 50 °C) has been reported earlier for the lectins *Amaranthus caudatus* [21], *Artocarpus hirsuta* [22], *Artocarpus integrifolia* [23] and *Cicer arietinum* [24]. These lectins showed progressive decrease in the hemagglutination activity as well as secondary structure around 45–55 °C. However, WFL gets aggregated above 80 °C and the rapid transitions lead to intense secondary structure. Thus, aggregation at much higher temperature with

pronounced secondary structure is the unusual thermal transition of WFL. This could be the soluble aggregation stage as no Thioflavin T or Congo red binding to the lectin was observed at higher temperature. In spite of the extensive denaturation studies on con A [25], pea seed [26], peanut [27] and soyabean lectin [28], very few studies are reported specifically on thermal denaturation. Investigations on *Artocarpus hirsuta* [15], *Artocarpus integrifolia* [23], *Moringa oliefera* [29], *Sauromatum guttatum* and *Arisaema tortuosum* [30], *Arisaema curvatum* [19], *Cicer arietinum* [17], *Sophora japonica* [18] and *Amaranthus caudatus* [21] include thermal transitions in addition to chemical folding and refolding. Similar kind of work has been carried out on phloem lectin belonging to Cucurbitaceae family [31] and banana lectin [32] using CD and fluorescence spectroscopy and differential scanning calorimetry (DSC).



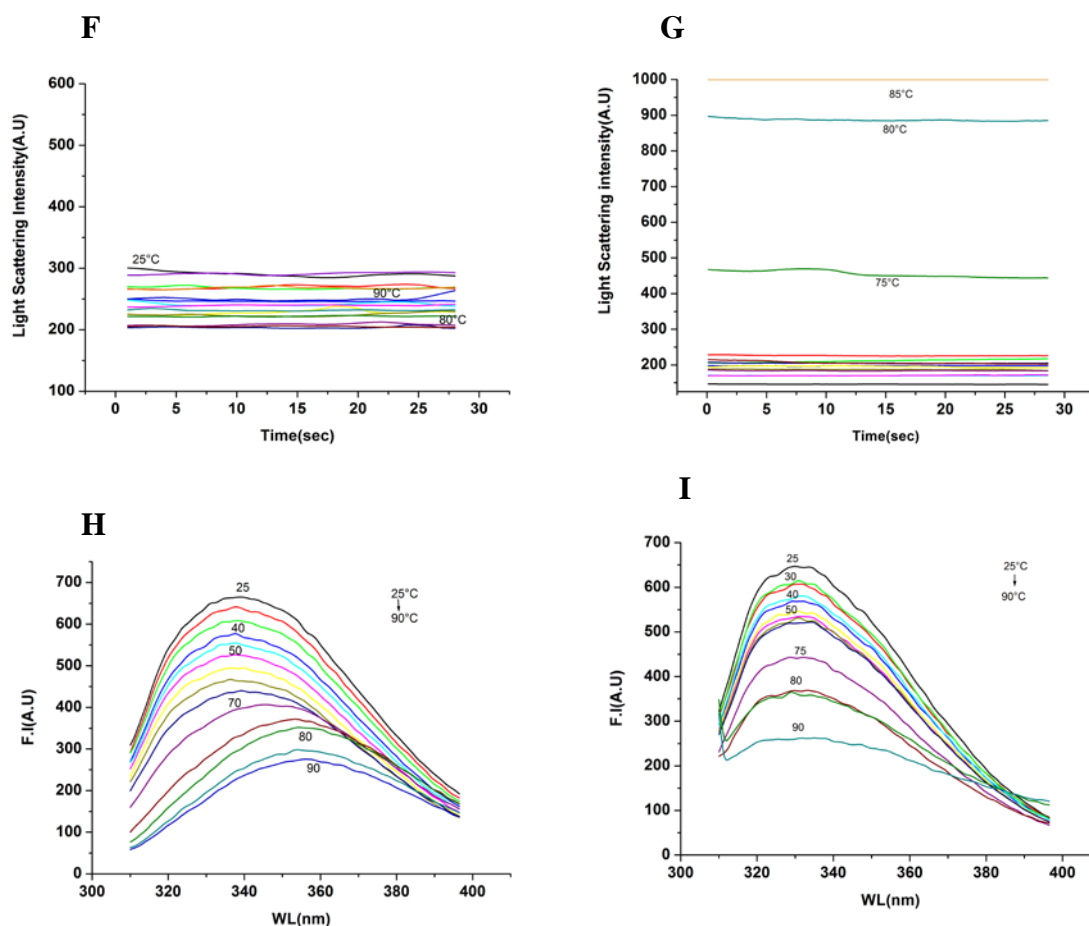


Figure 2: Thermal transition studies; A. and B. Relative hemagglutination activity (●), MRE (□) at 212/215 nm as a function of temperature (25–90 °C) for BPL and WFL, respectively. **C.** Native Far-UV CD spectra of BPL and WFL. **D and E.** Far-UV CD spectra of BPL and WFL at different temperature (25–90 °C). **F and G.** Light scattering intensity scan, **H and I.** Intrinsic fluorescence scan of BPL and WFL incubated at respective temperature (25–90 °C) for 5 min.

3.3.2.4 Molecular Dynamics (MD) Simulations

MD simulations reveal thorough information on the fluctuations and conformational changes of proteins. To study complex and dynamic processes of protein unfolding, thermal-MD simulations can be performed [33]. MD simulations of WFL (PDB ID: 5KXB) were performed using the Charmm 36 force field built-in GROMACS program. The structural variations were calculated with the help of Root Mean Square Deviation (RMSD) and Root-mean-square fluctuations (RMSF) of the lectin at two different temperatures. The simulations were run for 200 ns at 358 K as the aggregation in the protein was observed at this temperature. The results were compared with simulations at 298 K for native protein. The RMSD of the evolving structure increased rapidly after 116

ns as compared to the native structure representing the initiation of aggregation of the protein (Fig.3A). The per-residue C-alpha atom fluctuations (RMSF) calculations revealed the region of 100-125 amino acids show major fluctuations which are present in loop regions of the protein (Fig.3B). Similar studies have been performed earlier for *A. caudatus* lectin where RMSD increased above 12 ns and RMSF were higher in loop region at 358K [21] .

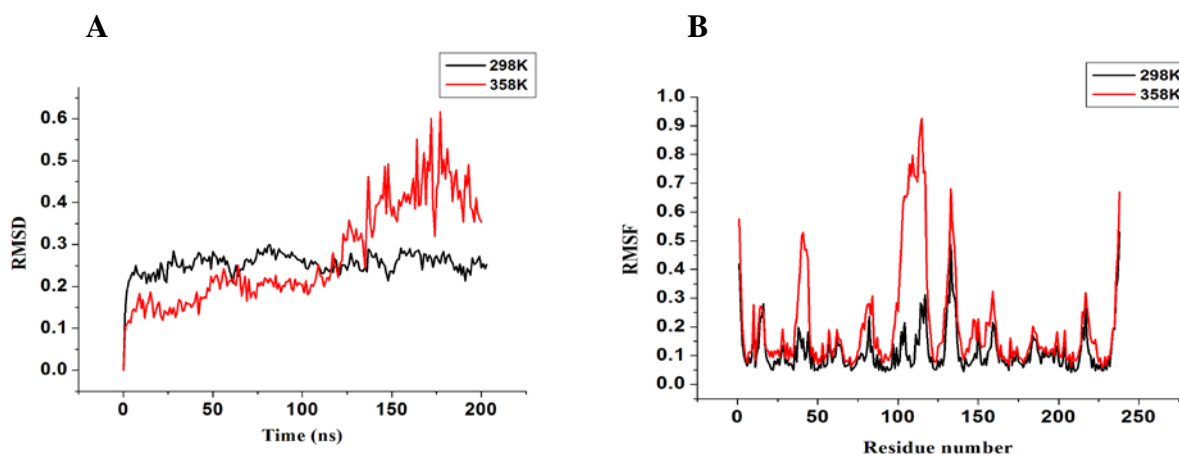


Figure 3: Structural parameters for conformation of WFL simulated for 200 ns: A. RMSD B. RMSF values for C- α atoms for respective temperatures, black line (298 K) and red line (358 K)

Section II: Chemical denaturation studies

3.3.3 GdnHCl induced denaturation of lectins

The unfolding pathways of several proteins in presence of GdnHCl have been shown to be either a simple two-state (monophasic) or a multi-state process (multiphasic) involving structured or partially folded intermediates. In case of oligomeric proteins unfolding can be two ways: 1. Dissociation of oligomer to monomer and then monomers are unfolded. 2. Simultaneous dissociation and unfolding.

3.3.3.1 Functional stability

Biological activity of the BPL and WFL incubated in GdnHCl (0.0–6.0 M) was checked by hemagglutination assay (Fig. 4A). The results indicated that both the lectins were stable in 2.0 M GdnHCl. $D_{1/2}$ of GdnHCl denaturation were deduced to be 2.8 M.

3.3.3.2 Fluorescence measurement

In presence of 2.0-6.0 M GdnHCl, λ_{\max} of fluorescence showed gradual red shift from 338 nm to 363 nm for BPL, while from 332 nm to 363 nm for WFL indicating increased polarity of tryptophan with progressive unfolding of protein (Fig. 4B, C). Intersubunit disulfide bonds in WFL could be preventing the dissociation of the subunits and contributing to the stability of the protein as indicated by higher $D_{1/2}$ for WFL (Fig. 4D). Loss in structure and function in 2.0-6.0 M GdnHCl was similar as seen in case of other lectins *Artocarpus integrifolia* [23] and *Sophora Japonica* [18]. Tryptophans in BPL and WFL denatured in GdnHCl (6.0 M) exhibited higher polar environment than in pH 8.0 due to unfolding.

Quenching with KI showed higher positive charge density around surface tryptophan residues with K_{sv} 8.35 and 2.66 M^{-1} for BPL and WFL, respectively (Figs. 4E and 4F). However, the accessibility of tryptophans was not 100 % indicating some residual structure still remaining even after denaturation in 6.0 M GdnHCl.

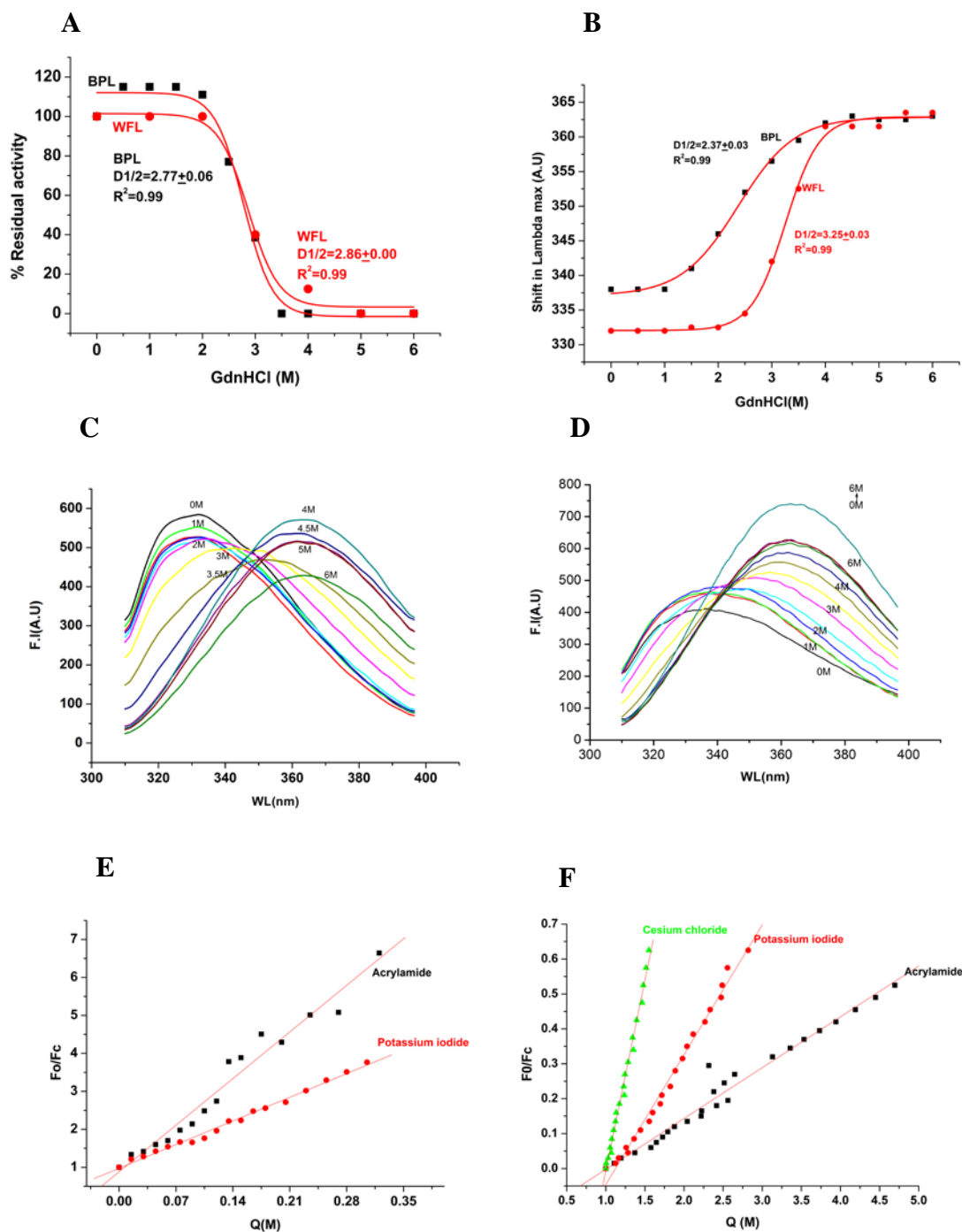
3.3.3.3 CD spectroscopic analysis

The far-UV CD spectra of BPL showed partial loss in structure in 3.0 M GdnHCl and complete loss in >3.0 M which correlated well with functional loss of activity (≥ 3.0 M). Similar results were observed in WFL, complete loss in structure was observed in 5.0 M GdnHCl (Fig 4G, 4H). Overall it's a multistate unfolding of protein (Fig. 4I). Hence, there could be difference in the $D_{1/2}$ values determined by fluorescence and CD spectroscopy.

3.3.3.4 Size exclusion chromatography (SEC)

Retention times of BPL and WFL subjected to SEC in different concentrations of GdnHCl have been summarized in Table 3. Substantial decrease in retention time (by 1.2–1.8 min) due to increase in Stoke's radius in presence of 1.0 M GdnHCl was observed. With further increase in concentration of GdnHCl, the retention time still decreased. In case of BPL, as the tetramer is formed only with the non-covalent interactions between monomers, the native protein could be gradually dissociating and unfolding to dimer and subsequently to monomer. The secondary structure was stable in GdnHCl up to 2.0 M concentration as observed in far UV CD spectra (Fig. 4G and 4H). In presence of 3.0 M GdnHCl, a broad peak with indication of two species was observed which could be due to

mixture of dimer and monomer. In 4.0 M GdnHCl, the BPL showed single peak of unfolded monomer. Denaturation of WFL showed emergence of additional peak at and above 2.0 M GdnHCl. The protein may not be getting completely dissociated into monomers due to presence of disulfide bonds. Some amount of monomer could be formed during the disulfide exchanges in the dimers [20].



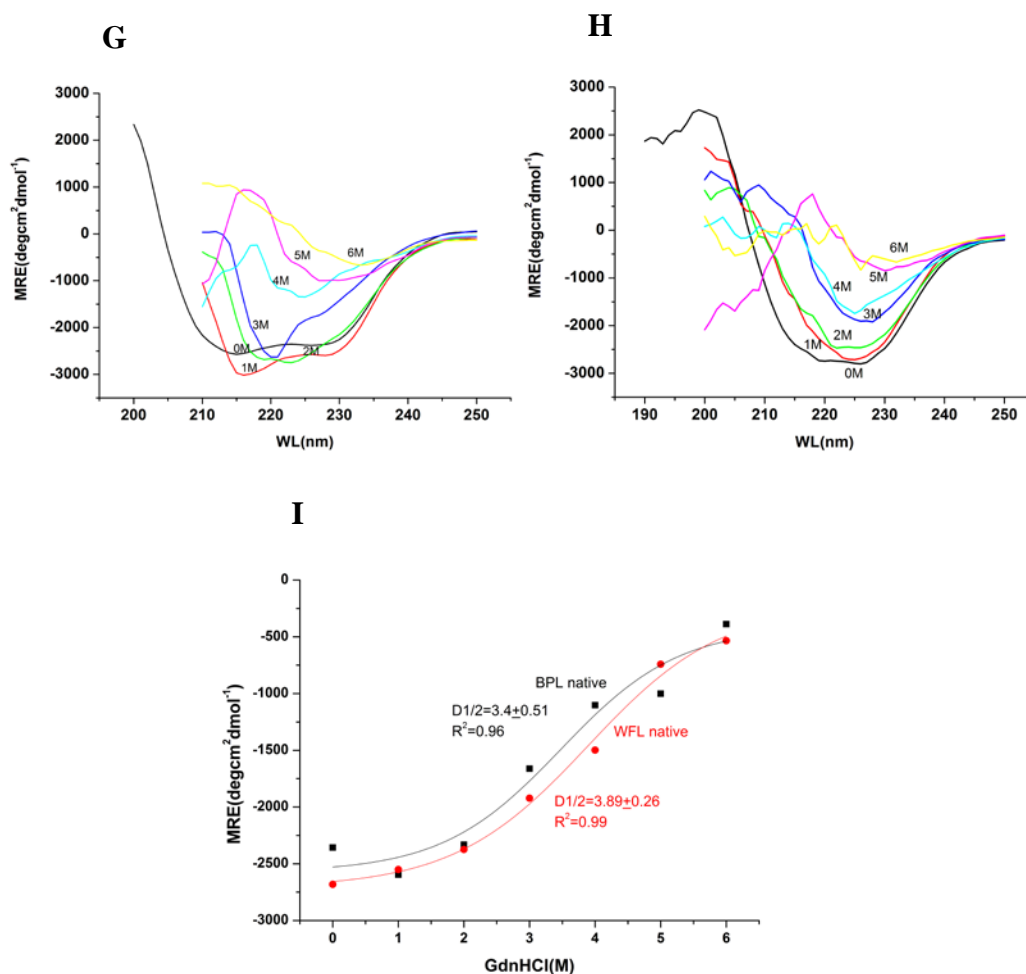


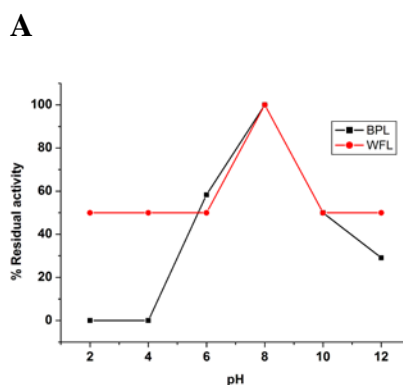
Figure 4: GdnHCl induced denaturation of lectin; A. Relative hemagglutination activity of BPL and WFL as a function of the different concentration of GdnHCl (0–6.0 M). **B** Shift in λ_{\max} of fluorescence BPL (70 $\mu\text{g/ml}$) and WFL (62 $\mu\text{g/ml}$) incubated in GdnHCl (0–6.0 M) for 24 h **C and D.** Fluorescence scans of BPL (70 $\mu\text{g/ml}$) and WFL (62 $\mu\text{g/ml}$) incubated in GdnHCl (0–6.0 M) for 24 h, respectively. **E and F.** Solute quenching studies of BPL (70 $\mu\text{g/ml}$) and WFL (62 $\mu\text{g/ml}$) incubated in GdnHCl (0–6.0 M) for 24 h, respectively. **G and H.** CD scans of BPL (0.29 mg/ml) and WFL (0.31 mg/ml) at incubated in GdnHCl (0–6.0 M) for 24 h, respectively **I.** Mean residue ellipticity of BPL (0.29 mg/ml) and WFL (0.31 mg/ml) at 228 nm incubated in GdnHCl (0–6.0 M) for 24 h.

Table 2: Summary of the size exclusion chromatography of BPL and WFL in GdnHCl.

GdnHCl(M)	BPL		WFL	
	Retention time (min)		Retention time (min)	
	Peak 1	Peak 2	Peak 1	Peak 2
0	16.15	-	17.8	-
1	14.97	-	16.00	-
2	15.60	-	15.30	16.30
3	13.30	14.17	15.10	16.40
4	14.80	-	14.90	16.50

3.3.4. Transitions due to protonation and deprotonation

. Changes in pH of the solution alter protein stability by altering hydrogen bond interactions and like-charge repulsion effects and various other mechanisms. Hemagglutination activity remained stable in the pH range of 6.0–8.0 (Fig 5A), whereas the secondary structure of BPL and WFL were found to be stable in wide range of pH (2.0–12.0) as observed in far-UV CD spectra (Figs. 5B and 5C). Gradual increase in protonation and deprotonation was observed as indicated by fluorescence scans of the lectins in different pH. The sugar binding ability of lectins was abolished due to protonation/ deprotonation but the major structure was retained.



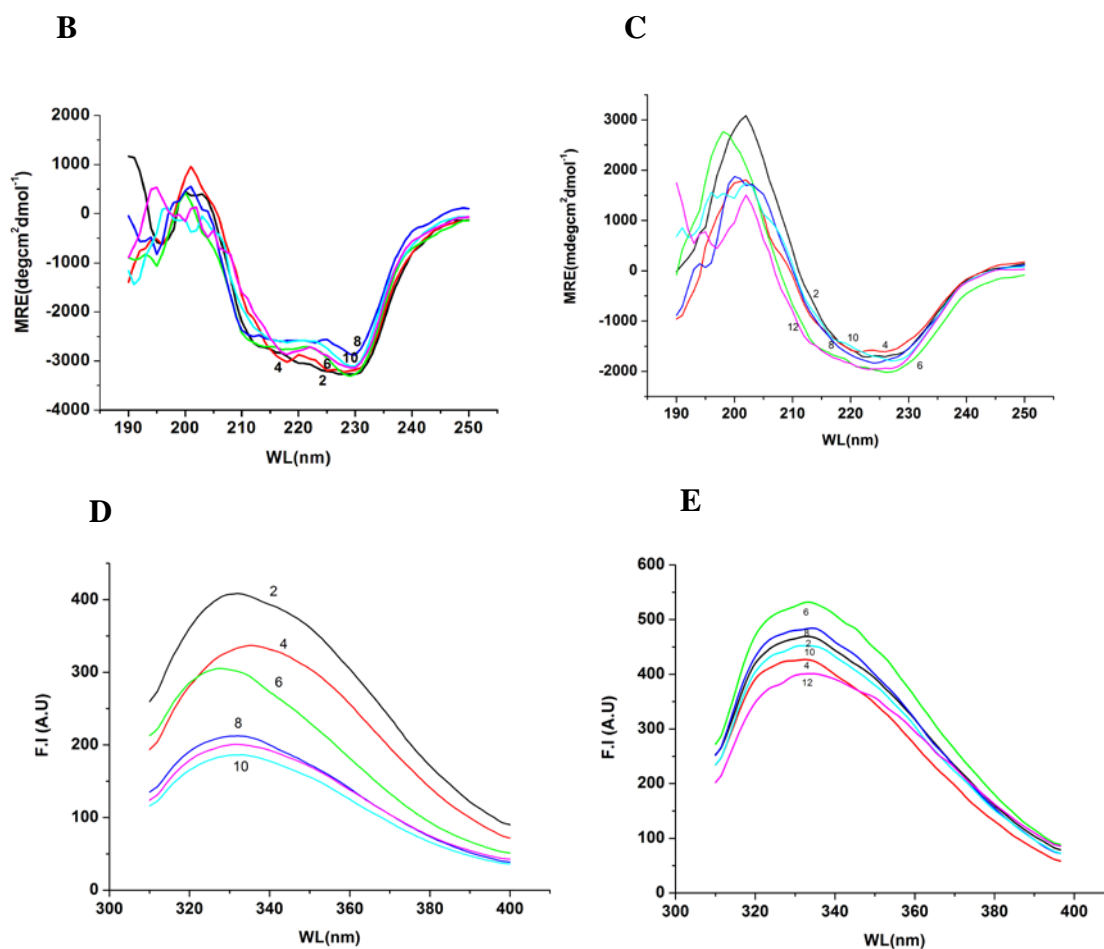


Figure 5: Studies of effect of pH on lectins **A.** Hemagglutination activity of BPL and WFL incubated in different pH buffers (2.0-12.0) for 24h. **B and C.** CD scan of BPL and WFL incubated in different pH buffers (2.0-12.0) for 24h. **D and E** Fluorescence scan of BPL and WFL incubated in different pH buffers (2.0-12.0) for 24h, respectively.

Section III: Characterization of molten globule like intermediate

3.3.5 Detection and Characterization of molten globule like intermediate

To investigate the non-native conformations of protein, 8-anilinoanthracene-1-sulfonic acid (ANS) fluorescence has been extensively used [34]. ANS is an extrinsic fluorescence probe that binds to loosely packed solvent accessible hydrophobic cores of proteins. It specifically exhibits intense fluorescence upon interaction with hydrophobic patches of proteins. Due to change in conformation of the protein, hydrophobic amino acids were exposed to surface which was seen in noticeable ANS binding to both the lectins BPL and WFL at pH 1.0 (Fig. 6A). Far UV CD spectra of both the lectins showed increase in

the secondary structure at pH 1.0 (Fig.6B). Near UV CD spectra in the wavelength range of 250–300 nm showed altered tertiary structure (Fig.6C). Shift in λ_{max} of fluorescence scan from 338 nm to 349 nm for BPL was observed due to exposure of tryptophan residues whereas no shift in λ_{max} was observed in WFL (Fig.6D). The acid-induced state having compact secondary and altered tertiary structure with exposed hydrophobic amino acid residues is named as a “molten-globule”. Above results indicate that BPL and WFL exist in molten globule like intermediate form at pH 1.0. To characterize them further, the proteins were subjected to different denaturing conditions gradually and the changes were monitored as described for the native proteins. Acid induced intermediate states have been reported earlier in lectins from *Sophora japonica* [18], *Amaranthus caudatus* [21], Banana [32] and *Artocarpus integrifolia* [23].

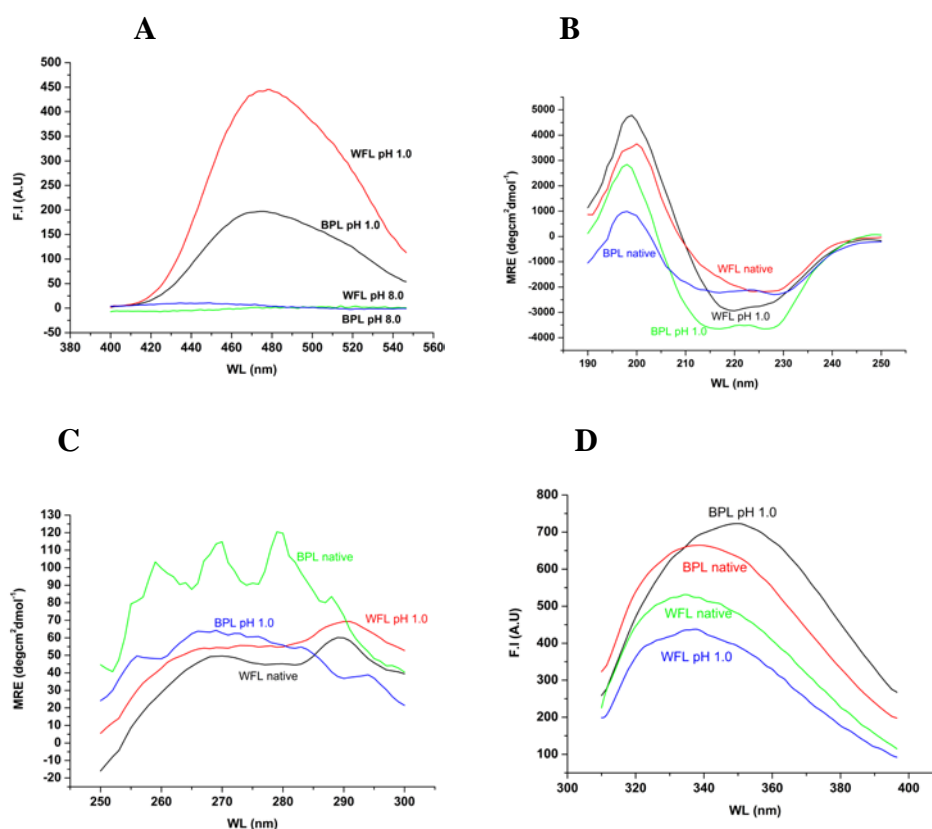


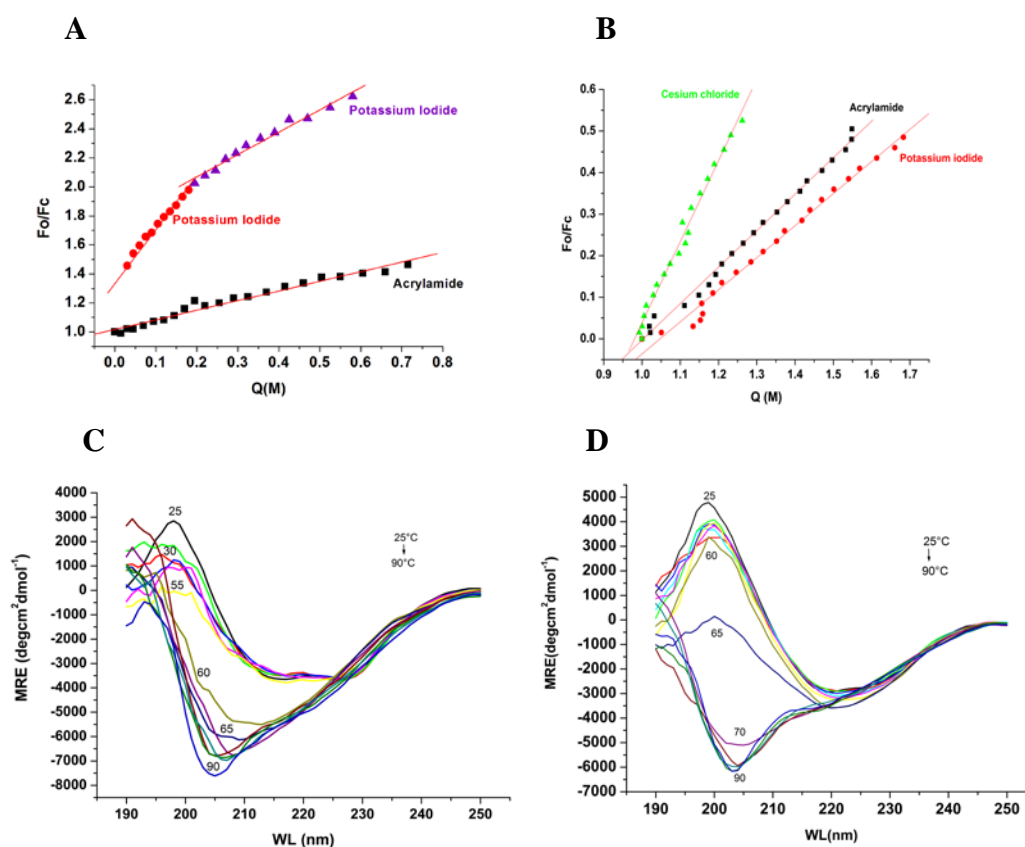
Figure 6: Characterization of molten globule; **A.** Extrinsic fluorescence spectra of BPL (70 $\mu\text{g/ml}$) and WFL (62 $\mu\text{g/ml}$) in presence of ANS **B.** Far UV CD scans of BPL (0.29 mg/ml) and WFL (0.31 mg/ml), **C.** Near UV CD scan of BPL (0.9 mg/ml) and WFL (1 mg/ml) incubated at pH 1.0 and 8.0 for 24 h. **D.** Intrinsic fluorescence spectra of BPL (70 $\mu\text{g/ml}$) and WFL (62 $\mu\text{g/ml}$) at pH 8.0 and pH 1.0.

3.3.5.1 Solute quenching studies at pH 1.0

At pH 1.0, the surface tryptophans in BPL were observed (higher K_{sv}) in higher positive charge density confirming the altered conformation of the molten globule (Table 1A and 1B). There was hardly any change in the microenvironment of molten globule of WFL (Fig. 7A and 7B).

3.3.5.2 Effect of temperature on acid induced intermediate species

Molten globule like intermediates of both the lectins are less stable compared to native protein as their thermal transitions started at lower temperature. For native BPL, transition was seen above 65 °C (Fig. 2D) and that at pH 1.0 was observed above 55 °C (Fig. 7C). For native WFL, transition was seen above 75 °C (Fig. 2E) and that at pH 1.0 was observed above 60 °C (Fig. 7D). No shift in λ_{max} was observed in BPL at pH 1.0. Whereas, WFL showed shift in λ_{max} from 332 nm to 365nm and unfolding was observed at 70 °C (Fig.7E, 7F).



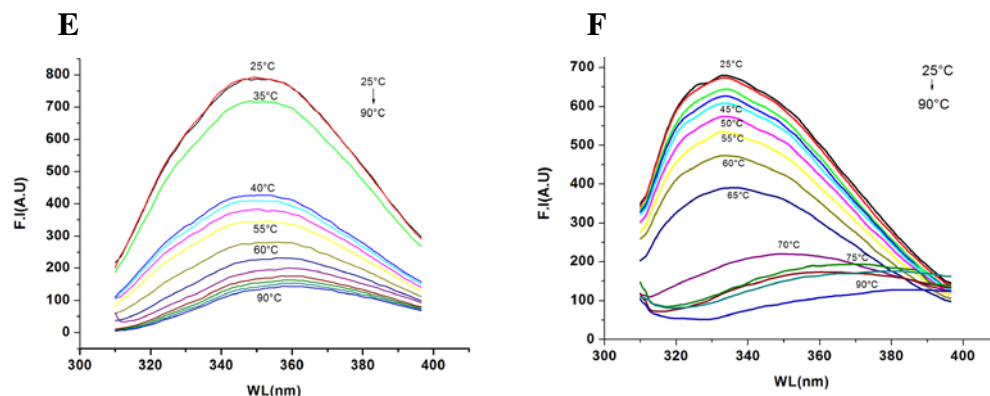
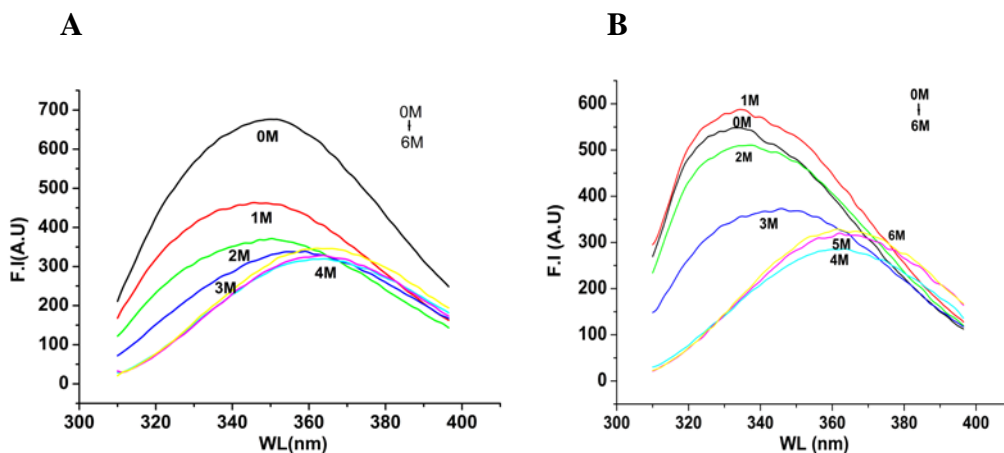


Figure 7: Effect of temperature on Molten globule intermediate: A and B. Solute quenching studies of BPL and WFL incubated at pH 1.0. **C. and D.** Far UV-CD spectra of BPL (0.29 mg/ml) and WFL (0.31 mg/ml) **E and F.** Intrinsic fluorescence scan of BPL and WFL at pH 1.0 incubated at temperatures (25–90 °C)

3.3.6 Effect of GdnHCl

Loss of structure in presence of 1.0 M- 6.0 M GdnHCl was observed in molten globule like forms of both the lectins. Red shift in the λ_{\max} of fluorescence from 349 nm to 363 nm in BPL, 330 to 368 in WFL was observed (Fig. 8A, 8B). Shift in negative ellipticity minima was monitored through Far-UV CD scans upto 24 h of incubation (Fig. 8C, 8D and 8E)

Unfolding transitions of molten globule species of both the lectins in presence of GdnHCl occur between 3.0 and 4.0 M, much similar to that observed in native BPL and WFL.



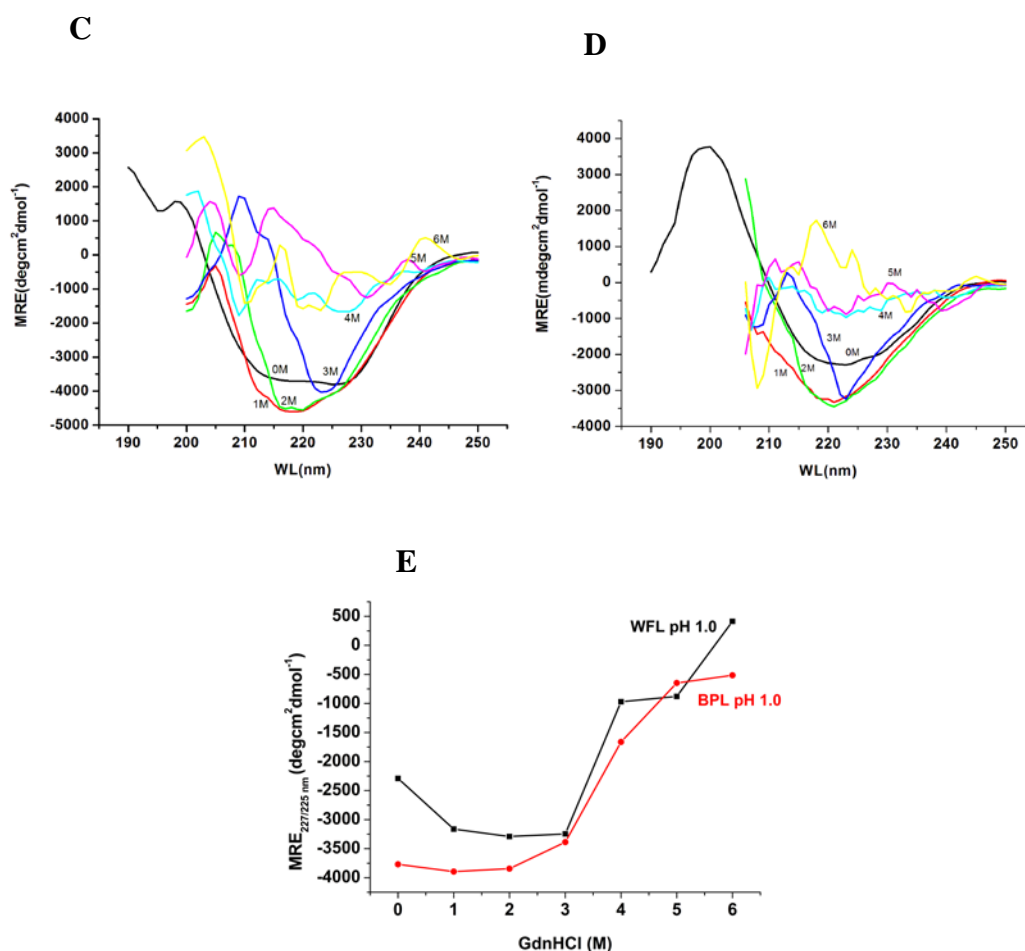


Figure 8: Effect of GdnHCl on molten globule intermediate: A and B. Intrinsic fluorescence scan of BPL and WFL at pH 1.0, **C and D.** CD scans of BPL and WFL at pH 1.0 **E.** MRE at 227 nm of BPL and at 225 nm of WFL at pH 1.0 incubated in GdnHCl (0–6.0 M) after 24 h, respectively.

3.4 Conclusion

Present studies have demonstrated systematic presentation of conformational and functional transitions of the two medicinally important legume lectins at molecular level. Detailed biochemical and biophysical characterization of the leguminous lectins from *Bauhinia purpurea* and *Wisteria floribunda* was performed. Fluorimetric characterization revealed different tryptophan microenvironment for both the lectins. These lectins were structurally stable in wide range of pH. BPL and WFL demonstrated multistate unfolding in presence of chemical denaturant whereas they behaved differently to thermal transitions. Lectins displayed formation of intermediate species at pH 1.0 which were further characterized as “molten globule like species”. Similar and differential transitions of BPL and WFL have been summarized in Fig. 9A and B. The studies showed complex

nature of protein. Although not proved unequivocally, plant lectins are proposed to be involved in defense mechanism. The lectins could be fulfilling this role due to the reasonable stability under harsh conditions. The above studies have provided valuable insights thereby offering perceptions into the molecular basis of their activity and stability.

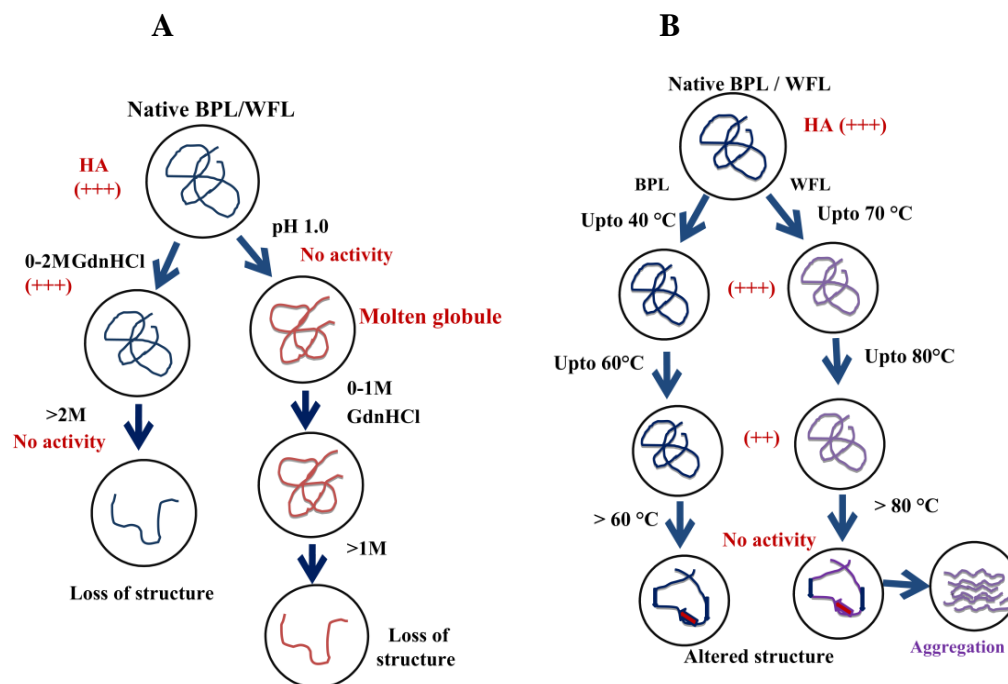


Figure 9: Schematic representation of **A. Similar (Chemical)** **B. Differential (Thermal)** transitions in BPL and WFL.

References

1. K. Dill and J. MacCallum (2012) The protein-folding problem, 50 Years on, *Science*. 338, 1042-1046.
2. D.T. Haynie and E. Freire (1993) Structural energetics of the molten globule state. *Proteins*. 16, 115-140.
3. M. Ohgushi and A. Wada (1983) 'Molten-globule state': a compact form of globular proteins with mobile side-chains, *FEBS Letters*. 164.
4. M.J.J. Dijkstra, W.J. Fokkink, J. Heringa, E. van Dijk and S. Abeln (2018) The characteristics of molten globule states and folding pathways strongly depend on the sequence of a protein, *Molecular Physics*, 116 (21-22), 3173-3180.

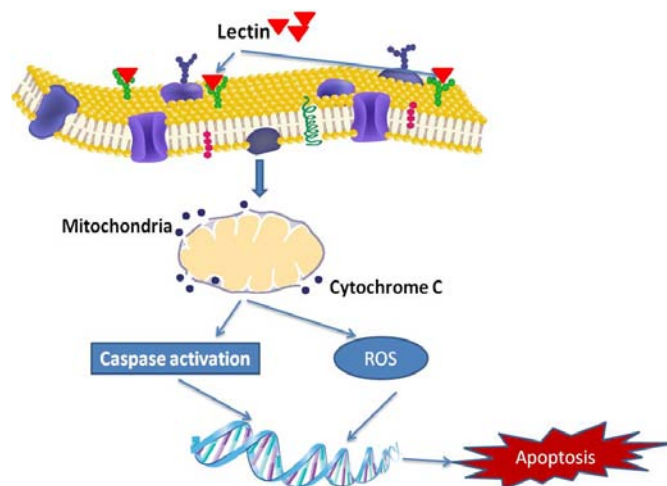
5. B.C. Lee, P.A. Croonquist, T.R. Sosnick, and W.D. Hoff (2001) PAS Domain Receptor photoactive Yellow Protein is converted to a Molten Globule State upon activation, *The Journal of Biological Chemistry*. 276 (24), 20821–20823.
6. W. Robert, A. Bailey, A.K. Dunker, C.J. Brown, E.C. Garner and M.D. Griswold (2001) Clusterin, a Binding Protein with a Molten Globule-like Region, *Biochemistry*. 40 (39), 11828-11840.
7. S.J. Park, B.N. Borin, M.A. Martinez-Yamout and H.J. Dyson (2011) The client protein p53 adopts a molten globule-like state in the presence of Hsp90, *Nat Struct Mol Biol*. 18(5), 537–541.
8. A.P. Bom, M.S. Freitas, F.S. Moreira, D. Ferraz, D. Sanches, A.M. Gomes, A.P. Valente, Y. Cordeiro and J.L. Silva (2010) The p53 core domain is a molten globule at low pH: functional implications of a partially unfolded structure. *J Biol Chem*. 285(4), 2857-66.
9. G.B. Reddy, V.R. Srinivas, N.Ahmad and A.Surolia (1999) Molten Globule-like state of peanut lectin monomer retains its carbohydrate specificity: implications in protein folding and legume lectin oligomerization, *J Biol Chem*. 274(8), 4500–4503.
10. F. Hart and M. Hayer-Hartl (2009) Converging concepts of protein folding in vitro and in vivo, *Nature Struct. Biol*. 16, 574-81.
11. A. Bartlett and S. Radford (2009) An expanding arsenal of experimental methods yields an explosion of insights into protein folding mechanisms. *Nature Struct. Biol*, 16, 582-588.
12. D. Van Der Spoel, L. Erik, B. Hess, G. Groenhof, A. Mark and H.J.C. Berendsen (2005) GROMACS: fast, flexible, and free. *J. Comput. Chem*. 26, 1701-18.
13. J. Klauda, M. Richard, J. Alfredo Freitas, J. W. O'Connor, D. J. Tobias, C. Mondragon-Ramirez, I. Vorobyov, A. D. MacKerell Jr. and W. Richard (2010) Update of the CHARMM all-atom additive force field for lipids: validation on six lipid types, *J. Phys. Chem. B*. 114, 7830-43.
14. T. Darden, Y. Darrin and L. Pedersen (1993) Particle Mesh Ewald: an N.log (N) method for Ewald sums in large systems, *J. of Chem. Phys*. 98, 10089-92.
15. G. Bussi, D. Donadio and M. Parrinello (2007) Canonical sampling through velocity rescaling, *J. Chem. Phys*. 126 doi: 10.1063/1.2408420.

16. M.F. Siddiqui and B. Bano (2018) Insight into the functional and structural transition of garlic phytocystatin induced by urea and guanidine hydrochloride: a comparative biophysical study, *Int. J. Biol. Macromol.* 106, 20–29.
17. A. Blumlein and J.J. Mcmanus (2013) Reversible and non-reversible thermal denaturation of lysozyme with varying pH at low ionic strength, *Biochim. Biophys. Acta Protein Proteomics.* 1834, 2064–2070.
18. P. Yadav, G. Shahane, S. Ramasamy, D. Sengupta and S. Gaikwad (2016) Structural-functional insights and studies on saccharide binding of *Sophora japonica* seed lectin, *Int. J. Biol. Macromol.* 91, 75–84 .
19. U. Sharma, S.M. Gaikwad, C.G. Suresh, V. Dhuna, J. Singh and S.S. Kamboj (2011) Conformational transitions in *Ariesaema curvatum* lectin: Characterization of an acid induced active molten globule, *J. Fluoresc.* 21, 753–763.
20. W. Wang, Protein aggregation and inhibition in biopharmaceutics, *Int. J. Pharm.* 289 (2005) 1–30.
21. P. Yadav, G. Shahane and S. Gaikwad (2017) *Amaranthus caudatus* lectin with polyproline II fold: conformational and functional transitions and molecular dynamics, *J. Biomol. Struct. Dyn.* 1102, 1–13
22. S.M. Gaikwad, M.M. Gurjar and M.I. Khan (2002) *Artocarpus hirsuta* lectin differential mode of chemical and thermal denaturation, *Eur. J. Biochem.* 269, 1413–1417.
23. A.A. Sahasrabudde, S.M. Gaikwad and M.V. Krishnasastry (2004) Studies on recombinant single chain Jacalin lectin reveal reduced affinity for saccharides despite normal folding like native Jacalin, *Protein Sci.* 3264–3273.
24. M. Wakankar, K. Patel, M. Krishnasastry and S. Gaikwad (2013) Solution and in silico ligand binding studies of *Cicer arietinum* lectin, *Biochem. Physiol.* S2.
25. M. Chatterjee and D.K. Mandal (2003) Denaturant-induced equilibrium unfolding of concanavalin A is expressed by a three-state mechanism and provides an estimate of its protein stability, *Biochim. Biophys. Acta.* 1648, 174–183.
26. D. Sen and D.K. Mandal (2011) Pea lectin unfolding reveals a unique molten globule fragment chain, *Biochimie.* 93, 409–417.
27. G. Ghosh and D.K. Mandal (2012) Differing structural characteristics of molten globule intermediate of peanut lectin in urea and guanidine-HCl, *Int. J. Biol. Macromol.* 51, 188–195.

28. M. Chatterjee and D.K. Mandal (2003) Kinetic analysis of subunit oligomerization of the legume lectin soybean, *Biochemistry*. 12217–12222.
29. U.V. Katre, C.G. Suresh, M.I. Khan and S.M. Gaikwad (2008) Structure-activity relationship of a hemagglutinin from *Moringa oleifera* seeds, *Int. J. Biol. Macromol.* 42, 203–207.
30. P.N. Dharker, S.M. Gaikwad, C.G. Suresh, V. Dhuna, M.I. Kahan, J. Singh and S.S. Kamboj (2008) Comparative studies of two araceous lectins by steady state and Timeresolved fluorescence and CD spectroscopy, *J. Fluoresc.* 9, 239–248.
31. P.K. Nareddy and M.J. Swamy (2018) Differential scanning calorimetric and spectroscopic studies on the thermal and chemical unfolding of cucumber (*Cucumis sativus*) phloem exudate lectin, *Int. J. Biol. Macromol.* 106, 95–100.
32. J.M. Khan, A. Qadeer, E. Ahmad, R. Ashraf, B. Bhushan, S.K. Chaturvedi and R.H. Khan (2013) Monomeric banana lectin at acidic pH overrules conformational stability of its native dimeric form, *PLoS One.* 8.
33. N. Salimi, B. Ho and D. Agard (2010) Unfolding simulations reveal the mechanism of extreme unfolding cooperativity in the kinetically stable a-lytic protease, *PLoS Comput Biol.* 6(2), e1000689.
34. G.V. Semisotnov, N.A. Rodionova, O.I. Razgulyaev, V.N. Uversky, A.F. Gripas and R.I. Gilmanshin (1991) Study of the “molten globule” intermediate state in protein folding by a hydrophobic fluorescent probe, *Biopolymers.* 31, 119–128.

Chapter 4

Anticancer activity of lectins from *Bauhinia purpurea* and *Wisteria floribunda* on Breast cancer MCF-7 cell lines



Abstract

The antiproliferative activity of two N-acetyl galactosamine specific lectins from *Bauhinia purpurea* and *Wisteria floribunda* was studied on MCF-7 Breast cancer cell lines. These agglutinins caused remarkable concentration-dependent antiproliferative effect on MCF-7 as determined using MTT assay. The values were approximately 446 μgml^{-1} (2.2 μM) and 329 μgml^{-1} (2.8 μM) for BPL and WFL, respectively. The inhibitory effect of these lectins was seen to be a consequence of binding of the lectin to cell surface and triggering S and G2 phase arrest revealed by flow cytometry studies. BPL and WFL induced apoptosis in MCF-7 cells associated with lactate dehydrogenase leakage, cell cycle arrest and reactive oxygen species generation. Apoptotic signal was observed to be amplified by activation of caspase-3 resulting in cell death. Therefore, these lectins could be called as a group of molecules possessing antitumor activity against breast cancer cells.

4.1 Introduction

Lectins, being saccharide binding specific proteins, are used as tools in the fields of cell biology, biochemistry, and immunology, as well as for therapeutic and diagnostic purposes in cancer research. Plant lectins as a bioactive principles received special attention in cancer prognosis because of their ability to activate various biological processes, such as cell agglutination and immune modulation. They also exhibit anti-viral and antimicrobial activities. Additionally, some lectins are able to recognize altered pattern of glycans on tumor cells and can differentiate them from normal cells [1]. Due to the specificity and selectivity properties of lectins they are known to induce cytotoxicity into tumor cells [2]. Among the major lectin families, significant amount of work has been done on legume and type 2 ribosome inactivating proteins (RIPs) due to their remarkable anti-neoplastic activity [3].

ConA by inducing apoptosis shows anti-tumor activity. The type 2 RIPs mistletoe lectins (MLs), trigger apoptosis through mitochondria/death receptor pathways [4]. One of the successful clinical translations of lectin used as diagnosis tools is *Lens culinaris* agglutinin (LCA). LCA, a plant lectin extracted from lentil seed, which bind specifically to α 1-6 fucose, has been used to diagnose hepato cellular carcinoma (HCC). Lectins have also been investigated for their potential in ovarian cancer diagnosis [5]. *Amaranthus caudatus* agglutinin (ACA), *Artocarpus integrifolia* agglutinin (AIA), *Arachis hypogea* agglutinin (AHA), *Vicia villosa* lectin (VVL), *Griffonia simplicifolia* agglutinin I (GSA I)

and *Ulex europaeus* agglutinin I (UEA I) are a group of lectins that recognize Thomsen-Friedenreich (T) antigen, Thomsen-nouvelle (Tn) and sialyl-Thomsen Friedenreich antigen. *Glycine max* agglutinin (GMA) could potentially be used for ovarian cancer diagnosis. Ricin (RCA), one of the first discovered lectins, is an ideal example of how lectins can both specifically target and induce cell death [6].

Furthermore, to distinguish metastatic from non metastatic breast cancer patients, Fry et al. designed lectin microarrays consisting of 45 lectins with different binding preferences. Serum and urine samples were then analyzed for binding differences. *Bauhinia purpurea* lectin (BPL) showed significantly higher binding in metastatic compared to non-metastatic urines samples [7]. Moreover, WFL binds to LacdiNAc which is a cancer glycomarker associated with leukemia, prostate, pancreatic, ovarian, and liver cancers [8]. WFL is currently considered as the most prominent diagnostic lectin against cholangiocarcinoma [9].

In the present study, we have tried to characterize two legume lectins, BPL and WFL for the antiproliferative and apoptosis activity.

4.2 Materials and Methods

4.2.1 Lectins

Bauhinia purpurea lectin (BPL) and *Wisteria floribunda* lectin (WFL) were procured from Vector Labs, USA.

4.2.2 Cell Line and Culture Conditions

Human breast cancer cell line (MCF-7) was procured from the National Centre for Cell Science (NCCS), Pune, India. These cells were grown and maintained in a high glucose concentration (4.5 g/L) Dulbecco's modified eagle medium (DMEM) supplemented with 10 % fetal bovine serum, 100 U/ml penicillin and 100 mg/ml streptomycin in a humidified CO₂ incubator at 37°C. Cells were counted using a haemocytometer and plated for 24 hr before the addition of lectin.

4.2.3. Antiproliferative effect of lectins on human cancer cell line

MTT assay

Tetrazolium derivative reduction assay (Sigma) was used to determine cell viability after cell-lectin incubation. As living cells respire, their mitochondrial dehydrogenases reduce yellow MTT (3-[4, 5- dimethylthiazol-2-yl]-2, 5-biphenyl tetrazolium bromide) to yield

purple crystals. The intensity of the coloured product formed, due to the formation of the formazon crystals, is directly proportional to the number of live cells in each sample. MTT cell count is similar to a direct cell count and it is an important method for studies of cell viability [10].

Cells were plated in a 96-well plate at a density of 5,000–7,000 cells per well and grown overnight in 10 % fetal bovine serum (FBS). After 24 hr, cells were replenished with fresh media. Then 100 µl of different concentrations of the lectin (100-500 µg/ml) were added to wells in triplicate. Cells were incubated with the lectin for 24 h after which 20 µl of MTT dye (5 mg/ml) was added to each well followed by further incubation for 4 h. Before read-out, precipitates of formazon crystal formed were dissolved in 200 µl of dimethyl sulphoxide (DMSO) using a shaker for 15 min. All steps after MTT additions were performed in the dark. Absorbance was measured at 550 nm. The cell % inhibition was calculated using the following formula:

$$\text{Cell proliferation inhibition (\%)} = [1 - (A_s/A_c)] \times 100$$

where: A_s – absorbance of sample; A_c – absorbance of control.

4.2.4. Lactate dehydrogenase leakage assay

To assess the cell membrane integrity, lactate dehydrogenase (LDH) cytotoxicity assay kit (Sigma-Aldrich USA) was employed. The assay takes the advantage of LDH measurement as released from the damaged cells into the medium [11]. Briefly, to the plated cells (1×10^4 cells per well), 100-500 µg/ml lectin was added and re-incubated for 24 hr. By adding 1 % triton to the control cells, positive control was prepared at 45 min prior to the centrifugation. Following centrifugation at 3000 x g for 5 min, 100 µl of the supernatant of each well was transferred to a new culture plate and absorbance was read at 490 nm.

The LDH leakage (% of positive control) is expressed as the percentage of

$$(\text{OD}_{\text{test}} - \text{OD}_{\text{blank}}) / (\text{OD}_{\text{positive}} - \text{OD}_{\text{blank}}),$$

Where OD_{test} is the optical density of lectin exposed cells, $\text{OD}_{\text{positive}}$ is the optical density of the positive control cells and OD_{blank} is the optical density of the wells without cells.

4.2.5. Reactive Oxygen Species Assay (ROS Assay)

The ROS assay was performed using a kit of Sigma-Aldrich (USA) employing 2, 7'-dichloro dihydro fluorescein diacetate (DCFH-DA) as a dye. Briefly, MCF-7 cells (1×10^6

cells per well) were treated either with 100-500 µg/ml lectin, tamoxifen or DMSO as a control. The 24 hr incubated cells having cell density of 1×10^6 cells per well were washed with 200 µl phosphate buffer saline (PBS). To each well, 100 µl of 1X dye was added and incubated at 37 °C for 30 min in dark. Thereafter, cells were washed with PBS for about 3-4 times and lectin with different concentrations was introduced. In addition, positive controls were maintained containing 200 mM H₂O₂. The DCFH oxidation induced fluorescence in the cells was read at 480 and 530 nm for excitation and emission wavelengths respectively. At every 5 min, data points were measured for 30 min.

The ROS level is expressed as the ratio of $(F_{\text{test}} - F_{\text{blank}}) / (F_{\text{control}} - F_{\text{blank}})$,

Where F_{test} is the fluorescence intensity of the cells exposed to lectin or the positive control, F_{control} is the fluorescence intensity of the control cells, and F_{blank} is the fluorescence intensity of the wells without cells.

4.2.6. Assay of Caspase-3 Activity

The caspase-3 activity in the cell lysate was determined following manufacturer's instructions given in the kit(Sigma-Aldrich USA) [12]. Briefly, MCF-7 cells (1×10^6 cells per well) were treated either with 100-500 µg/ml lectin, tamoxifen or DMSO as a control. After 24 hr incubation at 37° C in a humidified 5 % CO₂ incubator, 100 µl of caspase-3 reagent was added to each well containing 100 µl of blank, negative control cells, or treated cells in culture medium. After mixing the contents of wells using a plate shaker for 30 seconds, plates were incubated at room temperature for 2 hr and luminescence was measured.

4.2.7 Cell Cycle Analysis

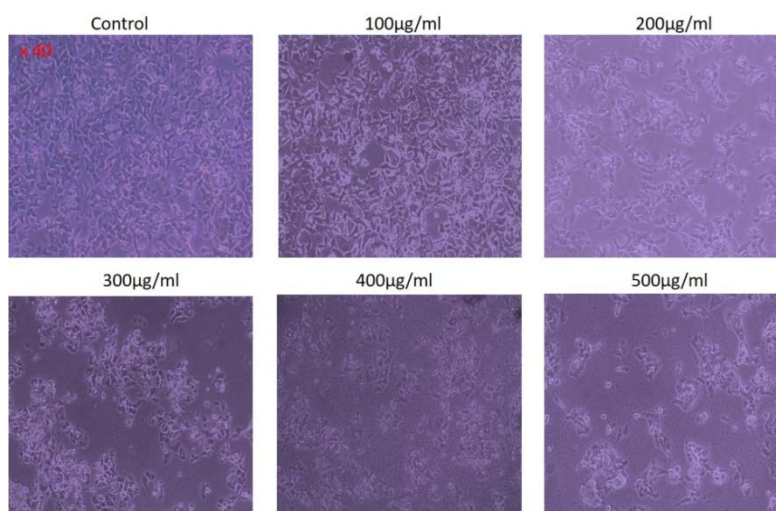
MCF-7 cells (5×10^5 per well) in a six well plate were incubated (37 °C, 5 % CO₂) with 80 µg/ml of purified lectin and DMSO as a control vehicle suspended in media for 24 hr. Following trypsinization, the washed cells were centrifuged at 2000 x g for 10 min and the pellet was resuspended in 0.5 ml PBS. By adding 1.2 ml of 70 % cold ethanol for 2 hr and the fixed cells were washed with PBS and subsequently centrifuged at 2000 x g for 10 min. To the suspending cells (0.3 ml in PBS), 20 mg/ml RNAase was added and incubated for 1 hr. Thereafter, propidium iodide (0.5 mg/ml) was added and cells were incubated at 4 °C for 30 min. The cell cycle parameters were studied using Beckman Coulter flow cytometer. The spectrum was recorded with an excitation wavelength of 488 nm and emission at 670 nm [13].

4.3 Results

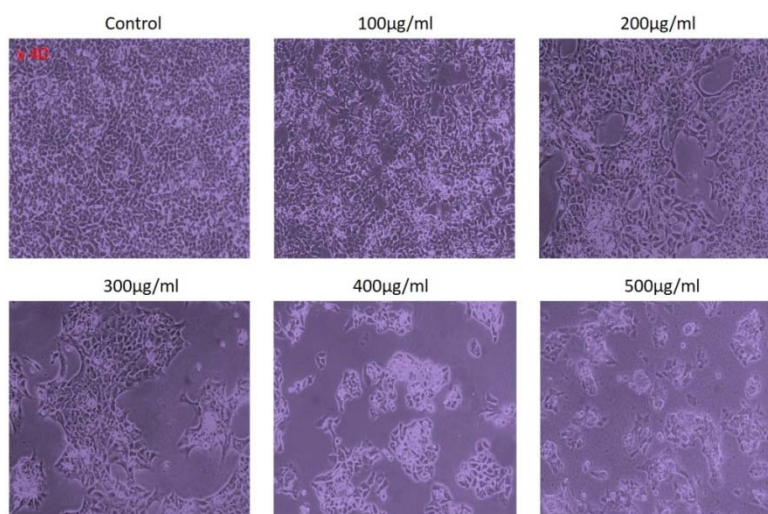
4.3.1 MTT assay

MTT assay on human breast cancer cell line MCF-7 was performed to examine cytotoxic effect of BPL and WFL. A standard anticancer drug tamoxifen was used as a positive control. The results on the survival of MCF-7 cells treated with the lectin and tamoxifen after 24 hr are expressed depicting that the response of MCF-7 cancer cells against lectin/tamoxifen is dose dependent with increased cytotoxicity. MCF-7 cells retained 35-38.5 % viability with 500 µg/ml of the lectins after 24 hr incubation, while the untreated cell showed only 5 % decrease in growth thereby retaining 95 % viability (Fig.1) indicating that the lectin exhibits significantly higher toxicity towards cancer cells. The cell viability of the cancer cells for lectins compared to the tamoxifen suggests that both the lectins BPL and WFL may possibly have potential as an anticancer agent.

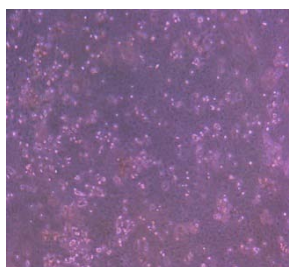
A.BPL



B.WFL



C. Tamoxifen



D.

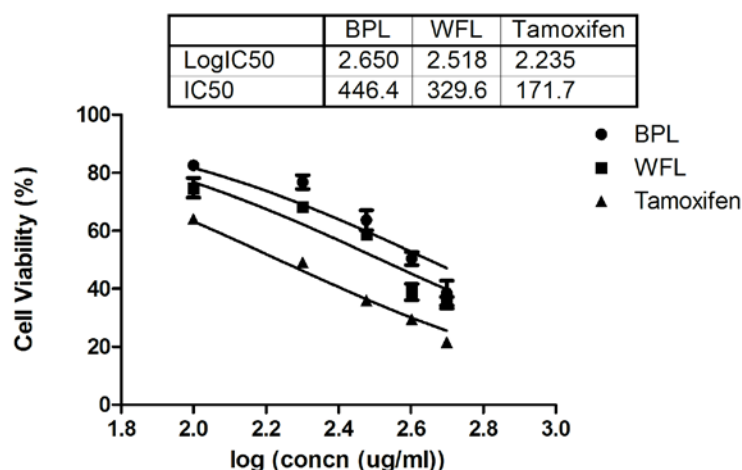


Figure 1: Morphological changes and microscopic analysis of MCF-7 cells after 24 hr treatment with lectins (100-500 $\mu\text{g/ml}$), A. BPL B. WFL C. tamoxifen (positive control) and DMSO (as a control) D. Cell viability.

4.3.2 LDH Release Assay

LDH activity in cell culture is an important indicator for cytotoxicity. LDH is an intracellular enzyme, leaking out of cells to cell culture medium, relates to unhealthy condition such as loss of cell membrane integrity. The level of LDH released from the cells significantly increased after 24 hr of exposure to 100-500 $\mu\text{g/ml}$ of lectins as compared to untreated cells (Fig.2) The pattern of LDH released from MCF-7 cells treated with lectin suggest that the cytotoxic effect of the lectin is concentration dependent. The percentage of LDH released from MCF-7 cells after 24 hr of exposure to 500 $\mu\text{g/ml}$ lectins were 76.62 % for BPL, 80.7 % for WFL while with tamoxifen it was 98.0 %.

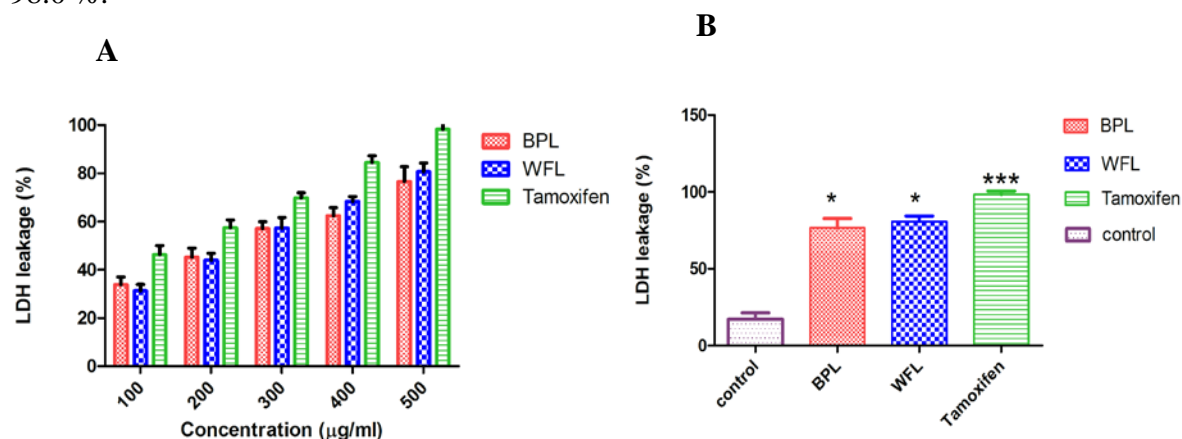


Figure 2: The levels of LDH released into the medium from untreated control and lectins treated MCF-7 cells for 24 hr. A. 100-500 $\mu\text{g/ml}$ B. At 500 $\mu\text{g/ml}$ concentration of BPL and WFL, Values are mean \pm SD (n=3)

4.3.3 ROS Generation

The reactive oxygen species (ROS) released on cell metabolism plays critical role in mediating cytotoxicity that contribute to cell cycle arrest leading to cellular apoptosis. The effect of lectin treatment on ROS generation in MCF-7 cells was therefore studied (Fig. 3). Intracellular ROS production was measured by DCFH oxidation in cells treated with lectin at a dosage of 100-500 $\mu\text{g/ml}$ for 24 hr. There was 2.5-2.7 times fold change in DCF fluorescence of lectin treated cells at 500 $\mu\text{g/ml}$ concentration of BPL and WFL indicating significant increase in the ROS generation as compared to control (tamoxifen treatment). It can be predicted that lectins at said concentration exhibited pro-oxidant activity through enhancement of intracellular ROS and are capable of modulating the redox state of MCF-7 cells.

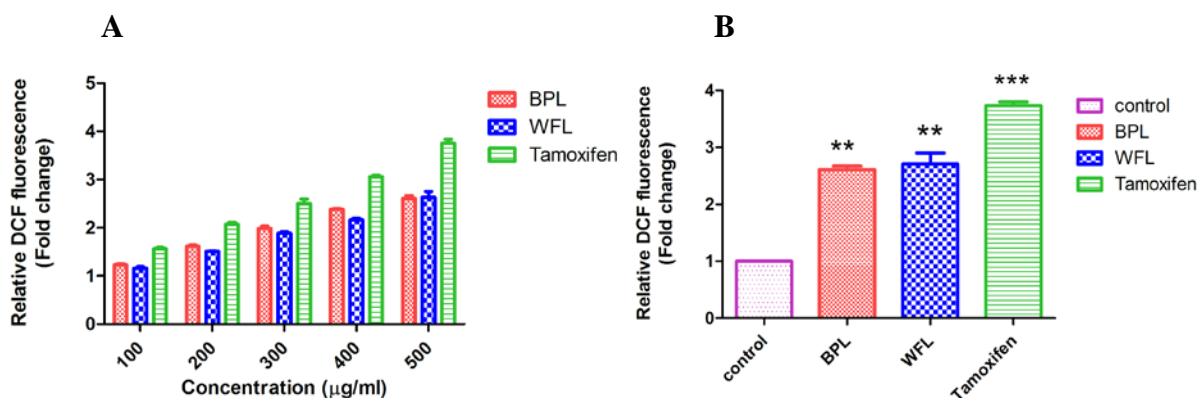


Figure 3: ROS production induced by lectins on MCF-7 cells for 24hr. A. 100-500 $\mu\text{g/ml}$ B. At 500 $\mu\text{g/ml}$ concentration of BPL and WFL Values are mean \pm SD (n=3)

4.3.4 Caspase 3 activity assay

Caspase-3 plays a central role in the caspase cascade showing characteristics of apoptotic pathway. The initiation and activation of caspases is studied in mitochondrial dependent apoptosis. The BPL and WFL at 500 $\mu\text{g/ml}$ treatment for 24 hr caused a significant ($P < 0.05$) increase in caspase-3 activation compared to tamoxifen and control (Fig. 4).

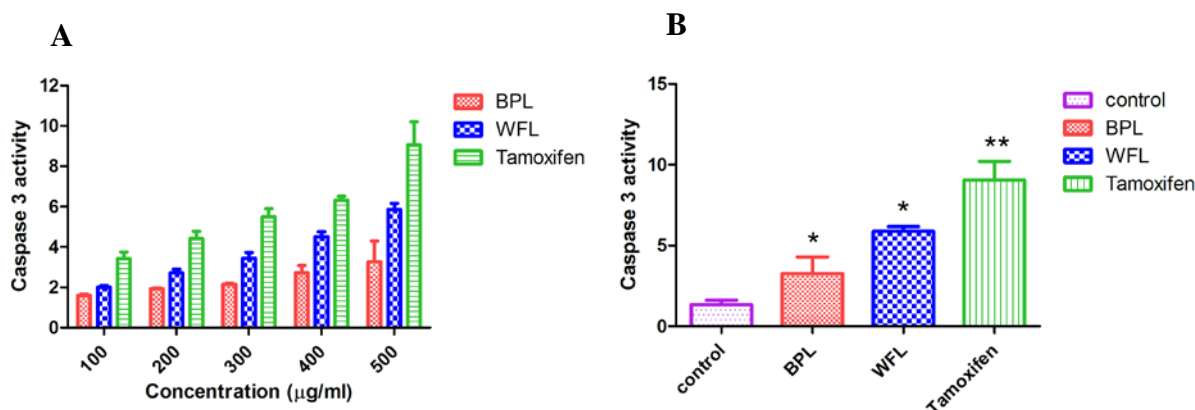
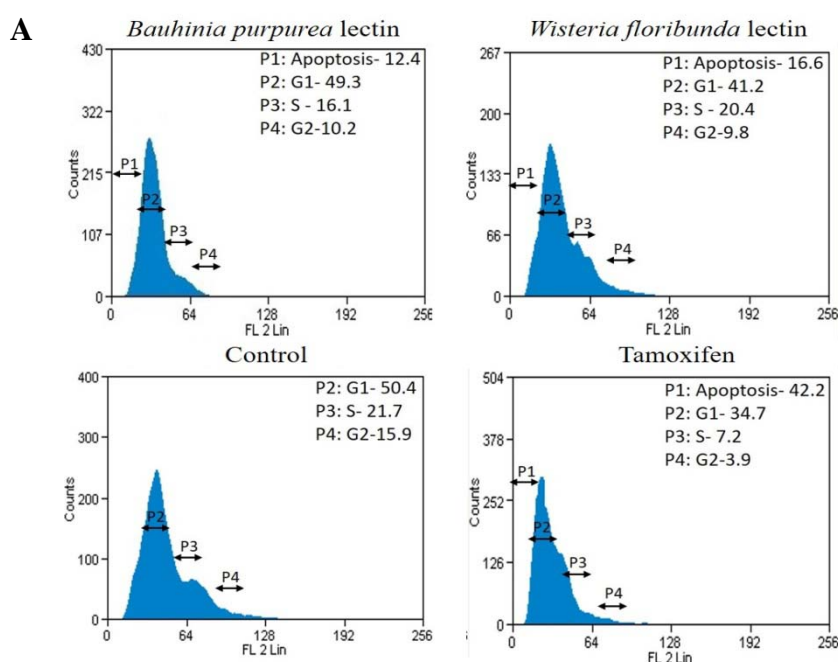


Figure 4: Effects of lectins on Caspase-3 activity of MCF-7 cells. A. 100-500 µg/ml B. At 500 µg/ml concentration of BPL and WFL Values are mean \pm SD (n=3)

4.3.5 Cell Cycle Assay

The effect of lectins on cell cycle progression using propidium iodide staining was analyzed. Untreated control cells showed all phases of the cell cycle; G0/G1, S and G2/M. Effect of both BPL and WFL on MCF-7 cells appeared similar at 500 µg/ml concentration arresting the cells at S and G2 phase with substantial decline of cell numbers. The percentage of lectin and tamoxifen treated cells partitioned between different phases of cell cycle is presented in Figure 5. BPL and WFL treatment resulted into decreased cell population leading to 12 and 16 % cell proportion, respectively damaged by apoptosis.



B

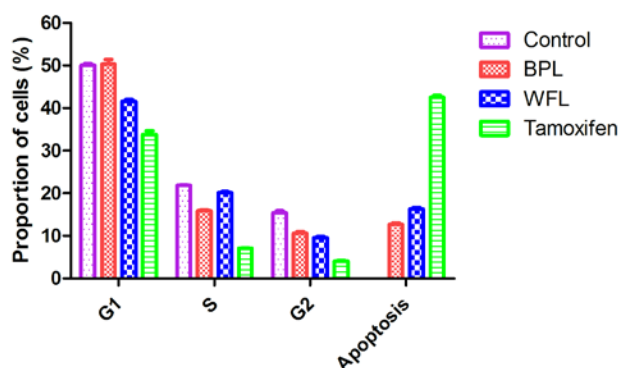


Figure 5: Induction of cell cycle arrest and apoptosis in lectin treated MCF-7 cells.

Cell cycle analysis output of MCF-7 A. cells after 24 hr of incubation with BPL, WFL (500 $\mu\text{g/ml}$). Proportion of MCF-7 B. Cells in apoptosis, G1, S, G2 and apoptosis phases after 24 hr of treatment with lectin.

4.4 Discussion:

Numerous anticancer agents from natural sources including plants, animals, microbes and marine organisms have been obtained. Lectins, have gained more attention in identification of cancer and degree of metastasis due to the property of selectivity and specificity. Several reports are available on apoptotic and cytotoxic activity of lectins on tumor cells. In previous study, we have shown that both the lectins from *Bauhinia purpurea* and *Wisteria floribunda* bind to T-antigen (Gal β 1-3 GalNAc) which is over expressed in cancer cells; WFL has extended binding to LacdiNAc which is also a glycomarker [16]. In the present study, we have investigated potential anticancer property of BPL and WFL. MCF-7 cell lines are flat and spread before treatment. However, on treatment with lectins and tamoxifen, significant changes in the cell structure were observed in microscopic images. Lectin treated cells showed cell shrinkage, membrane breakage with few cells detached from the plate and coming out in the medium as floating cells. LDH is a reliable and accurate marker of cytotoxicity. The cytotoxic agents exert damage to cell membranes and permit intracellular LDH molecules to leak into culture medium. Cell membrane integrity associated with necrosis is thus reflected by LDH leakage [17]. In the present study, the LDH leakage increased significantly in high dose of lectin compared to the control cells.

Reactive oxygen species (ROS) such as superoxide and hydrogen peroxide are continuously produced during metabolism. ROS generation is often counterbalanced by the action of antioxidant enzymes and other redox molecules. However, excess ROS can

lead to cellular injury in the form of damaged DNA, lipids and proteins [18]. In the present studies, significant increase in ROS was observed with treatment with lectins.

Caspases belong to cysteine proteases family. Caspase-3 plays an important role in apoptosis. Signaling from cell death receptors or mitochondria activate caspases. The occurrence of apoptosis is correlated to increase in caspase 3 activity [19]. Previously, in case of two chitotriose specific lectins, Singh et al. (2016) demonstrated the mechanism of cell death leading to apoptosis is through caspase-3 activity [20].

Flow cytometric analysis showed the lectin induced cell cycle arrest and apoptosis in MCF-7 cells. The proposed mechanism for the interconnection between cell cycle regulation and apoptosis rely on the up-regulation of p21 upon treatment with therapeutic agents [21]. The induction of cell cycle arrest leading to apoptosis is a common mechanism through which studies on a number of anticancer drugs inhibiting tumor growth can be undertaken. In this study, we found that BPL and WFL arrest S and G2-phase of cell cycle at 500 µg/ml concentration. This dose resulted in 12-16 % apoptosis in the cell density. Moreover, as a hallmark of apoptosis, fragmentation could be observed in lectin treated MCF-7 cells. Our results correlate well to similar studies carried out earlier in case of chickpea lectin [14].

The plant lectins show differential cytotoxic impact on cancer cell lines. Several earlier reports describe lectin induced apoptosis through caspase activity in different cancer cell lines [15]. Moreno-Celis et al (2017) examined the cytotoxic effects of tepary bean lectins on colon cancer cells for its apoptotic activity. This lectin exhibited anti-proliferative and pro-apoptotic properties associated with the reduction of signal transduction pathway protein Akt and rise in caspase 3 activity, however not to p53 activation [22]. Estrada-Martínez et al. (2017) reviewed the efficacy of plant lectins as a modern tool against digestive system cancers [23]. Some of the *in vitro* studies described preferential attachment of certain lectins to the cancer cell [24]. Wheat germ agglutinin has displayed a feature of daunorubicin anti-resistant liposomes demonstrating anticancer efficacy in treatment of drug-resistant breast cancer [25]. Such studies may open up new vista to force plant lectins as a tool to increase the effectiveness of anticancer therapies.

References

1. E.G. De Mejía and V.I. Prisecaru (2005) Lectins as bioactive plant proteins: a potential in cancer treatment. *Crit Rev Food Sci.* 45, 42–445.
2. E.J.M. Van Damme, N. Lanno and W.J. Peumans (2008) Plant Lectins. In: J.C. Kader, M. Delseny (eds) *Advances in botanical research.* 48(Elsevier Ltd, San Diego),107–209.
3. B. Liu, H.J. Bian and J.K. Bao (2010) Plant lectins: potential antineoplastic drugs from bench to clinic. *Cancer Lett.* 287(1), 1–12.
4. S.Y. Lyu, S.H. Choi and W.B. Park (2002) Korean mistletoe lectin-induced apoptosis in hepatocarcinoma cells is associated with inhibition of telomerase via mitochondrial controlled pathway independent of p53. *Arch Pharm Res.* 25(1), 93–101.
5. F.S. Coulibaly and B.C. Youan (2017) Current status of lectin-based cancer diagnosis and therapy. *AIMS Molecular Science.* 4(1), 1-27
6. N. Sharon and H. Lis (2004) History of lectins: from hemagglutinins to biological recognition molecules. *Glycobiology.* 14, 53-62.
7. S.A. Fry, B. Afrough, H. Lomax-browne, J.F. Timms, L.S. Velentzis and A.J.C. Leathem (2011) Lectin microarray profiling of metastatic breast cancers. *Glycobiology.* 21, 1060–1070.
8. O. Haji-Ghassemi, M. Gilbert, J. Spence, M.J. Schur, M.J. Parker, M.J. Jenkins and S.V. Evans (2016) Molecular basis for recognition of the cancer glyco biomarker, LacdiNAc (GalNAc[β 1→4]GlcNAc), by *Wisteria floribunda* agglutinin. *J. Biol. Chem.* 29, 24085–24095.
9. A. Matsuda, A. Kuno, T. Kawamoto, H. Matsuzaki, T. Irimura, Y. Ikehara, Y. Zen, Y. Nakanuma, M. Yamamoto, N. Ohkohchi, J. Shoda, J. Hirabayashi and H. Narimatsu (2010) *Wisteria floribunda* agglutinin positive mucin-1 is a sensitive biliary marker for human cholangiocarcinoma. *Hepatology.* 52, 174–182.
10. M. Remmelink, F. Darro, Decaestecker, R. Decker, N. Bovin, Gebhart, H. Kaltner, H.J. Gabius, R. Kiss, I. Salmon and A. Danguy (1999) In vitro influence of lectins and neoglycoconjugates on the growth of three human sarcoma cell lines, *Journal of Cancer Research and Clinical Oncology*, 125(5), 275-285.
11. G. Fotakis and J.A. Timbrell (2006) In vitro cytotoxicity assays: comparison of LDH, neutral red, MTT and protein assay in hepatoma cell lines following exposure to cadmium chloride. *Toxicol. Lett.* 160(2), 171-177.

12. P.K. Ajji, M.J. Binder, K. Walder and M. Puri (2017) Balsamin induces apoptosis in breast cancer cells via DNA fragmentation and cell cycle arrest. *Mol. Cell. Biochem.* 432(1-2), 189-198.
13. B.B. Mishell and S.M. Shiigi (1980) Selected methods in cellular immunology. W H Freeman and Co. Oxford, UK. 1980.
14. N. Gupta, P.S. Bisen and S.S. Bhagyawant (2018) Chickpea lectin inhibits human breast cancer cell proliferation and induces apoptosis through cell cycle arrest. *Protein and Peptide Letters.* 25, 1-8.
15. L.H. Huang, Q.J. Yan, N.K. Kopparapu, Z.Q. Jiang and Y. Sun (2012) *Astragalus membranaceus* lectin (AML) induces caspase-dependent apoptosis in human leukemia cells, *Cell Prolif.* 45, 15–21.
16. S.B. Agrawal, D. Ghosh and S.M. Gaikwad (2019) Investigation of structural and saccharide binding transitions of *Bauhinia purpurea* and *Wisteria floribunda* lectins. *Arch. Biochem. Biophys.* 662, 134-142.
17. T. Decker and M.L. Lohmann-Matthes (1988) A quick and simple method for the quantitation of lactate dehydrogenase release in measurements of cellular cytotoxicity and tumor necrosis factor (TNF) activity. *J. Immunol. Methods.* 115(1), 61-69.
18. S. Kumari, A.K. Badana, G. Murali Mohan, G. Shailender and R.R. Malla (2018) Reactive Oxygen Species: A Key Constituent in Cancer Survival. *Biomarker Insights.* 13, 1–9.
19. G.S. Salvesen and V.M. Dixit (1999) Caspase activation: the induced proximity model. *Proc. Natl. Acad. Sci. USA*, 96(20):10964-10967.
20. R. Singh, L. Nawale, D. Sarkar and C.G. Suresh (2016) Two chitotriose-specific lectins show anti-angiogenesis, induces caspase-9-mediated apoptosis and early arrest of pancreatic tumor cell cycle. *PLoS ONE* 11(1): e0146110. doi:10.1371/ journal.pone.
21. D. Mundekkad, S. Thavamani, P.K. Satheeshkumar and P. Sulochana (2012) Purified mulberry leaf lectin (MLL) induces apoptosis and cell cycle arrest in human breast cancer and colon cancer cells. *Chem. Biol. Interact.* 200(1), 38-44.
22. U. Moreno-Celis, J. López-Martínez, A. Blanco-Labra, R. Cervantes-Jiménez, L.E. Estrada-Martínez, A.E. García-Pascalín, M.J. Guerrero-Carrillo, A.J. Rodríguez-Méndez, C. Mejía, R.A. Ferríz-Martínez and T. García-Gasca (2017) *Phaseolus acutifolius* lectin fractions exhibit apoptotic effects on colon cancer: Preclinical studies using dimethylhydrazine or azoxi-methane as cancer induction agents. *Molecules.* 22:E1670.

23. L.E. Estrada-Martínez, U. Moreno-Celis, R. Cervantes-Jiménez, R.A. Ferriz-Martínez, A. Blanco-Labra and T. García-Gasca (2017) Plant lectins as medical tools against digestive system cancers, *Int. J. Mol. Sci.* 18(7), 1403.
24. S. Mukhopadhyay, P.K. Panda, B. Behera, C.K. Das, M.K. Hassan, D.N. Das, N. Sinha, A. Bissoyi, K. Pramanik, T.K. Maiti et al.(2014) *In vitro* and *in vivo* antitumor effects of peanut agglutinin through induction of apoptotic and autophagic cell death. *Food Chem. Toxicol.* 64, 369–377.
25. S. Liu, X.L. Song, Y.H. Wang, X.M. Wang, Y. Xiao, X. Wang, L. Cheng and X.T. Li (2017) The efficacy of WGA modified daunorubicin anti-resistant liposomes in treatment of drug-resistant MCF-7 breast cancer. *J. Drug Target.* 25, 541-553.

Summary and Conclusion



Summary and Conclusion

The study of protein folding started as a challenge in basic sciences and still motivates researchers for understanding structure-function relationship. To understand the correlation, information is rendered by the primary structure i.e amino acid sequence and associated tertiary structure of protein. Development and advancement of classical techniques have accelerated the research in this field. Due to their different carbohydrate binding specificity, lectins from different sources i.e plants, animals, microorganisms have been studied for stability, folding/unfolding transitions and different applications.

In the present study, we have characterized two N-acetyl galactosamine binding lectins; 1. *Bauhinia purpurea* seed lectin and 2. *Wisteria floribunda* seed lectin, for their functional and conformational dynamics. We even have tried to investigate their effect on MCF-7 breast cancer cell lines.

The highlights of the study are:

Seed lectin from *Bauhinia purpurea* (BPL)


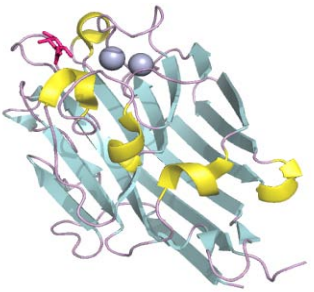
- **BPL homology model showed a Jelly roll motif**
- **It was functionally stable in presence of chaotropic agent indicating structural rigidity of the protein**
- **Higher affinity of BPL towards T-antigen specifies the extended binding site and application in cancer studies**
- **Structural rearrangements over the wide temperature range and no aggregation reflect complex structure of the protein**
- **BPL formed a molten-globule like structure at pH 1.0**
- **It showed cytotoxicity towards breast cancer cell lines MCF-7**

Lectin from *Wisteria floribunda*

- **Detailed investigation of sugar binding to WFL showed higher affinity and extended binding site for LacdiNAc over T-antigen.**
- **WFL showed simultaneous unfolding and aggregation at 80 °C**
- **It formed a molten-globule like structure at pH 1.0**
- **It showed cytotoxicity towards breast cancer cell lines MCF-7**

Comparative analysis of the conformational changes taking place in both the lectins is summarised below in Table 1:

Table 1: Comparison of the conformational changes in both the lectins BPL and WFL.

Lectin		<i>Bauhinia purpurea</i>	<i>Wisteria floribunda</i>
			
Secondary structure		β-sheet rich	
Specificity		N-acetylgalactosamine T-antigen disaccharide	N-acetylgalactosamine T-antigen disaccharide LacdiNAc
Thermal stability	Activity	50 °C	75 °C
	Structure	70 °C	80 °C
Stability in pH	Activity	8.0	
	Structure	Stable in pH 6.0-8.0 alteration in structure at acidic (2.0-4.0)and basic pH(10.0-12.0)	
Stability in GdnHCl	Activity	2M upto 24 hrs	
	Structure	2M upto 24 hrs	
Thermal aggregation		Not observed	At 85 °C
Molten Globule		At pH 1.0	

Our basic understanding of structure and function in detail has provided valuable insights into molecular basis of activity and stability. The cytotoxicity studies have further paved way for the use of these lectins in cancer diagnosis and treatment.

Publications

From thesis work

1. **Sanskruthi B. Agrawal**, Deepanjan Ghosh, Sushama M. Gaikwad (2019) Investigation of structural and saccharide binding transitions of *Bauhinia purpurea* and *Wisteria floribunda* lectin. **Archives of Biochemistry and Biophysics**, 662, 134–142. I.F 3.5.
2. **Sanskruthi B. Agrawal**, Neha Gupta, Sameer Bhagyawant , Sushama M. Gaikwad, Anticancer activity of *Bauhinia purpurea* and *Wisteria floribunda* lectin on Breast cancer MCF-7 cell lines.(Manuscript under review)

Other work

1. Ekta Shukla, **Sanskruthi B. Agrawal**, Sushama Gaikwad (2017) Conformational and functional transitions and in silico analysis of a serine protease from *Conidiobolus brefeldianus* (MTCC 5185). **International journal of biological macromolecule**,98, 387–397.I.F 3.9
2. Krishna Adeshara, **Sanskruthi Agrawal**, Sushama Gaikwad , Rashmi Tupe (2018) Pioglitazone inhibits advanced glycation induced protein modifications and down-regulates expression of RAGE and NF- κ B in renal cells. **International journal of biological macromolecule**, 119, 1154–1163. I.F 3.9

Oral and Poster presentations

Oral Presentations

1. **“Investigation of structural and saccharide binding transitions of *Bauhinia purpurea* and *Wisteria floribunda* lectin”** at NCL-RF Annual student conference 2018, NCL, Pune.
2. **“Biochemical and Biophysical Characterization of *Bahuina purpurea* lectin”** at International conference on ‘Nutrigenomics & Nutrigenetics Present and Future Scenario’ (ICONN 2016), held at K.T.H.M College, Nashik. **(Awarded Best Prize)**

Poster Presentations

1. **“GalNAc specific *Bauhinia purpurea* lectin: Characterization of acid induced molten globule”** at NCL Science Day 2017, NCL, Pune .
2. **“Investigation of structural and saccharide binding transitions of *Bauhinia purpurea* and *Wisteria floribunda* lectin”** at NCL science Day 2019, NCL, Pune **(Awarded Best Prize)**



Investigation of structural and saccharide binding transitions of *Bauhinia purpurea* and *Wisteria floribunda* lectins[☆]

Sanskruthi B. Agrawal^{a,b}, Deepanjan Ghosh^{a,b}, Sushama M. Gaikwad^{b,*}

^a Academy of Scientific and Innovative Research (AcSIR), India

^b CSIR-National Chemical Laboratory, Dr Homi Bhabha Road, Pune, 411008, India

ARTICLE INFO

Keywords:

Lectin
Saccharide binding
Homology model
Conformation
Thermal aggregation
Molten globule

ABSTRACT

Two novel medicinally important legume lectins from *Bauhinia purpurea* (BPL) and *Wisteria floribunda* (WFL) possessing extended sugar binding site were investigated for functional and conformational transitions using biochemical and biophysical techniques as well as bioinformatical tools. Homology model of BPL was constructed using the Schrodinger suite and docked with N-acetyl galactosamine and T-antigen disaccharide (Gal β 1-3GalNAc α O-Me). The longer loop D in the structure of WFL compared to that in BPL was found to be responsible for its specificity to LacdiNAc (β -D-GalNAc-[1 \rightarrow 4]-DGlcNAc) over Gal β 1-3GalNAc. BPL remained functionally stable up to 40 °C whereas WFL remained stable upto 70 °C indicating the strength of the sugar binding site geometry. Both the lectins showed intense but non-specific secondary structure in the range of 65–90 °C. WFL showed rapid aggregation above 80 °C as indicated by light scattering intensity. The lectins showed simultaneous dissociation and multistate unfolding in the vicinity of GdnHCl. At pH 1.0, both the lectins exhibited molten globule like structures, which were characterized further and were found to respond in a different way towards denaturants. The results have provided valuable insights into the molecular basis of the activity and stability of the two lectins.

1. Introduction

Proteins fold with different energies and with enormous combinations of secondary structural elements which is dictated by the primary sequence. Accurately folded protein governs its functional life. Principles of protein folding have applications in the understanding of different pathologies, in the design of novel proteins with special functions [1]. In order to understand and appreciate the contributions of protein folding on function and stability of a protein, biophysical characterizations of the partially folded and unfolded state of the protein is important. Due to the emergence of computational biology, the advancement of biophysical techniques now, seems to have shifted protein folding field from hypothesis driven to data mining [2].

Lectins are the proteins conferred with carbohydrate binding property. Apart from their applications in cell biology as well as in medical field and extensive research in investigating the biological role, lectins are still an interesting topic for the structure-function studies at molecular level. The two lectins selected for the present studies are from *Bauhinia purpurea* and *Wisteria floribunda* (Family: Fabaceae), leguminous plants commonly called as Camel foot's tree or Butterfly tree

and *Japanese wisteria*, respectively. *Bauhinia purpurea* is used as anti-dysenteric, astringent and as a poison antidote [3]. *Bauhinia purpurea* lectin (BPL) binds to T-antigen and has also displayed elevated binding in metastatic urine [4,5]. *Wisteria floribunda* lectin (WFL) binds N-glycans terminating in β -linked N-acetylgalactosaminides particularly ones with LacdiNAc (β -D-GalNAc-[1 \rightarrow 4]-DGlcNAc) termini, and to terminal galactose residues with lower affinity [6–8]. LacdiNAc is a cancer glycomarker associated with leukemia, prostate, pancreatic, ovarian, and liver cancers [7]. WFL is currently considered as the most prominent diagnostic lectin against cholangiocarcinoma [9]. Thus, both the lectins have high medicinal values.

The seed lectins from the plants *Bauhinia purpurea* and *Wisteria floribunda* are tetrameric proteins with molecular mass of 197 kDa and 116 kDa, respectively, show maximum stability at pH 8.0 and specificity towards N-acetyl D-galactosamine (GalNAc) [6,10]. Molecular cloning of the *Bauhinia purpurea* lectin has been reported earlier [4], whereas cloning and crystal structure of *Wisteria floribunda* lectin has been recently reported [7,11]. The lectins show 43% sequence identity. We have tried to investigate the functional and/or structural novelty by monitoring the respective transitions of these two lectins under various

[☆] Note: SBA is a student enrolled in AcSIR and Dr. Gaikwad is the mentor.

* Corresponding author. Biochemical sciences Division, CSIR-National Chemical Laboratory, Pune, 411008, India.

E-mail address: sm.gaikwad@ncl.res.in (S.M. Gaikwad).